

Blade manipulator for offshore wind turbine installation by WIV

A new approach to the installation of enormous wind turbine blades on a state of the art installation vessel while increasing safety and workability

K.J. van Dinther

Master Thesis

2022



Blade manipulator for offshore wind turbine installation by WIV

A new approach to the installation of enormous wind turbine blades on a state of the art installation vessel while increasing safety and workability

by

K.J. van Dinther

Master Thesis

to obtain the degree of Master of Science in Mechanical Engineering
at the Department Maritime and Transport Technology of Faculty Mechanical, Maritime and Materials
Engineering of Delft University of Technology
to be defended publicly on Monday October 31, 2022 at 13:30 PM.

| | | |
|-------------------|---|--|
| Student number: | 4596048 | |
| MSc track: | Multi-Machine Engineering | |
| Project duration: | April 19, 2022 – October 31, 2022 | |
| Report number: | 2022.MME.8647 | |
| Supervisor: | Dr.ir. H. Polinder, Ir. W. van den Bos, D. Wijning, | TU Delft, Committee Chair TU Delft, Supervisor Huisman, Company Supervisor |

*This thesis is **confidential** and cannot be made public until October 31, 2024.*

An electronic version of this thesis is available at <http://repository.tudelft.nl/>.

Summary

Demand for offshore wind farms is growing rapidly, as is the size of the wind turbines themselves. Currently, Huisman is working on the design of a Windfarm Installation Vessel (WIV), which approaches the installation of offshore wind turbines as an industrial robotised process. Fast installation capability and high workability of this vessel leads to a higher installation capacity of wind turbines. In theory, the WIV is up to three times faster than conventional jack-up vessels.

The objective of this thesis is to develop a blade manipulator to install wind turbine blades on a customised floating vessel, the WIV, in severe weather conditions. The following research question is formulated:

How can a blade manipulator be used to quickly and accurately install blades on a 15 MW wind turbine on a floating vessel?

Currently, standard wind turbine installation is done by a jack-up vessel during favourable weather conditions. The process starts with the transportation of the components to the offshore installation site. The foundation is already installed. The tower is upended and placed on the transition piece on the foundation. Subsequently, the nacelle, hub, and blades are installed. This is done by using the single blade installation method. Single blade installation is done by a yoke connected to a hook of a crane. This installation process is severely influenced by environmental conditions. The goal is to install wind turbines 85 % of the year instead of the 2 months which is now the case. To increase the installation capacity per year, Huisman has developed the WIV. The WIV is a semi-submersible vessel that robotises the installation of both wind turbines and monopiles. The wind turbine components are placed on deck at port or by means of a delivery vessel. The WIV navigates to the appropriate location at sea, where a wind turbine foundation is located, and a wind turbine can be installed on top of the foundation after assembly. The offshore wind turbine selected for this thesis is the IEA 15-MW wind turbine. This is the largest reference wind turbine with all the blade properties and specifications available. This 15 MW wind turbine is used as a reference part for the capacity of the WIV.

The VDI 2221 guideline is used for a systematic development of concepts. There are a number of boundary conditions that each concept must meet. The blade manipulator should be installed on top of the installation tower, above the swing bearing. The manipulator has a working area between the blade rack on the deck and station 3 of the WIV. The rotation of the installation tower on the WIV requires clearance to prevent the protruding material from colliding with the wind turbine. The blade must be installed horizontally on the hub of the wind turbine. The blades of the wind turbine are stored in a blade rack on the deck of the WIV. This rack is adapted so that the manipulator has access to the blades. Using a morphological overview with several sub-functions, six different concepts were created. Using the analytic hierarchy process together with the weight factors, the results of the concept selection can be calculated. The rotational arm is the most feasible concept.

The purpose of the manipulator is to transport a blade from the blade rack to the hub of the wind turbine. The rotational arm lifts the blade from the blade rack around the Centre of Gravity (CoG) of the blade. Consequently, the gripper slides over a distance towards the pivot point to obtain the correct radius for installation. After this, the manipulator move upwards by means of a rotating movement, after which the blade can be installed on the hub of the wind turbine. When the arm of the manipulator is in a horizontal position to grab a blade from the blade rack, there are three positions the gripper should be able to reach. Furthermore, the gripper comes from the side to pick up the blade. A hydraulic cylinder and a hinge point provide a rotational movement to reach these locations. To keep the gripper horizontal in any circumstance, a slew bearing is used. To ensure that the gripper can tilt, cylinders are used. For the sliding movement along the arm of the manipulator, a slider with an rack and pinion is used. A winch with a wire rope helps to lift the manipulator.

The manipulator is designed to be operational with an average wind speed of 12 m/s and a significant wave height of 3.5 m. This enables the WIV to operate through most of the year. As larger wind

turbines will make their appearance in the future, a WIV equipped to install these wind turbines is needed. Due to the slider mechanism, the manipulator is able to handle increasing blade sizes.

Follow-up research is required before realisation of the blade manipulator. The steel structure of the boom should be optimised. The wind loads and ship movements should be added to the load cases. This can then be used to consider the optimal cross section for each section. Additionally, the actuators in the current design are determined fundamentally. They should be more extensively designed and optimised. Finally, a control system needs to be added and the accuracy calculated and determined with model tests. The largest wind turbine currently available is 15 MW. There is already a plan for 20 MW wind turbines. The results from this thesis can be used for these kinds of larger wind turbines by applying the argumentation analysis and calculations to a larger wind turbine than 15 MW. However, it is advisable to use the 20 MW reference wind turbine when doing so, assuming it will be published in the near future.

Summary in Dutch (Samenvatting)

De behoefte aan windparken op zee groeit snel, evenals de omvang van de windturbines zelf. Huisman werkt momenteel aan het ontwerp van een Windfarm Installation Vessel (WIV), die de installatie van offshore windturbines benadert als een industrieel gerobotiseerd proces. De snelle installatie en hoge werkbaarheid van dit schip zullen leiden tot een grotere installatiecapaciteit van windturbines. Het schip is theoretisch tot 3 keer sneller dan installatie met conventionele jack-up schepen.

Het doel van dit afstudeerproject is het ontwikkelen van een bladmanipulator om windturbinebladen te installeren op een speciaal drijvend schip, de WIV, in zware weersomstandigheden. De volgende onderzoeksvraag is geformuleerd:

Hoe kan een bladmanipulator worden gebruikt om snel en nauwkeurig bladen te installeren op een 15 MW windturbine op een drijvend schip?

Momenteel wordt de standaardinstallatie van windturbines uitgevoerd vanaf een jack-up schip bij gunstige weersomstandigheden. Het proces begint met het vervoer van de onderdelen naar de offshore-installatieplaats. De fundering is al geïnstalleerd. De toren wordt opgetild en op de fundering geplaatst. Vervolgens kunnen de nacelle, de hub en de bladen worden geïnstalleerd. Momenteel gebeurt dit met de installatiemethode waarbij één blad per keer wordt geïnstalleerd. De installatie van een enkel blad gebeurt met een yoke die aan een haak van een kraan is bevestigd. Dit huidige installatieproces wordt sterk beïnvloed door de weersomstandigheden. Het doel is om 85 % van het jaar windturbines te installeren in plaats van de huidige 2 maanden. Om de installatiecapaciteit per jaar te verhogen, heeft Huisman de WIV ontwikkeld. De WIV is een semi-submersible schip dat de installatie van zowel windturbines als monopiles robotiseert. De onderdelen van de windturbines worden aan dek geplaatst in de haven of door middel van een leveringsschip. De WIV navigeert naar de juiste locatie op zee, waar zich een windturbinefundatie bevindt. Na assemblage wordt de windturbine boven op de fundatie geïnstalleerd. De voor dit afstudeerproject geselecteerde offshore-windturbine is de IEA-windturbine van 15 MW. Dit is de grootste referentiewindturbine met alle beschikbare bladkarakteristieken en specificaties. Deze 15 MW-windturbine wordt gebruikt als referentie voor het bepalen van de capaciteit van de WIV.

De VDI 2221 richtlijn wordt gebruikt voor het systematisch ontwikkelen van concepten. Elk concept moet voldoen aan een aantal randvoorwaarden. De bladmanipulator moet boven op de installatietoren worden geïnstalleerd, boven het lager. De manipulator heeft een werkgebied tussen het bladrek op het dek en station 3 van de WIV. De rotatie van de installatietoren op de WIV vereist ruimte om te voorkomen dat uitstekend materiaal in conflict komt met de windturbine. Het blad moet horizontaal op de hub van de windturbine worden geïnstalleerd. De bladen van de windturbine worden opgeslagen in een bladenrek op het dek van de WIV. Dit rek is zodanig aangepast dat de manipulator toegang heeft tot de bladen. Met een morfologisch overzicht van verschillende sub functies zijn zes verschillende concepten gecreëerd. Met behulp van het analytisch hiërarchisch proces en weegfactoren zijn de resultaten van de conceptkeuze berekend. De roterende arm is het meest haalbare concept.

Het doel van de manipulator is een blad te transporteren van het bladrek naar de hub van de windturbine. De roterende arm tilt het blad uit het bladrek rond het zwaartepunt van het blad. Vervolgens schuift de grijper over een afstand richting het draaipunt om de juiste radius voor de installatie te verkrijgen. Vervolgens beweegt de manipulator met een roterende beweging omhoog, waarna het blad op de hub van de windturbine kan worden geïnstalleerd. Wanneer de arm van de manipulator zich in een horizontale positie bevindt om een blad uit het bladrek te grijpen, zijn er drie posities die de grijper moet kunnen bereiken. Bovendien komt de grijper van opzij om het blad op te pakken. Een hydraulische cilinder en een draaipunt zorgen voor een roterende beweging om deze posities te bereiken. Om de grijper onder alle omstandigheden horizontaal te houden, wordt een lager gebruikt. Om ervoor te zorgen dat de grijper kan kantelen, worden cilinders gebruikt. Voor de schuifbeweging langs de arm van de manipulator wordt een rechtgeleiding met tandheugel en rondsel gebruikt. Een lier met een

staalkabel helpt om de manipulator op te tillen.

De manipulator is ontworpen om te functioneren bij een gemiddelde windsnelheid van 12 m/s en een significante golfhoogte van 3,5 m. Aangezien in de toekomst grotere windturbines hun intrede zullen doen, is er behoefte aan een WIV die is uitgerust om de grotere windturbines te installeren. Dankzij de rechtgeleiding kan de manipulator toenemende bladafmetingen aan.

Voor de realisatie van de bladmanipulator is vervolgonderzoek nodig. De staalconstructie van de giek moet worden geoptimaliseerd. De windbelastingen en scheepsbewegingen moeten aan de belastingengevallen worden toegevoegd. Dit kan dan worden gebruikt om de optimale doorsnede voor elke sectie te bepalen. Daarnaast zijn de actuatoren in het huidige ontwerp fundamenteel bepaald. Zij moeten uitgebreider worden ontworpen en geoptimaliseerd. Tenslotte moet het regelsysteem worden toegevoegd en moet de nauwkeurigheid van dit systeem worden berekend en bepaald met modelproeven.

Het ontwerp is gebaseerd op de grootste beschikbare referentiewindturbine, namelijk 15 MW. Er is al een plan voor windturbines van 20 MW. De resultaten uit dit onderzoek kunnen worden gebruikt voor dit soort grotere windturbines door de argumentatieanalyse en berekeningen toe te passen op een grotere windturbine dan 15 MW. Het is raadzaam om daarbij de 20 MW referentiewindturbine te gebruiken, ervan uitgaande dat deze in de nabije toekomst wordt gepubliceerd.

Contents

| | |
|---|-------------|
| Summary | iii |
| Summary in Dutch (Samenvatting) | v |
| Contents | viii |
| Symbols | ix |
| Abbreviations | xi |
| List of Figures | xiv |
| List of Tables | xv |
| 1 Introduction | 1 |
| 1.1 Offshore Wind Market | 1 |
| 1.2 Problem Definition | 2 |
| 1.3 Objective | 3 |
| 1.4 Outline | 3 |
| 2 Problem Analysis | 5 |
| 2.1 Current Wind Turbine Installation Methods | 5 |
| 2.2 Reference Location. | 8 |
| 2.3 Reference Wind Turbine | 10 |
| 2.4 Windfarm Installation Vessel. | 11 |
| 2.5 Conclusion | 13 |
| 3 Concepts | 15 |
| 3.1 Concept Requirements. | 16 |
| 3.1.1 Clearance on Deck | 16 |
| 3.1.2 Wind Turbine Blade Installation Angle. | 17 |
| 3.1.3 Blade Rack Layout | 17 |
| 3.1.4 Gripper Specifications | 18 |
| 3.1.5 Overview of Boundary Conditions and Functional Constraints. | 19 |
| 3.2 Conceptual Design | 20 |
| 3.2.1 Function Structure | 20 |
| 3.2.2 Morphological Overview | 20 |
| 3.2.3 Blade Buffer and Pickup Blade. | 22 |
| 3.2.4 Concept 1 – Rotational Arm | 23 |
| 3.2.5 Concept 2 – Knuckle Boom Crane. | 24 |
| 3.2.6 Concept 3 – Four-bar Linkage | 25 |
| 3.2.7 Concept 4 – Conventional Crane | 26 |
| 3.2.8 Concept 5 – Translational Arm. | 27 |
| 3.2.9 Concept 6 – Robotic Arm | 28 |
| 3.3 Concept Selection | 29 |
| 3.4 Conclusion | 35 |
| 4 Final Concept | 37 |
| 4.1 Functional Design | 37 |
| 4.2 Material | 39 |
| 4.3 Load Factor | 39 |
| 4.4 Load Cases | 40 |
| 4.5 Load Calculation | 40 |
| 4.5.1 Gravitational Load | 40 |

| | | |
|----------|--|-----------|
| 4.5.2 | Wind Load Manipulator | 43 |
| 4.5.3 | Wind Load Gripper | 43 |
| 4.5.4 | Wind Load Blade | 43 |
| 4.6 | Structural Design | 47 |
| 4.6.1 | Allowable Deflection | 47 |
| 4.6.2 | Allowable Stress | 48 |
| 4.7 | Drive Systems | 48 |
| 4.7.1 | Winch | 48 |
| 4.7.2 | Hydraulic Cylinder | 49 |
| 4.7.3 | Slew Drive | 49 |
| 4.7.4 | Slider | 50 |
| 4.8 | Safety | 50 |
| 4.9 | Conclusion and Storyboard | 50 |
| 5 | Conclusion and Recommendations | 53 |
| 5.1 | Recommendations | 53 |
| | Bibliography | 55 |
| A | Scientific Research Paper | 59 |
| B | Nomenclature | 67 |
| B.1 | Wind Turbine | 67 |
| B.2 | Foundation | 68 |
| B.3 | Installation Vessels | 69 |
| C | Additional Information Windfarm Installation Vessel | 71 |
| D | Concept Selection | 73 |

Symbols

| Symbol | Description | Unit |
|-----------------------|---------------------------------------|------------|
| A | Surface Area | $[m^2]$ |
| AoA | Angle of Attack | $[^\circ]$ |
| $A_{segment}$ | Area per Segment | $[m^2]$ |
| C_D | Drag Coefficient | $[-]$ |
| CI | Consistency Index | $[-]$ |
| C_L | Lift Coefficient | $[-]$ |
| C_M | Moment Coefficient | $[-]$ |
| CR | Consistency Ratio | $[-]$ |
| d_{CoG} | Distance Between the Node and the CoG | $[m]$ |
| D/d | Ratio Drum Diameter per Rope Diameter | $[-]$ |
| E | Young's Modulus | $[N/mm^2]$ |
| F_D | Drag Force | $[kN]$ |
| $F_{g,blade}$ | Gravitational Force Blade | $[kN]$ |
| $F_{g,blade+gripper}$ | Gravitational Force Blade and Gripper | $[kN]$ |
| $F_{g,boom}$ | Gravitational Force Boom | $[kN]$ |
| $F_{g,boom/m}$ | Gravitational Force Boom per Meter | $[kN/m]$ |
| $F_{g,gripper}$ | Gravitational Force Gripper | $[kN]$ |
| F_L | Lift Force | $[kN]$ |
| F_W | Wind Force | $[kN]$ |
| G | Shear Modulus | $[GPa]$ |
| g | Gravitational Acceleration | $[m/s^2]$ |
| H_S | Significant Wave Height | $[m]$ |
| I | Mass Moment of Inertia | $[mm^4]$ |
| J | Polar Moment of Inertia | $[mm^4]$ |
| L | Length Boom | $[m]$ |
| LF | Load Factor | $[-]$ |
| $l_{segment}$ | Span Length per Segment | $[m]$ |
| m_{blade} | Mass Wind Turbine Blade | $[mt]$ |
| $M_{blade+gripper}$ | Moment Blade and Gripper | $[kNm]$ |
| m_{boom} | Mass Boom Manipulator | $[mt]$ |
| $m_{gripper}$ | Mass Gripper | $[mt]$ |
| $r_{CoG,blade}$ | Distance CoG Blade and Boom | $[m]$ |
| RCI | Random Consistency Index | $[-]$ |
| $r_{CoG,gripper}$ | Distance CoG Gripper and Boom | $[m]$ |
| SF_{actual} | Actual Safety Factor | $[-]$ |

| Symbol | Description | Unit |
|------------------------------|---------------------------------|----------------------|
| $SF_{required}$ | Required Safety Factor | [–] |
| T_P | Peak Peak Period | [s] |
| t_{rel} | Relative Thickness of the Chord | [–] |
| T_z | Zero Up-Crossing Period | [s] |
| UTS | Ultimate Tensile Strength | [N/mm ²] |
| U_W | Mean Wind Speed | [m/s] |
| V_{rel} | Relative Wind Velocity | [m/s] |
| α | Angle of Incoming Wind | [°] |
| β | Pitch Angle | [°] |
| δ | Deflection | [m] |
| $\delta_{distributed\ load}$ | Deflection Distributed load | [m] |
| $\delta_{point\ load}$ | Deflection Point Load | [m] |
| θ | Twist Angle | [°] |
| λ_{max} | Eigenvalue | [–] |
| ν | Poisson Ratio | [–] |
| ρ_{air} | Air Density | [kg/m ³] |
| ρ_{steel} | Steel Density | [g/cm ³] |
| $\sigma_{occurring}$ | Occuring stress | [N/mm ²] |
| σ_y | Yield strength | [N/mm ²] |
| ϕ | Torsion | [°] |

Abbreviations

AHP Analytic Hierarchy Process. 29

CoG Centre of Gravity. iii, ix, 6, 10, 37, 41, 45, 49

DD Direct Drive. 67

DoF Degree of Freedom. 27, 48

IEA International Energy Agency. xiii, xv, 10, 13, 18, 32, 44, 45, 53

MBL Minimum Breaking Load. 48

MP Monopile. xiv, 71

OWT Offshore Wind Turbine. xiii, 11, 16

RAO Response Amplitude Operator. 8, 9

SWL Safe Working Load. 19, 69

TRL Technology Readiness Level. xv, 29, 30, 31

WIV Windfarm Installation Vessel. iii, iv, v, vi, xiii, xiv, 2, 3, 5, 9, 10, 11, 12, 13, 15, 16, 17, 18, 19, 20, 35, 47, 50, 53, 71

List of Figures

| | | |
|------|--|----|
| 1.1 | Installed offshore wind energy per year [4] | 1 |
| 1.2 | Current and future limiting conditions for a wind turbine [21] | 3 |
| 2.1 | Flowchart foundation and wind turbine installation process | 5 |
| 2.2 | Foundation installation | 6 |
| 2.3 | Flowchart single blade installation | 7 |
| 2.4 | Single blade installation | 7 |
| 2.5 | Nautical zones for estimation long term wave distribution parameters [32] | 8 |
| 2.6 | The IEA 15-MW reference wind turbine dimensions [12] | 10 |
| 2.7 | Black box of Offshore Wind Turbine (OWT) installation | 11 |
| 2.8 | Coordinate system of the Windfarm Installation Vessel (WIV) | 11 |
| 2.9 | Top view Windfarm Installation Vessel (WIV) with the four different stations | 12 |
| 2.10 | Flowchart of the assembly and installation process by the Windfarm Installation Vessel | 12 |
| 2.11 | Assembling and installation of a wind turbine by Windfarm Installation Vessel (WIV) | 13 |
| 3.1 | VDI 2221 guideline [33] | 15 |
| 3.2 | Black box representation of blade installation on an Offshore Wind Turbine (OWT) | 16 |
| 3.3 | Top view of the WIV with the needed clearance and working area | 16 |
| 3.4 | Allowable blade orientation angle | 17 |
| 3.5 | Current methods of storing wind turbine blades on deck of a jack-up vessel | 17 |
| 3.6 | Storage method of wind turbine blades on deck of the Windfarm Installation Vessel (WIV) | 18 |
| 3.7 | Gripper | 18 |
| 3.8 | Function flowchart | 20 |
| 3.9 | Possible combinations of Blade Buffer and Pickup Blade | 22 |
| 3.10 | Concept 1 – Rotational arm | 23 |
| 3.11 | Concept 2 – Knuckle boom crane | 24 |
| 3.12 | Concept 3 – Four-bar linkage | 25 |
| 3.13 | Concept 4 – Conventional crane | 26 |
| 3.14 | Concept 5 – Translational arm | 27 |
| 3.15 | Concept 6 – Robotic arm | 28 |
| 4.1 | General layout | 37 |
| 4.2 | New blade rack size, the blade supports at the top level have been removed | 38 |
| 4.3 | Overview of manipulator movement | 38 |
| 4.4 | Locations (P1, P2, and P3) shown in red of the blade the gripper must be able to reach | 38 |
| 4.5 | Drawing manipulator | 39 |
| 4.6 | Schematic 3D representation of the manipulator | 41 |
| 4.7 | Shear force and bending moment diagrams for different load cases | 42 |
| 4.8 | Different surfaces of a wind turbine blade [44] | 43 |
| 4.9 | Blade segments and coordinate system top view | 44 |
| 4.10 | Intersection wind turbine blade and coordinate system | 44 |
| 4.11 | Distribution of wind forces on the blade. The nodes represent the different segments of the blade. | 46 |
| 4.12 | cross-section boom | 47 |
| 4.13 | Crosssection wire rope 8xK36WS+EPIWRC [45] | 48 |
| 4.14 | Dimensions winch | 49 |
| 4.15 | Layout cylinder | 49 |
| 4.16 | Cross-section bearing | 50 |
| 4.17 | Storyboard | 51 |

| | | |
|-----|--|----|
| B.1 | Schematic overview of a wind turbine [21] | 67 |
| B.2 | Water depth | 68 |
| B.3 | Types of offshore wind turbine foundation | 68 |
| B.4 | Offshore Wind Turbine Installation Vessels | 69 |
| C.1 | Flowchart for installing a Monopile (MP) | 71 |
| C.2 | Monopile installation by WIV | 71 |

List of Tables

| | | |
|------|---|----|
| 1.1 | Wind turbine capacity and dimensions [5–16] | 2 |
| 2.1 | Scatter Diagram Area 11, North Sea | 8 |
| 2.2 | Environmental considerations | 9 |
| 2.3 | Blade properties IEA 15 MW reference wind turbine[12] | 10 |
| 3.1 | Gripper specifications | 19 |
| 3.2 | Boundary conditions | 19 |
| 3.3 | Geometric constraints | 19 |
| 3.4 | Operational conditions | 19 |
| 3.5 | Morphological overview the different sub-functions and their solution options | 22 |
| 3.6 | Criteria for concept selection with description | 29 |
| 3.7 | Scale of relative importance [39] | 29 |
| 3.8 | Judgement matrix | 30 |
| 3.9 | Random Consistency Index values for different values of n [41] | 30 |
| 3.10 | Criterion 1 – Ease of manufacturing | 31 |
| 3.11 | Criterion 2 – Technology Readiness Level (TRL) | 31 |
| 3.12 | Criterion 3 – Economic feasibility | 32 |
| 3.13 | Criterion 4 – Scalability | 32 |
| 3.14 | Criterion 5 – Installation time | 33 |
| 3.15 | Criterion 6 – Reliability | 33 |
| 3.16 | Criterion 7 – Safety | 34 |
| 3.17 | Criterion 8 – Sustainability | 34 |
| 3.18 | Local and global priority vectors | 34 |
| 3.19 | Results | 35 |
| 4.1 | Material properties ST52-3N-Plate | 39 |
| 4.2 | Location nodes as shown in Figure 4.6 | 40 |
| 4.3 | Wind force on wind turbine blade | 43 |
| 4.4 | Parameters per section | 45 |
| 4.5 | Blade nodes | 45 |
| 4.6 | Blade segments | 46 |
| 4.7 | Dimensions segment | 47 |
| 4.8 | Characteristics 8xK36WS+EPIWRC [45] | 48 |
| 4.9 | Characteristics hydraulic cylinder [46] | 49 |

Introduction

Recently, the drawing up of climate goals has been prioritized worldwide, notably the 2015 Paris Agreement. 196 countries signed this agreement stipulating that global warming must be limited to a maximum of 2°C compared to the pre-industrial level [1]. The European Union has drawn up the European Green Deal targeting to become climate neutral with zero net greenhouse gas emissions by 2050 [2, 3]. In order to meet these goals, the way energy sources are used needs major change. All parts of society and economic sectors have to play their role, including the offshore industry. The offshore sector is changing to meet the established global climate goals by investing in renewable energy sources, specifically wind energy.

1.1. Offshore Wind Market

Demand for offshore wind farms is growing rapidly, as is the size of the wind turbines themselves. Figure 1.1 shows that the total installed capacity of offshore wind power in Europe is growing significantly. The total cumulative installed capacity of offshore wind energy in Europe was 28.4 GW at the end of June 2022 [4]. The pledge is that this will grow to a capacity of about 160 GW by 2030. This growth means that at least 8,776 wind turbines of 15 MW need to be realized in the following 8 years. Resulting in 1097 wind turbines per year, in other words at least 3 wind turbines needed to be installed per day. In 2022 one monopile is placed every 2.7 days, which is far off from the goal of 3 per day. To meet the targets, wind turbine installation needs to intensify.

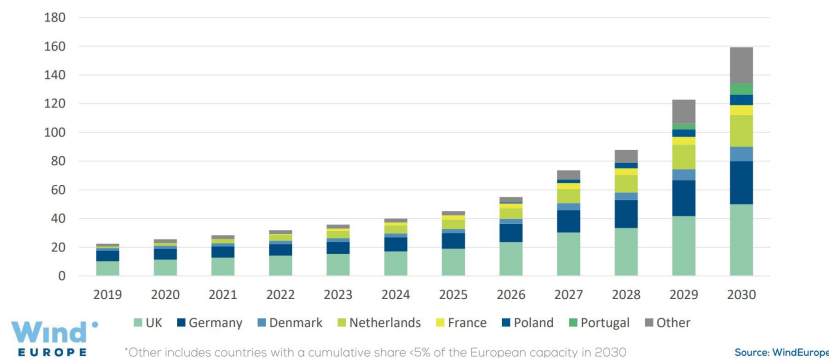


Figure 1.1: Installed offshore wind energy per year [4]

A wind turbine is a turbine that converts the energy of the wind into electricity by means of a generator. Further information on the wind turbine itself is described in Appendix B. Currently, most wind turbines placed at sea have a capacity of about 10 MW with a rotor diameter of approximately 160 m [5]. In the future, wind turbines will inevitably become larger to meet the growing demand for renewable energy. Wind turbines of about 20 MW with a rotor diameter of approximately 260 m are considered. Table 1.1 lists the capacity of different wind turbines together with the dimensions and the

reference wind farm. As wind turbines become larger in size, the challenge of installation grows with it and the foundations also have to scale accordingly. Furthermore, accessible shallow locations for placing wind turbines, with water depths of 30-50 m have already been exploited. Locations with water depths exceeding 50 m should therefore be considered, using floating foundations. Appendix B gives an overview of offshore wind turbine foundations.

Table 1.1: Wind turbine capacity and dimensions [5–16]

| Turbine Model | Capacity [MW] | Rotor Diameter [m] | Blade Length [m] | Blade Weight [mt] | Hub Height [m] | Reference Wind Farm |
|-------------------------------|---------------|--------------------|------------------|-------------------|----------------|----------------------------|
| Vestas V80-2.0 | 2.0 | 80 | 39 | 6.4 | 67 | North Hoyle (2004) |
| Siemens SWT-3.6-107 | 3.6 | 107 | 52 | 15.8 | 80 | Burbo Bank (2007) |
| NREL 5MW | 5.0 | 126 | 61.5 | 17 | 90 | Reference model (2009) |
| DTU 10MW | 10 | 178 | 86.4 | 41.7 | 119 | Reference model (2013) |
| Vestas V164-10.0 MW | 10 | 164 | 80 | 35 | 105 | Seagreen (2023) |
| Siemens Gamesa SG 11.0-200 DD | 11 | 200 | 97 | Unknown | ca. 140 | Hollandse Kust Zuid (2023) |
| GE Haliade-X | 13 | 220 | 107 | 55 | 135 | Dogger Bank A (2023) |
| IEA 15MW | 15 | 240 | 117 | 65.2 | 150 | Reference model (2020) |
| Siemens Gamesa SG 14-222 DD | 14 | 222 | 108 | 65.6 | ca. 150 | Prototype Denmark (2021) |
| Vestas V236-15 MW | 15 | 236 | 116 | Unknown | ca. 150 | Prototype (2022) |
| 20 MW RWT | 20 | 252 | 122 | 118 | 168 | Research model (2017) |

Additionally, the challenge to install wind turbines in a larger weather window arises. The blades of wind turbines up to 10 MW are currently installed by single blade installation. A gripper, yoke, is suspended from a hook on a crane. The yoke is lowered and fixed to the blade. The blade is lifted to hub height and the alignment phase begins. During this phase, the blade root is properly aligned with the hub. If there are no job-stopping critical events and the blade is properly aligned with the hub, then the mating and mounting can take place. After the blade is attached to the hub, the yoke is released and lowered back to the deck for the next blade until all three blades are attached. Wind turbines are usually installed in the summer months when the weather window is favourable. This is because the maximum wind speed for the installation of blades is only about 10 m/s, to avoid critical events [17, 18]. Due to the use of jack-up vessels, the allowable significant wave height (H_s) is currently limited to 1.5 - 2.0 m [19, 20]. However, increasing the weather window means that wind turbine installations should also be feasible with wind speeds up to 12 m/s and sea conditions with H_s of up to 3.5 m. A summary of these numbers is shown in Figure 1.2.

1.2. Problem Definition

Currently, Huisman is working on the design of a Windfarm Installation Vessel (WIV), which approaches the installation of offshore wind turbines as an industrial robotised process. The WIV has four workstations, where different stages of the wind turbine assembly and installation take place simultaneously. Each station has its own purpose: upending the tower; lifting the nacelle; installing the blades; placing the entire assembled wind turbine on top of the foundation. Moving the wind turbine to the different workstations is carried out by rotating the installation tower in the centre of the WIV [22]. The fast installation and high workability of this vessel lead to a higher installation capacity of wind turbines. In theory, the WIV is up to three times faster than conventional jack-up vessels. As wind turbines are getting larger, installation of the larger wind turbine blades will be more challenging. This is compounded by the harsh weather conditions during the installation process. The objective of this paper is to develop a blade manipulator for wind turbine blade installation in severe weather conditions on a customized floating vessel, the WIV.

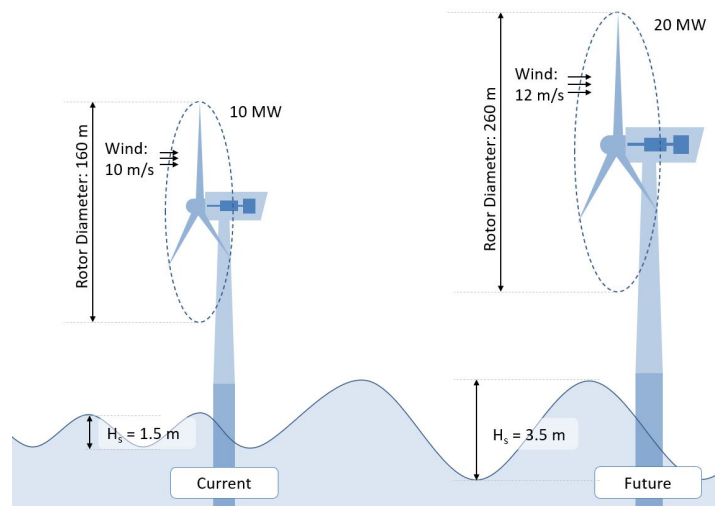


Figure 1.2: Current and future limiting conditions for a wind turbine [21]

1.3. Objective

The goal of this research is to detail the blade manipulator with respect to (1) boundary conditions, (2) functionality, and (3) mechanical design. The following research question is formulated:

How can a blade manipulator be used to quickly and accurately install blades on a 15 MW wind turbine on a floating vessel?

To answer this question, several sub-questions have been formulated:

1. *What are the boundary conditions that need to be taken into account at the Windfarm Installation Vessel?*
2. *What is the most feasible method to install a blade on a wind turbine on the Windfarm Installation Vessel?*
3. *What is the best mechanical design for the selected method?*

1.4. Outline

The main question with the sub-questions described above is answered in this report.

Chapter 2 This chapter presents the problem analysis for this design assignment and answers the first sub-question. The current installation methods of a wind turbine, focused on the single blade installation, are explained. A reference location and a reference wind turbine which is selected as the foundation for the design of the blade manipulator are presented, and the WIV from Huisman is explained.

Chapter 3 This chapter answers the second sub-question by listing the concept requirements and the different concepts for the blade manipulator that have been drawn up based on these requirements. A selection process leads to the choice of the preferred installation method.

Chapter 4 This chapter answers the third sub-question and explains the functional design and its different drive systems.

Chapter 5 This chapter answers the main research question and gives recommendations to proceed with the realisation of the design.

In addition, there are a number of appendices. The scientific research paper of this project is added in Appendix A. Appendix B presents the nomenclature of all terms used in this report by means of (schematic) figures. Appendix C contains additional information on the WIV. Appendix D provides the code for the concept selection process.

2

Problem Analysis

This chapter presents the case for the design of the blade manipulator and answers the first sub question: *What are the boundary conditions that need to be taken into account at the Windfarm Installation Vessel?* First, the current method of wind turbine installation is explained, focusing on the installation of a single blade [21]. Afterwards, the environmental factors for the blade manipulator are defined based on the location where the WIV should be operational, the type of wind turbine and further environmental conditions. Finally, the current design of the WIV is explained, focusing on the process of simultaneous installation of the wind turbine on the vessel.

2.1. Current Wind Turbine Installation Methods

Currently, standard wind turbine installation by a jack-up vessel during favourable weather conditions follows a clear step-by-step path, shown in Figure 2.1. In the flow chart, each step is represented by a block with a letter. Each block is explained below. The green box in Figure 2.1 stating 'Install Blade' is further detailed in Figure 2.3.

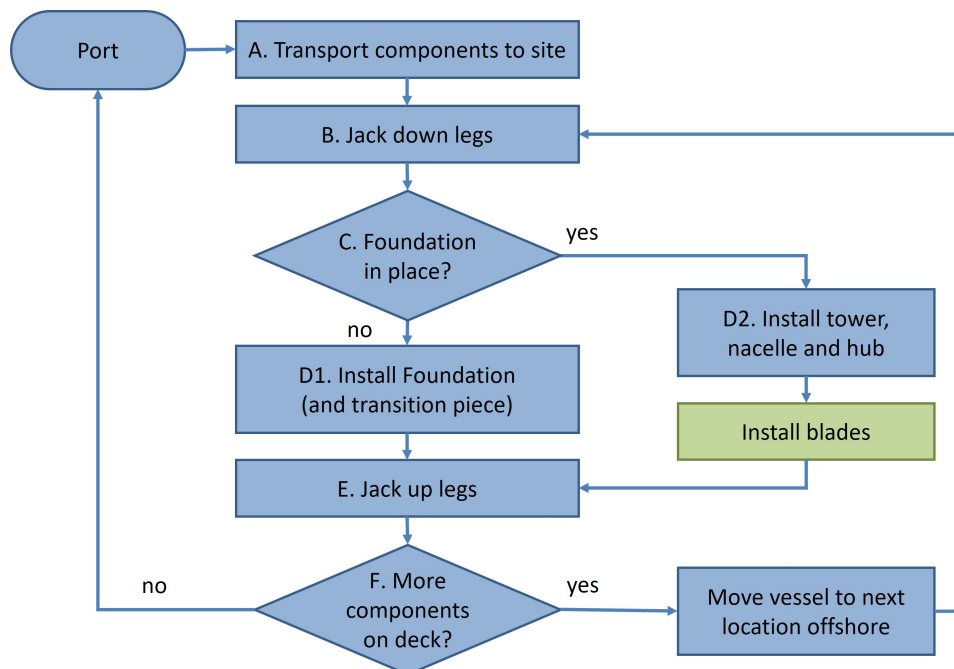


Figure 2.1: Flowchart foundation and wind turbine installation process

Block A. The process starts with the transportation of the components to the offshore installation site.

This is often done with jack-up vessels. The types of offshore vessels are further described in Appendix B.

Block B. At the installation site, the jack-up vessel lowers its legs to stabilize the vessel.

Block C. First, the foundations are placed on site (Block D1). At this stage, there are only foundation pieces present on the vessel during this phase of installing the wind farm. When the foundations are in place, the installation of the wind turbine on the foundation can take place (Block D2). During this phase, only components of the wind turbine are present on the vessel.

Block D1. The foundation of the wind turbine is installed. Because there are three different types of foundations, this can be achieved in different ways:

- **Monopile installation** – First, the monopile is upended. Then the monopile is hammered into the seabed, shown in Figure 2.2a. Finally, the transition piece, the connection between foundation and tower, is installed on top of the monopile.
- **Jacket or tripod installation** – First, the piles are secured to the seabed. Then the piles are attached to the jacket structure by grouting. The transition piece is pre-assembled. The installation is shown in Figure 2.2b [23].
- **Floating foundation installation** – A floating wind turbine is fully assembled in a port and towed to the desired location by a tugboat, shown in Figure 2.2c [24].

Block D2. The tower is upended and placed on the transition piece on the foundation. Subsequently, the nacelle, hub and blades can be installed. Currently, this is done using the single blade installation method [21].

Block E. The jack-up vessel lowers back into the water after the foundation installation and moves on.

Block F. The vessel moves to a new location and repeats the process until there are no components left after which the vessel makes a port call.



(a) Monopile [25]



(b) Jacket [26]



(c) Floating Foundation [27]

Figure 2.2: Foundation installation

The flowchart for single blade installation is shown in Figure 2.3. Each block is numbered and explained below. All components are lifted and assembled separately at the location. The nacelle and the hub are pre-assembled. This method is shown in Figure 2.4a. This method requires relatively less lifting capacity compared to pre-assembled configurations [28, 29]

Block 1. The hub is first rotated to the right angle so that the blade can be inserted properly.

Block 2. A yoke grabs a blade. The yoke is a specially designed lifting tool suspended at the crane hook, see Figure 2.4c, which is used to pick up the blade around its CoG. Sometimes, the tasks of the yoke are not limited to only gripping, in which case it is generally called the "blade manipulator".

Block 3. The yoke lifts the blade out of the rack to hub height. Tag lines, also called tugger lines or tack lines, can be attached to the yoke and the crane boom to ensure that the blade does not move too much in the wind and to be able to manipulate the load horizontally.

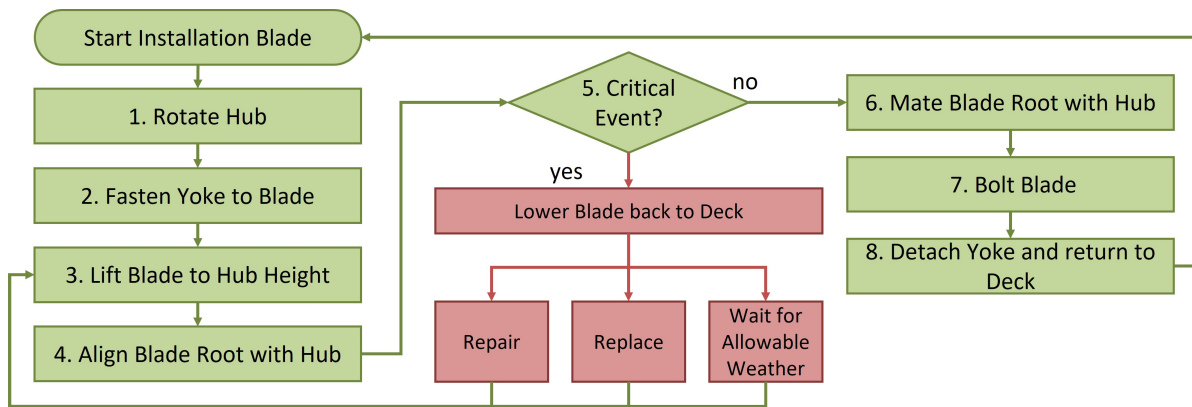


Figure 2.3: Flowchart single blade installation

Block 4. The blade root is aligned with the hub. Figure 2.4b shows the lineup of a blade with the hub during the installation of the Gemini Wind Farm installing a relatively small wind turbine (Siemens Gamesa SWT-4.0).

Block 5. If there is no critical event, such as a collision or severe weather conditions, Block 6 can continue, otherwise, the blade must be brought back to deck. The blade has to be repaired, replaced or the installation is halted until weather conditions allow further installation.

Block 6. If there is no critical event, the root is mated with the hub.

Block 7. The blade is mounted to the hub.

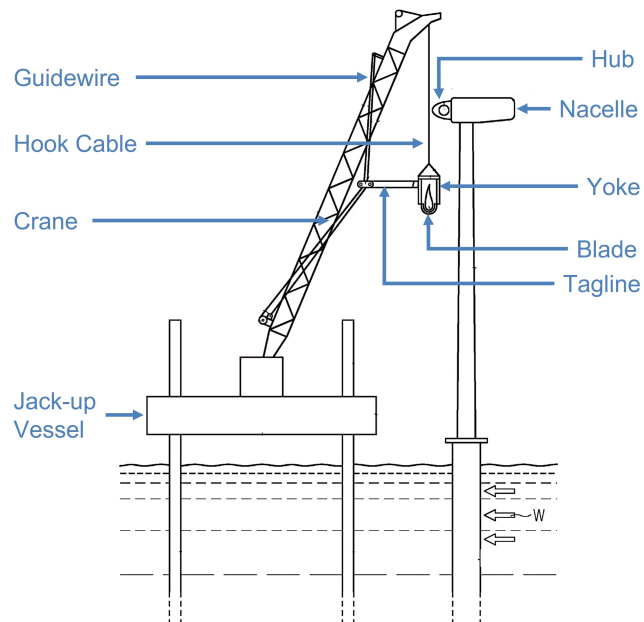
Block 8. After successful installation, the yoke is detached and returned to deck. Then the process is repeated until all three blades are installed [21].



(a) Lift blade to hub height



(b) Lineup of a blade with a hub [30]



(c) Schematic representation of single blade installation [31]

Figure 2.4: Single blade installation

2.2. Reference Location

At each location at sea different environmental conditions occur. For example, the wind speeds, significant wave height (H_S), peak period (T_P), and wave zero up-crossing period (T_z) all affect what the design of the blade manipulator must be able to handle. The H_S is the average of the highest third of the waves. About half of H_S is the most common wave height (mode). About 14% of the waves are higher than the average H_S . The peak wave period is the wave period with the most energetic waves. The T_z is the period between a wave crossing the mean water level in an upward and downward direction. Figure 2.5 shows a map with the different areas in which estimates of the wave heights and their probability of occurrence are available. Area 11, the North Sea is coloured red in this figure. The scatter diagram of area 11 is shown in Table 2.1. This diagram gives the probability of a significant wave height (H_S) against wave zero up-crossing period (T_z). The last column represents the probability of the wave height. The top row represents the probability of the wave period. As all the values in this table are rounded, the total value in the top right does not equal exactly 100 % (1005 in Table 2.1).

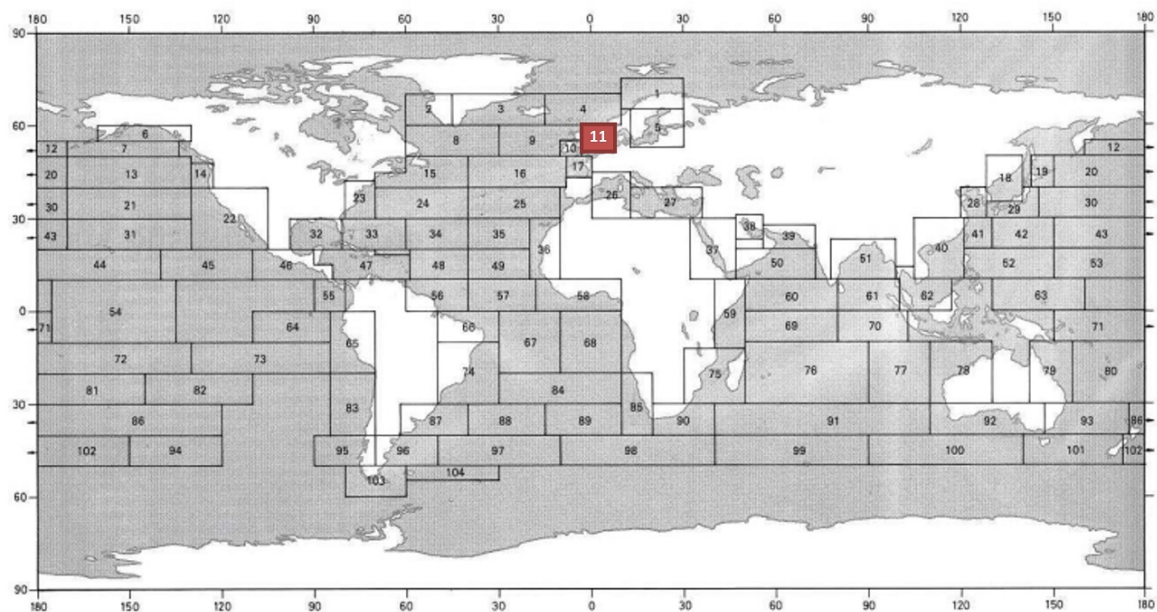


Figure 2.5: Nautical zones for estimation long term wave distribution parameters [32]

Table 2.1: Scatter Diagram Area 11, North Sea

| | | North Sea | | | | | | | | | | |
|-----------|-------|-----------|-----|-----|-----|-----|-----|------|-------|-------|------|-------|
| Total | | 23 | 161 | 323 | 288 | 145 | 49 | 13 | 3 | 0 | 0 | 1005 |
| H_S [m] | >14 | 14.5 | | | | | | | | | | 0 |
| | 13-14 | 13.5 | | | | | | | | | | 0 |
| | 12-13 | 12.5 | | | | | | | | | | 0 |
| | 11-12 | 11.5 | | | | | | | | | | 0 |
| | 10-11 | 10.5 | | | | | | | | | | 0 |
| | 9-10 | 9.5 | | | | 1 | 1 | | | | | 2 |
| | 8-9 | 8.5 | | | | 1 | 1 | 1 | | | | 3 |
| | 7-8 | 7.5 | | | 1 | 2 | 2 | 1 | 1 | | | 7 |
| | 6-7 | 6.5 | | | 2 | 4 | 4 | 2 | 1 | | | 13 |
| | 5-6 | 5.5 | | | 1 | 4 | 9 | 7 | 4 | 1 | | 26 |
| | 4-5 | 4.5 | | 2 | 11 | 19 | 14 | 6 | 2 | 1 | | 55 |
| | 3-4 | 3.5 | | 6 | 27 | 39 | 26 | 10 | 3 | 1 | | 112 |
| | 2-3 | 2.5 | 1 | 17 | 63 | 73 | 40 | 13 | 3 | 1 | | 211 |
| | 1-2 | 1.5 | 3 | 49 | 121 | 99 | 40 | 10 | 2 | | | 324 |
| | 0-1 | 0.5 | 19 | 86 | 94 | 41 | 10 | 2 | | | | 252 |
| | | 3.5 | 4.5 | 5.5 | 6.5 | 7.5 | 8.5 | 9.5 | 10.5 | 11.5 | 12.5 | Total |
| | | 0-4 | 4-5 | 5-6 | 6-7 | 7-8 | 8-9 | 9-10 | 10-11 | 11-12 | >12 | |
| | | T_z [s] | | | | | | | | | | |

The Response Amplitude Operator (RAO) is an engineering statistic to determine the behaviour

of a ship at sea. These RAOs can be calculated or measured during model tests. The calculations and model tests for the WIV were done for all ship motions in all wave headings. The calculations deviate from the tests. This is mainly because the rotational accelerations have many second order effects and therefore deviate. The WIV moves approximately around its centre of gravity, so the further away from the centre of gravity the more the linearised RAO calculations deviate from reality. As acceleration for further calculations, the maximum calculated accelerations are used: $[a_x, a_y, a_z] = [0.50, 0.75, 0.60] m/s^2$. This is all calculated with a significant wave height (H_S) of 4 m, which is more than the arm should be designed for.

In summary, all environmental considerations are listed in Table 2.2.

Table 2.2: Environmental considerations

| Description | Value |
|--|---------------------------------------|
| Minimum ambient temperature | $-20\text{ }^{\circ}C$ |
| Maximum ambient temperature | $+45\text{ }^{\circ}C$ |
| Maximum operational acceleration x-direction | $\pm 0.50\text{ m/s}^2$ |
| Maximum operational acceleration y-direction | $\pm 0.75\text{ m/s}^2$ |
| Maximum operational acceleration z-direction | $\pm 0.60\text{ m/s}^2$ excl. gravity |
| Mean wind speed (U_W) | 12 m/s |
| Maximum wind speed | 12 m/s |
| Significant wave height (H_S) | $\leq 3.5\text{ m}$ |

2.3. Reference Wind Turbine

A reference wind turbine is a fictional turbine that has not been and will not be manufactured in real life. Several reference wind turbines have been developed. The reason why reference wind turbines are developed is to serve as open benchmarks that can be used freely by the public as a basis for projects. The open design enables cooperation between different parties and industries. In addition, this model can be used as an educational tool for newcomers to the offshore energy industry [12]. The first reference wind turbine was published in 2009. This was the 5-MW Reference Wind Turbine [8]. Four years later, the 10-MW Reference Wind Turbine was introduced [5]. In 2020, the largest reference wind turbine to date was published, the International Energy Agency (IEA) 15-MW Reference Wind Turbine. This wind turbine has a capacity of 15 MW [12]. The IEA 15-MW Wind turbine is shown in Figure 2.6 together with its most important dimensions. Table 2.3 lists the key parameters for the blades.

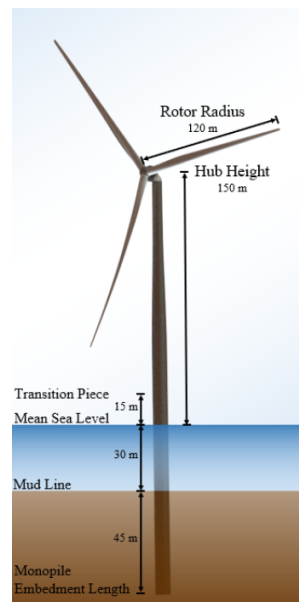


Figure 2.6: The IEA 15-MW reference wind turbine dimensions [12]

Table 2.3: Blade properties IEA 15 MW reference wind turbine[12]

| Description | Value | Units |
|----------------------------------|--------|-------|
| Blade length | 117 | m |
| Root diameter | 5.20 | m |
| Root cylinder length | 2.34 | m |
| Max chord | 5.77 | m |
| Max chord spanwise position | 27.2 | m |
| Tip prebend | 4.00 | m |
| Precone | 4.00 | ° |
| Blade mass | 65,250 | kg |
| Blade CoG | 26.8 | m |
| Design tip-speed ratio | 9.00 | - |
| First flapwise natural frequency | 0.555 | Hz |
| First edgewise natural frequency | 0.642 | Hz |
| Design CP | 0.489 | - |
| Design CT | 0.799 | - |
| Annual energy production | 77.4 | GWh |

The IEA 15-MW wind turbine is the biggest reference wind turbine with all the blade properties and specifications available. This 15 MW wind turbine is used as a reference part for the capacity of the WIV.

2.4. Windfarm Installation Vessel

Installation of a wind turbine, as can be seen in Figure 2.1, can be simplified and represented as a black box. The black box is shown in Figure 2.7. The input for this black box is the wind turbine components and the output is an installed wind turbine. The requirements for the installation are the number of wind turbines to be assembled; the location of wind turbines; the wind farm planning; the weather forecast; and de wind turbine specifications. The performance is measured by the number of wind turbines installed and the duration of the installation.

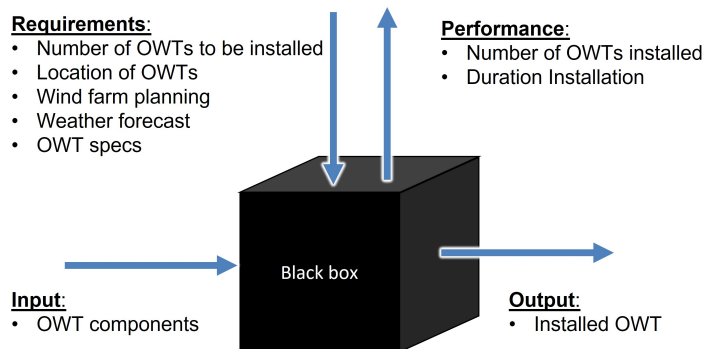


Figure 2.7: Black box of Offshore Wind Turbine (OWT) installation

Based on the black box model from Figure 2.7, the installation of the wind turbine can be performed as stated in Section 2.1. However, the process could also be performed differently.

The WIV is a semi-submersible vessel that robotises the installation of both wind turbines and monopiles. The WIV is operational 85 % per year. The wind turbine components are placed on deck at port or offshore supplied by a vessel. The WIV navigates to the appropriate location at sea, where a wind turbine foundation is located. The wind turbine is assembled on deck and installed on the foundation afterwards. A schematic isometric view of the WIV is shown in Figure 2.8. The origin of the coordinate system of the WIV is at the stern and at the bottom of the vessel. The x-axis points to the bow of the vessel; the y-axis points to the starboard side; and the z-axis points upwards.

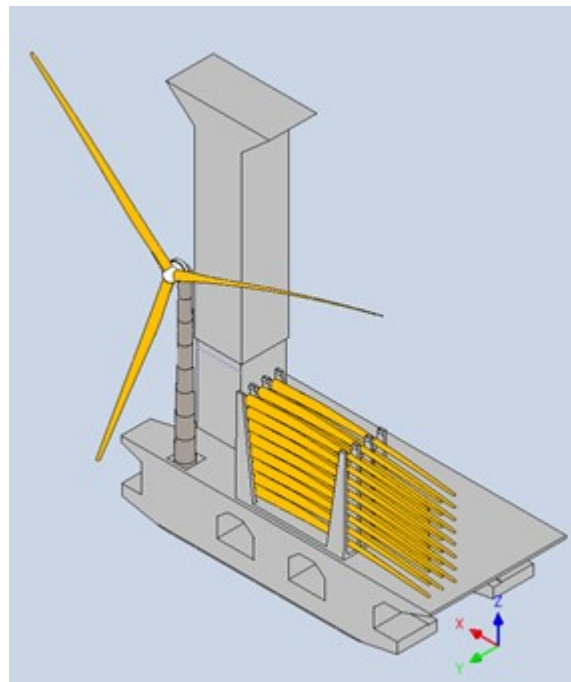


Figure 2.8: Coordinate system of the Windfarm Installation Vessel (WIV)

Figure 2.9 shows a top view of the WIV with the different stations to enable simultaneous assembly and installation. Station 1 is located on the starboard side of the vessel. Station 2 is located on the stern side of the vessel, station 3 on the port side and station 4 at the bow of the vessel.

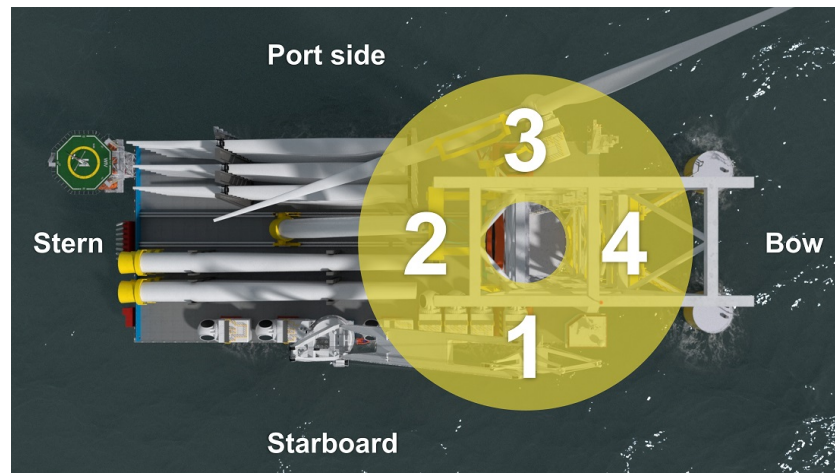


Figure 2.9: Top view Windfarm Installation Vessel (WIV) with the four different stations

Figure 2.10 shows the flowchart of the assembling and installation of the wind turbine. The same colours used in this flowchart are also used in Figure 2.11. The tower of the wind turbine is upended at station 2, as is shown in Figure 2.11a, after which the electrical cabling is made ready for the nacelle. The nacelle is skid to the right place on deck to make it possible for it to be picked up at station 1. The installation tower rotates and picks up the nacelle at station 3, see Figure 2.11b. The installation tower rotates back and installs the nacelle on top of the tower in station 2, as can be seen in Figure 2.11c. The electrical cabling is connected between the tower and the nacelle. Processes at all stations run simultaneously, increasing workability.

During these first steps in the assembly process, the grippers at station 2 are tucked away, to create enough clearance to be able to rotate the installation tower. The grippers pick up the tower-nacelle assembly at station 2, after which the installation tower rotates, see Figure 2.11d, and the tower-nacelle assembly is placed in the hole at station 3. Here, the blades are installed by the blade manipulator, shown in Figure 2.11e. Note that the method of installing the blades is an initial method used for problem analysis purposes, which is different from the final method described in this report. After installing the blades, the wind turbine is picked up, the installation tower rotates, see Figure 2.11f, and the wind turbine is installed on the foundation.

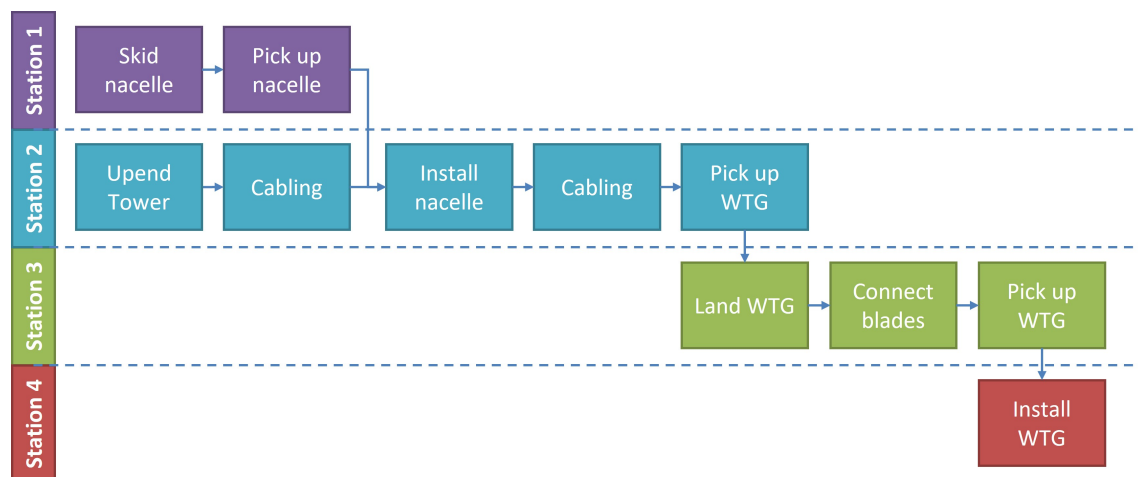


Figure 2.10: Flowchart of the assembly and installation process by the Windfarm Installation Vessel (WIV) divided per station

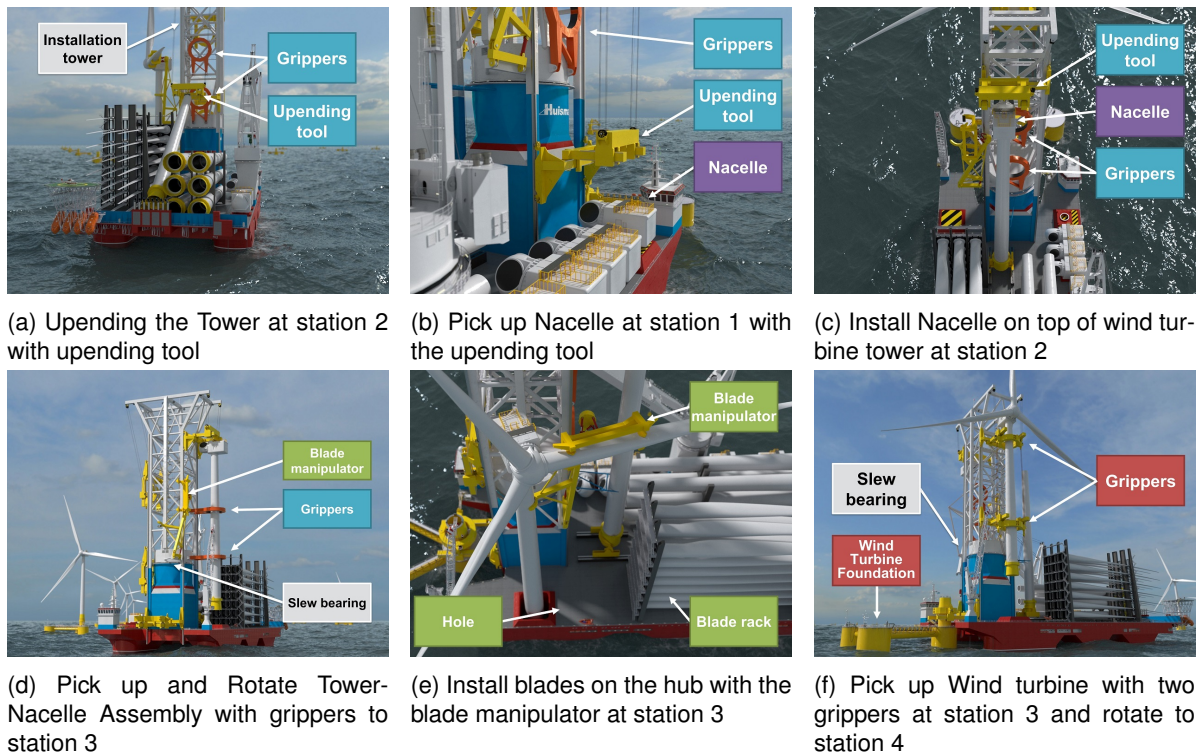


Figure 2.11: Assembling and installation of a wind turbine by Windfarm Installation Vessel (WIV)

The blade manipulator is mounted on the rotating part of the installation tower, so height, as well as clearance, is needed. Just under the slew bearing extra support is added between the installation tower and the wind turbine. This means the manipulator must be mounted above the slew bearing on the rotating part of the installation tower: 50 m above deck.

2.5. Conclusion

Currently, standard wind turbine installation is done by a jack-up vessel during favourable weather conditions. The process starts with the transportation of the components to the offshore installation site. The foundation is already installed. The tower is upended and placed on the transition piece on the foundation. Subsequently, the nacelle, hub and blades are installed. Currently, this is done using the single blade installation method. Single blade installation is done by a yoke connected to a hook of a crane.

This current installation process is severely influenced by environmental conditions. The goal is to install wind turbines 85 % of the year instead of the 2 months which is now the case. To increase the installation capacity per year, Huisman has developed the WIV. The WIV is a semi-submersible vessel that robotises the installation of both wind turbines and monopiles. The wind turbine components are placed on deck at port or by means of a delivery vessel. The WIV navigates to the appropriate location at sea, where a wind turbine foundation is located, and a wind turbine can be installed on top of the foundation after assembly.

The offshore wind turbine selected for this thesis is the IEA 15-MW wind turbine. This is the largest reference wind turbine with all the blade properties and specifications available [12]. This 15 MW wind turbine is used as a reference part for the capacity of the WIV.

3

Concepts

With a clear overview of the problem analysis, concepts toward the design objective can be made. This chapter answers the second sub-question: *What is the best method to install a blade on a wind turbine on the Windfarm Installation Vessel?* Multiple concepts are developed based on the guideline VDI 2221 [33]. Figure 3.1 shows the process and phases described by the guideline VDI 2221. Section 3.1 provides a list of requirements and assumptions with which the concepts must comply. This section represents *Phase I*. Section 3.2 describes *Phase II* and lists the functions that must be performed in order to reach the objective and their structure. Once the function structure is clear, a morphological overview with principal solutions is drawn up. In concluding this chapter, a concept selection takes place. The resulting single concept is developed in Chapter 4, representing *Phase III*, after which an overview of the complete concept with the final designs of the manipulators is presented in the same chapter. This represents *Phase IV*.

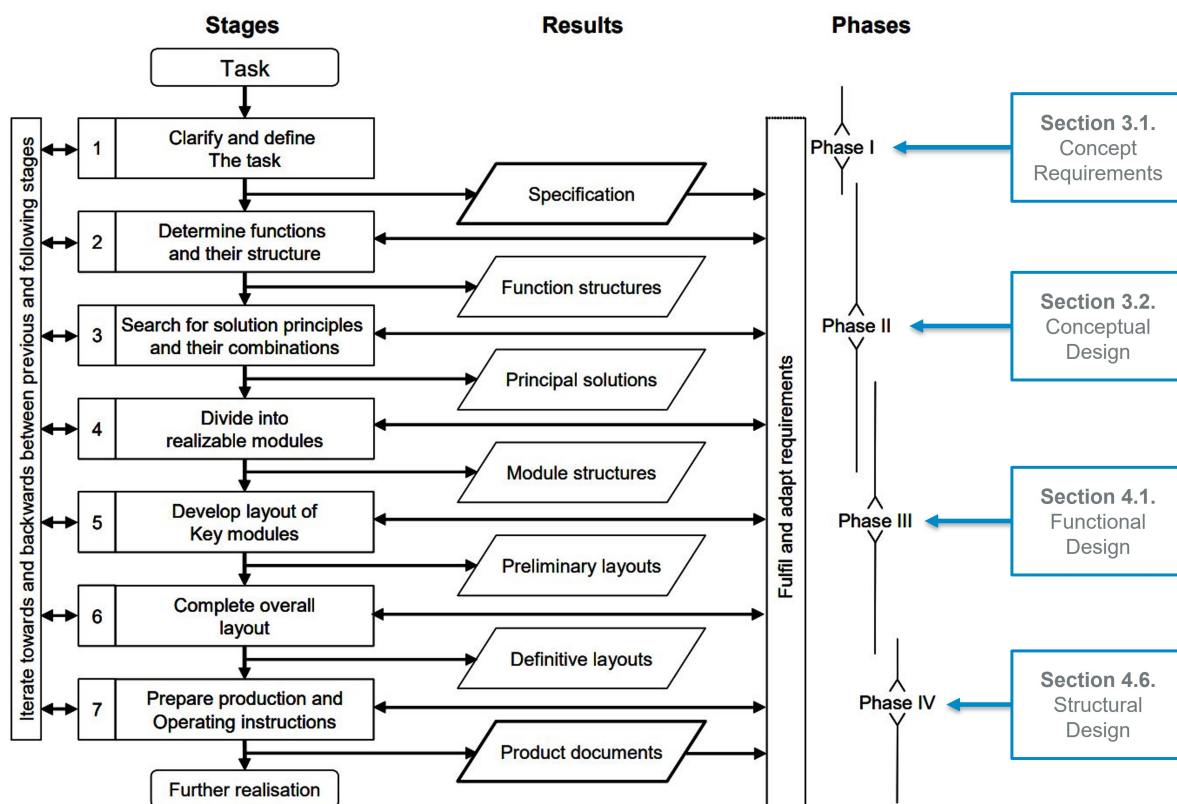


Figure 3.1: VDI 2221 guideline [33]

3.1. Concept Requirements

The process of blade installation can be seen as a black box as stated in Section 2.4. Here the initial state is the tower with nacelle at station 3 of the WIV. The blades are stacked next to the tower as shown in Figure 3.2 as the initial state. In the final state, the blades are installed on the wind turbine. The requirements for this black box model can be found below. The performance is measured by the installation time per blade. The black box involves the design of equipment to transport and install the blades on the hub of the wind turbine.

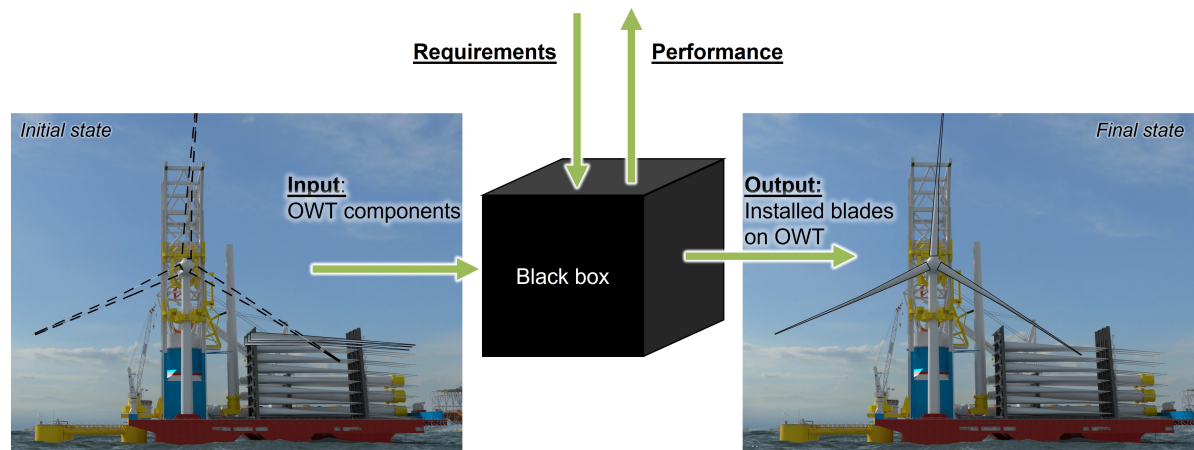


Figure 3.2: Black box representation of blade installation on an Offshore Wind Turbine (OWT)

3.1.1. Clearance on Deck

Figure 3.3 shows the top view of the WIV. The support structure between the installation tower and the wind turbine tower is shown in blue. This support structure is needed to reduce the movement of the wind turbine tower during blade installation. The WIV moves the wind turbine tower from 'station' to 'station' around its centre at a 35 m radius, shown in red. Due to the rotation of the WIV, clearance is needed for the protruding equipment not to clash with the wind turbine. This maximum protrusion is shown as the green circle. This green circle has a radius of 32.2 m. The working area of the blade installation equipment is between the blade rack on deck and station 3 of the WIV, shaded grey in Figure 3.3. On the installation tower, only the area between the wind turbine tower and the blade rack may be used. On the other locations on the vessel and on the installation tower, other processes are executed, see Section 2.4, and therefore there is no room for the manipulator to use these locations.

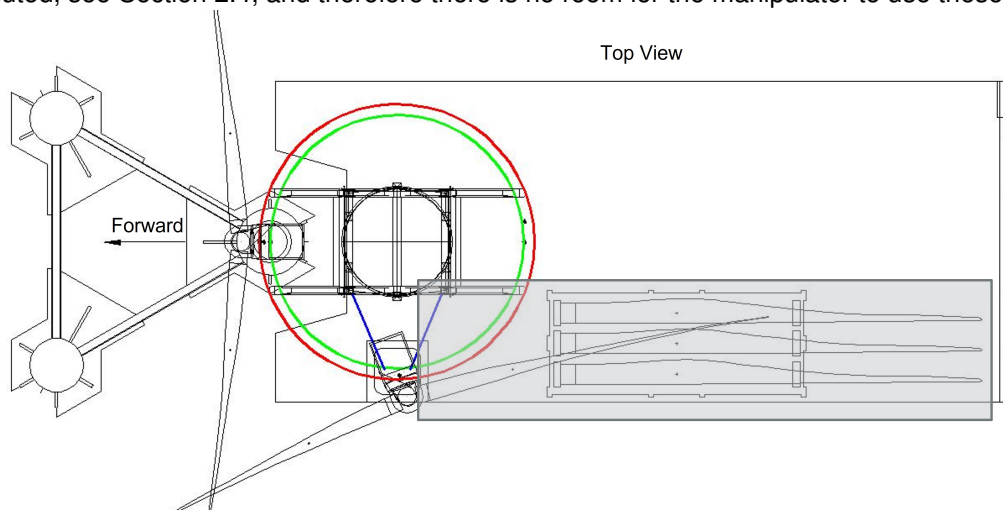


Figure 3.3: Top View of the WIV with the support between installation tower and the wind turbine tower at station 3 (blue), the path wind turbine tower (red), the clearance needed due to path wind turbine tower (green), and the working area (grey)

3.1.2. Wind Turbine Blade Installation Angle

The maximum allowable angle is limited by the water level. Blades are not allowed to contact water or other equipment, because this can cause damage. Therefore, the limits are determined based on the maximum water level and dimensions of deck equipment. Figure 3.4a shows the default installation orientation of the blades, with a reference angle of 0° . Rotating the hub counterclockwise results in a limiting angle of 7° , before one of the installed blades touch the water. The clockwise rotation of the hub can have two limit angles depending on the nacelle orientation. The nacelle, as shown in Figure 3.4b can be rotated 0° (situation 1) or rotated clockwise 5° (situation 2). In situation 1 the limiting angle of the hub is dependent on the maximum water level, resulting in a maximum clockwise rotation of 63° , shown in Figure 3.4c. In situation 2 the turbine blades can clash with deck equipment resulting in a maximum clockwise rotation of 17° . As the nacelle could rotate during installation, situation 2 is considered. This means that the limits of the hub rotation during installation is $-17^\circ < \theta < 7^\circ$, Due to the small range of rotation, the preferred blade installation is considered horizontal.

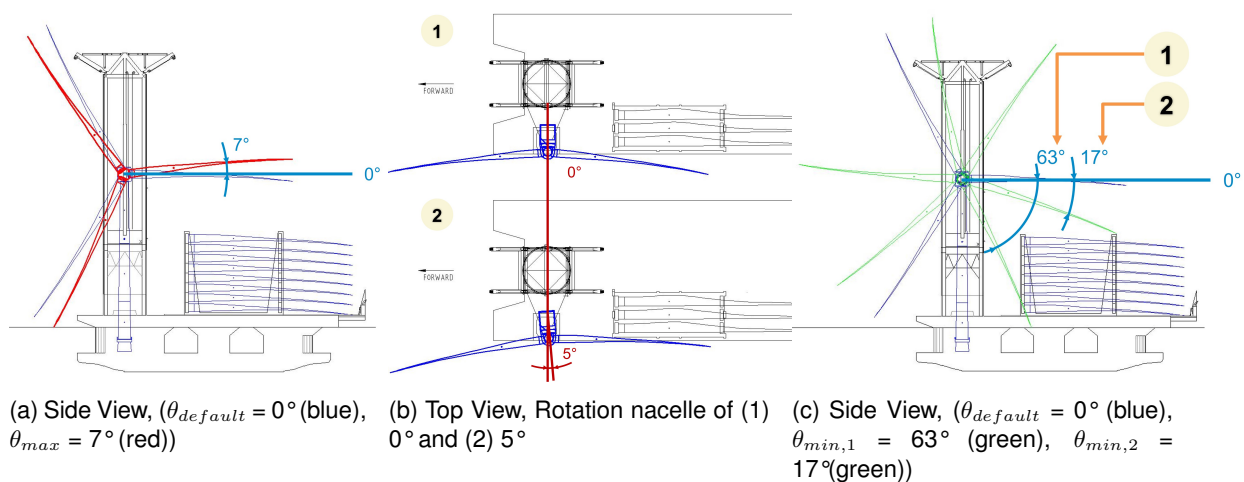


Figure 3.4: Allowable blade orientation angle due to the water level and other objects.

3.1.3. Blade Rack Layout

As can be seen in Figure 3.5, the blades are usually stacked on the deck in a rack. The specific way of storing blades is dependent on the specific project characteristics. In the case of the WIV, the blades are loaded onto the WIV in a series of 3 blades. These groups of blades are then placed in a large blade rack on the WIV. This is shown in Figure 3.6. This creates some restrictions on the accessibility of the blades to the manipulator. Figure 3.6c shows the front view of the blade rack. The large blade rack is shown in red. The manipulator should stay clear of this red area.



Figure 3.5: Current methods of storing wind turbine blades on deck of a jack-up vessel

A solution to ensure that the manipulator does not touch the rack is to move the rack. However, this is not possible, as then the rack clashes with the wind turbine tower during the transportation with the rotation of the installation tower. Since the clearance is 5 m, moving the blade rack is not possible.

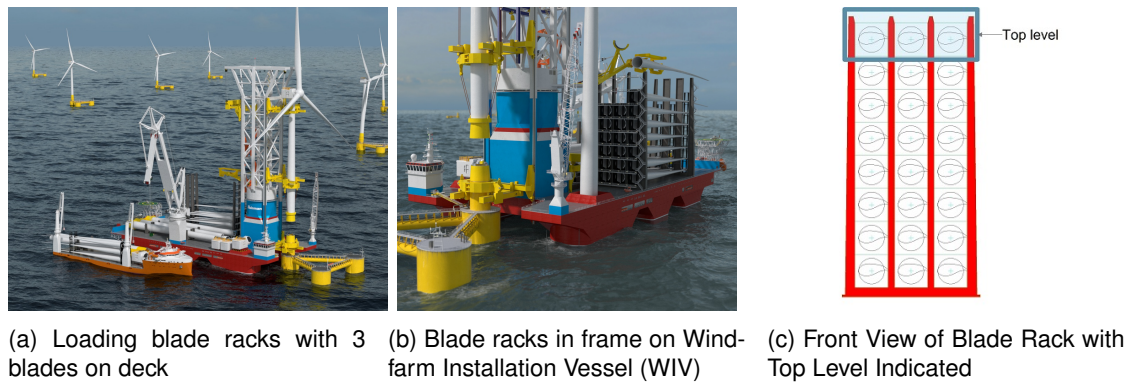


Figure 3.6: Storage method of wind turbine blades on deck of the Windfarm Installation Vessel (WIV)

Furthermore, the rack can not be moved in the y direction due to potential clashes with the wind turbine tower upending at station 2. Therefore, the position of the blade rack is fixed.

To ensure that the blade manipulator does not touch the blade rack, a mechanism could be added to the rack to transport the blades to the top level, ready to be picked up by the manipulator. The top level is shown in Figure 3.6c. There are four examples of possibilities for moving the blades upwards:

1. Use the crane on the starboard side of the vessel to hold the blades at the upper level. At this upper level, the blade can be picked up from the side with the manipulator.
2. A mechanism with trolleys can be used to move the blades upwards.
3. An overhead crane can be used to place the crane in a pickup station. The advantage is that the blade is lifted from one position only.
4. A piston or a similar mechanism under the blades can lift the entire column each time a blade has been removed from the rack by the manipulator.

Ideally, however, a static rack is preferred. Without moving parts, there are fewer modes of failure. This rules out the above possibilities. In the case of such a static rack, some adjustments must be made to the large rack in which the blades are placed. The stairs by the root of the blades must be replaced by ladders or moved to create enough space for the manipulator. In this case, the manipulator must be larger to reach all the blades in the rack.

3.1.4. Gripper Specifications

To pick up the turbine blades, a gripper is used. The gripper that is used is shown in Figure 3.7a. This gripper is adapted to the larger size blades of the IEA 15 MW wind turbine. The current yokes are connected at the top of the gripper to the crane. Here, the interface between the gripper and the manipulator is at the back of the gripper, as can be seen in Figure 3.7. The front, side and top view of the modified gripper can be seen in Figure 3.7b. This figure also shows the dimensions. Table 3.1 shows the specifications of the gripper.

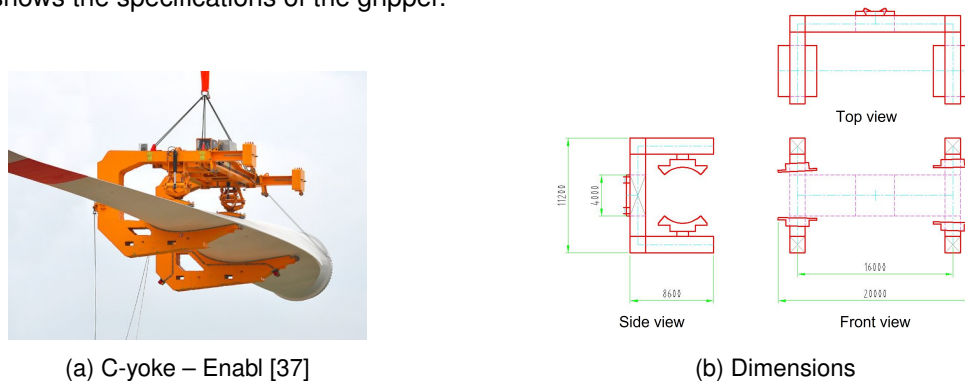


Figure 3.7: Gripper

Table 3.1: Gripper specifications

| Description | Value |
|---------------------------|----------------|
| Weight of the yoke | 80 <i>mt</i> |
| Safe Working Load (SWL) | 78 <i>mt</i> |
| Tilt angle | $\pm 10^\circ$ |
| Distance Blade interfaces | 16.0 <i>m</i> |
| Total length | 20.0 <i>m</i> |
| Total height | 11.2 <i>m</i> |
| Total depth | 8.6 <i>m</i> |
| Slew bearing diameter | 4.0 <i>m</i> |

3.1.5. Overview of Boundary Conditions and Functional Constraints

Tables 3.2, 3.3 and 3.4 list the boundary conditions, geometric constraints, and the operational constraints respectively.

Table 3.2: Boundary conditions

| Nr. | Description |
|-----|--|
| 1 | The blade installation equipment must be able to handle currently existing wind turbines , see Section 2.3 for the parameters of the <i>15 MW reference model</i> |
| 2 | The blade installation equipment should be able to handle different sizes of wind turbines, P = 13- 20 MW |
| 3 | Cycle time blade installation 2.5 hours |
| 4 | Holes or any other modifications to the blades are not allowed |
| 5 | Holes or any other modifications to the wind turbine tower are not allowed |
| 6 | The installation zone is -17° till $+7^\circ$ when facing the front of the wind turbine (hub side) |
| 7 | Hub rotation is possible by wind turbine during installation |
| 8 | Gripper must be an existing design able to operate autonomously or remotely |

Table 3.3: Geometric constraints

| Nr. | Description |
|-----|--|
| 1 | The blades must be stored parallel and horizontal on deck |
| 2 | Hub rotation is counterclockwise during installation, due to the clearance available on the WIV |
| 3 | Nacelle yaw $> \pm 10^\circ$ is not possible due to clearance available on the WIV |
| 4 | The blade installation equipment should be able to create enough clearance for the installation tower to rotate |
| 5 | Outreach 15-80 m |
| 6 | Safe Working Load (SWL) > 78 mt |

Table 3.4: Operational conditions

| Nr. | Description |
|-----|--|
| 1 | The blade installation equipment should be able to operate with a mean wind speed (U_W) of 12 m/s |
| 2 | The blade installation equipment should be able to operate with a significant wave height (H_S) of 3.5 m |

3.2. Conceptual Design

This section describes the design process of the concepts. First, the function structure is elaborated, describing the process to install the blade on the wind turbine. Following, different solutions are given for each function. This is presented in a morphological overview. Based on this morphological overview, different combinations of options are presented, followed by a number of different concepts for the design of the blade manipulator. These concepts undergo a selection after which one preferred concept emerges. That concept is further designed in the next chapter.

3.2.1. Function Structure

The black box in Figure 2.7 can be filled with different functions. There are three main functions, namely grabbing the blade with a gripper, transporting the blade to the hub, and mounting the blade on the hub. Disconnecting the gripper from the blade and lowering the gripper is not included in this function sequence, as these are the inverse of gripping and transporting respectively.

By adding some relevant sub-functions to these main functions, the function structure as shown in Figure 3.8 is created. Blade grabbing is divided into two actions: feeding the process with blades, which are stored in a particular configuring in the storage rack, which is called *Blade Buffer*, and picking up the blades with a gripper from the storage rack, which is called *Blade Pickup*. The *Transportation* of the blades to the hub remains one function. However, there are two main methods of doing this, namely *Translation* and *Rotation*. During the transportation of the blade and during the *Alignment* of the blade and hub, the movement is closely monitored, *Monitoring Movement*. This is important to prevent a critical event. After this, the *Installation* can take place. Installation includes inserting the blade into the hub, *Mating*, and bolting the blade root to the hub, *Mounting*. Figure 3.8 also shows the final steps of the function structure, namely *Disconnect Gripper*, and *Lower Gripper*, leading to the final state as shown in the black box representation in Figure 3.2.

For the design, it is also important to consider the *Storage* and *Maintenance* functions that need to be carried out after the blades are installed. The installation tower of the WIV, on which the manipulator is mounted, rotates after all blades have been installed to ensure that the next wind turbine can be put on station 3 and the blades installed on it. To do this, the manipulator must be folded up.

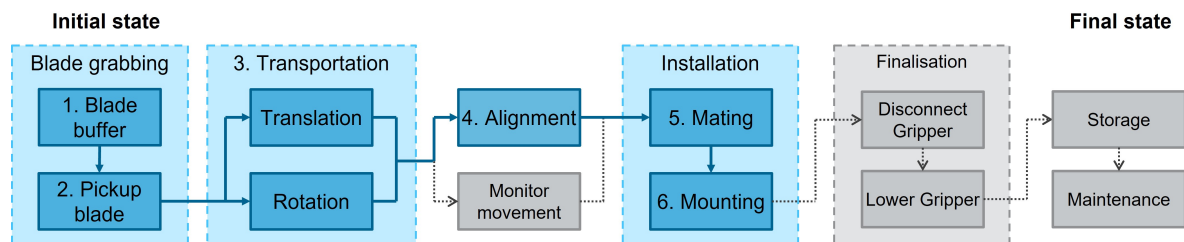


Figure 3.8: Function flowchart

3.2.2. Morphological Overview

For each numbered function in Figure 3.8, an overview has been made of possible solutions. These functions can be seen in Table 3.5. Transportation stays one function in this overview.

The location where the manipulator is attached to the system can theoretically be in four different locations: on the installation tower, on the wind turbine tower, on the nacelle, and on the deck. In practice, the manipulator cannot be placed on the deck because there is no space available. Moreover, there is no possibility for the blade installation equipment can be attached to the wind turbine, neither to the tower nor to the nacelle, given constraint 5 in Table 3.2.

1. Blade Buffer

Parts of six to eight wind turbines are carried on the deck. This means that there are 18 to 24 wind turbine blades on the deck. Storage can be done in different configurations, taking into account the way the manipulator grabs the blades. The different options are: parallel or radial storage; horizontal or vertical storage; and chord horizontal or vertical. This allows six different options. However, in Table 3.3 that describes geometric constraints, a limitation is already given. It states that the blades

may only be stored horizontally and parallel. This is also the most efficient use of deck space and has the fewest moving parts. Therefore, the options *Parallel, Horizontal, Chord Horizontal* (Option 1) and *Parallel, Horizontal, and Chord Vertical* (Option 2) are the only options in Table 3.5.

2. Pickup Blade

Table 3.2 which sums up the boundary conditions, contains constraint 4, which states that holes or other modifications to the blades are not allowed. Constraint 8 requires the use of existing blade grippers. It must be possible to operate the gripper remotely or autonomously. This means that the blades should not be fixed manually. That leaves two options: a gripper grabbing from above and a gripper grabbing from the side.

3. Transportation

Table 3.5 presents actuators as options for transportation. These types of actuators can be divided into two movements: translation and rotation. A combination of these is taken as a third option.

4. Alignment

Alignment is an important step before the mating process. Alignment and mating can be performed together as a pre connection, to prevent movement between the hub and the blade. There are then three possible methods to prevent movement:

- **Stiffness** – increase the stiffness of the entire structure;
- **Interconnection** – add an interconnection between the blade and the tower, nacelle, or hub;
- **None** – manual alignment, which is currently the most used option for installing the blade to the hub.

5. Mating

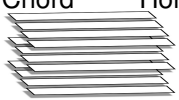
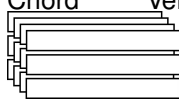


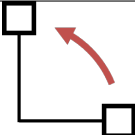

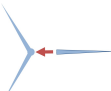

The mating can be performed in different orientations. The orientation is stated as seen from the front of the wind turbine hub. The blades can be mated to the hub horizontally, vertically, or inclined. Only horizontal installation is possible due to the clearance with the water and equipment on deck, see constraint 6 in Table 3.2.

6. Mounting

Mounting can be accomplished in various ways. Currently, manual mounting is performed as a standard operation in the industry. Autonomous or remote mounting are possibilities, but developing these solutions falls outside the scope of this study. Therefore, only manual mounting is considered.

The complete morphological overview is shown in Table 3.5.

Table 3.5: Morphological overview the different sub-functions and their solution options

| Sub-function | Option 1 | Option 2 | Option 3 |
|-------------------------------|---|--|---|
| 1 Blade Buffer | Chord Horizontal  | Chord Vertical  | |
| 2 Pickup Blade | From above [38]  | From the side [37]  | |
| 3 Blade Transportation |  Rotation |  Translation | Combination of rotation and translation |
| 4 Alignment | Stiffness | Interconnection (blade-tower, blade-nacelle, blade-hub) | None (Manual) |
| 5 Mating | Orientation Horizontal  | | |
| 6 Mounting | Manual  | | |

3.2.3. Blade Buffer and Pickup Blade

The first two sub-functions of Table 3.5 (blade buffer and pickup blade) are merged into three possible modules, which are shown in Figure 3.9. Blade Buffer option 1 (Chord Horizontal) can be combined with Pickup Blade option 2 (Grab from the side). An example is shown in Figure 3.9a. Blade Buffer option 2 (Chord Vertical) can be combined with two blade pickup options. The first combination with a vertical chord can be picked up with a gripper from above (option 1), as shown in Figure 3.9b. The blade can be picked up with a gripper from the side (option 2), as shown in Figure 3.9c.

Note that a vertical chord refers to a chord that is not horizontal, but rather reasonably angled.



Figure 3.9: Possible combinations of Blade Buffer and Pickup Blade

3.2.4. Concept 1 – Rotational Arm

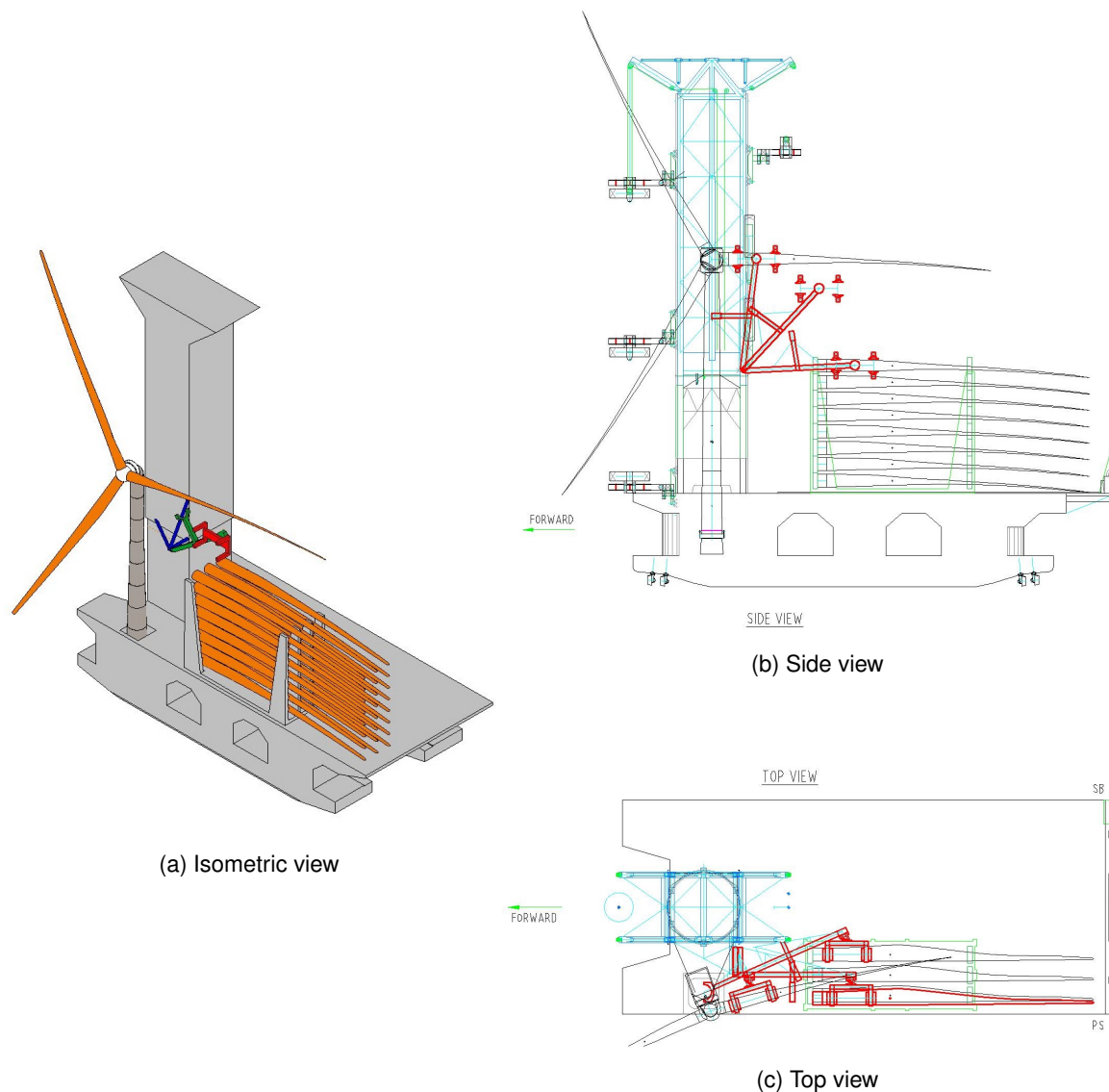


Figure 3.10: Concept 1 – Rotational arm

The first concept consists of an arm with a gripper attached to it. Figure 3.10a shows a 3D presentation of the concept and Figure 3.10b and Figure 3.10c present the more detailed 2D representation. The gripper picks up the blade from the side and a rotational movement of the arm lifts the blade to the hub height. A rotating movement is also used for the movement in the xy-plane to pick up the blades from all three places. An interconnection between the arm of the manipulator and the tower of the wind turbine is used for alignment to reduce the relative motion between the two.

The advantage of this concept is a relatively compact system with few moving parts.

The disadvantage of this concept is that this movement can only be applied when the blades to be picked up are at the top of the rack, because the reach of this rotating arm is not large enough to reach blades lower than the third level. Furthermore, there is no clearance with the blade rack and the manipulator lower than the first level. In order to ensure that the blades are at the top level of the blade rack, an additional system is required that moves the blades upwards as described in Section 3.1.

3.2.5. Concept 2 – Knuckle Boom Crane

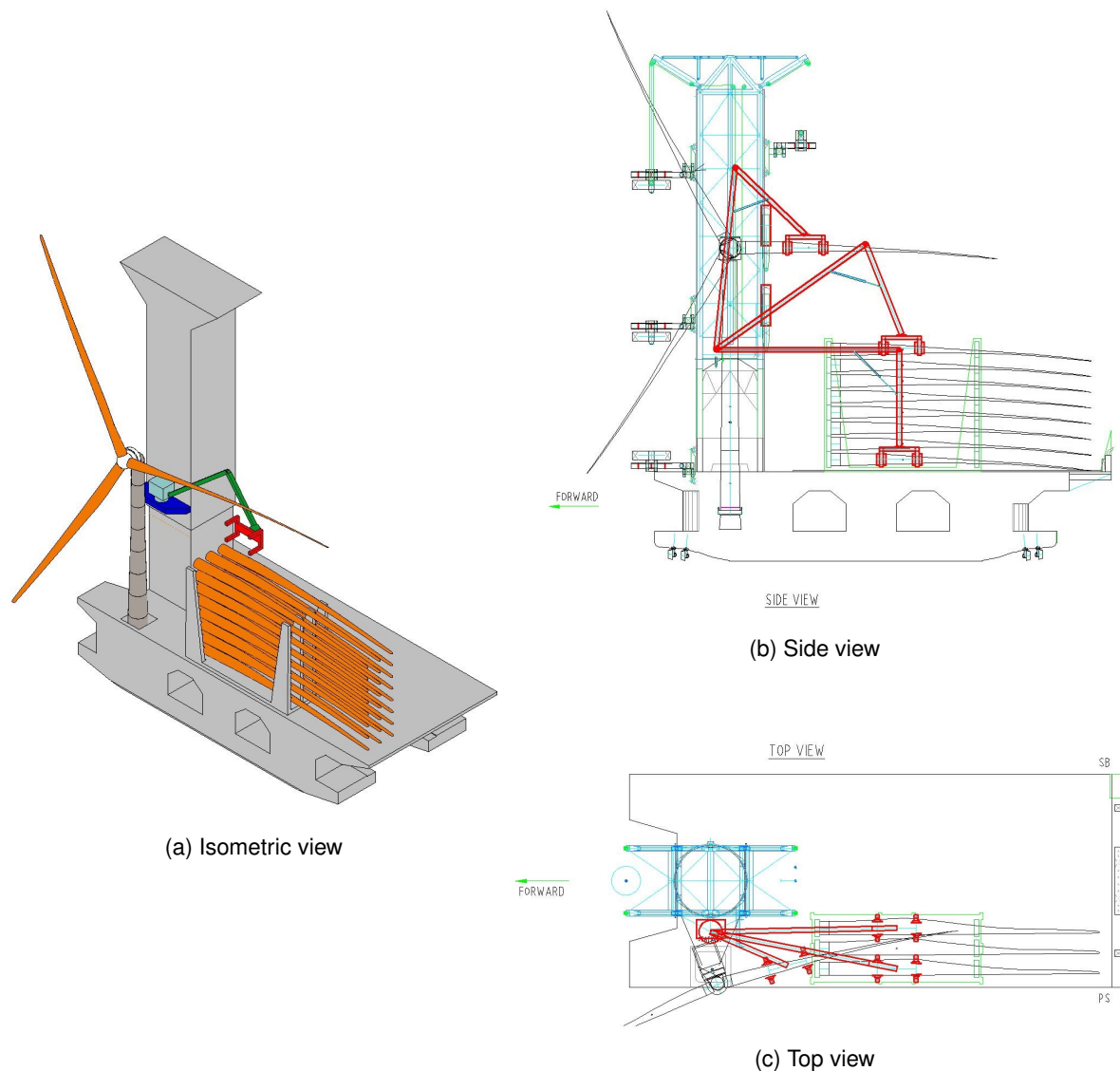


Figure 3.11: Concept 2 – Knuckle boom crane

The second concept is based on a knuckle boom crane, shown in Figure 3.11. Instead of a hook, the gripper is attached to the end of the outer boom. The gripper picks up the blade out of the rack and lifts it to hub height. There is a swing bearing at the bottom of the manipulator to ensure that the manipulator has a large working area in the xy-plane. The inner boom is approximately 80 m and the outer boom is approximately 40 m. These dimensions leave enough space between the blade rack and the manipulator for the gripper to pick up the blades anywhere in the rack.

The advantage of this concept is that the rack can be passive because the manipulator can reach all blades. No extra system needs to be added to move the blades to a specific location where they can then be picked up by the manipulator.

The disadvantage is that this design has large dimensions. The inner and outer boom must have a relatively large cross-section in order not to fail, which also makes the concept relatively heavy.

3.2.6. Concept 3 – Four-bar Linkage

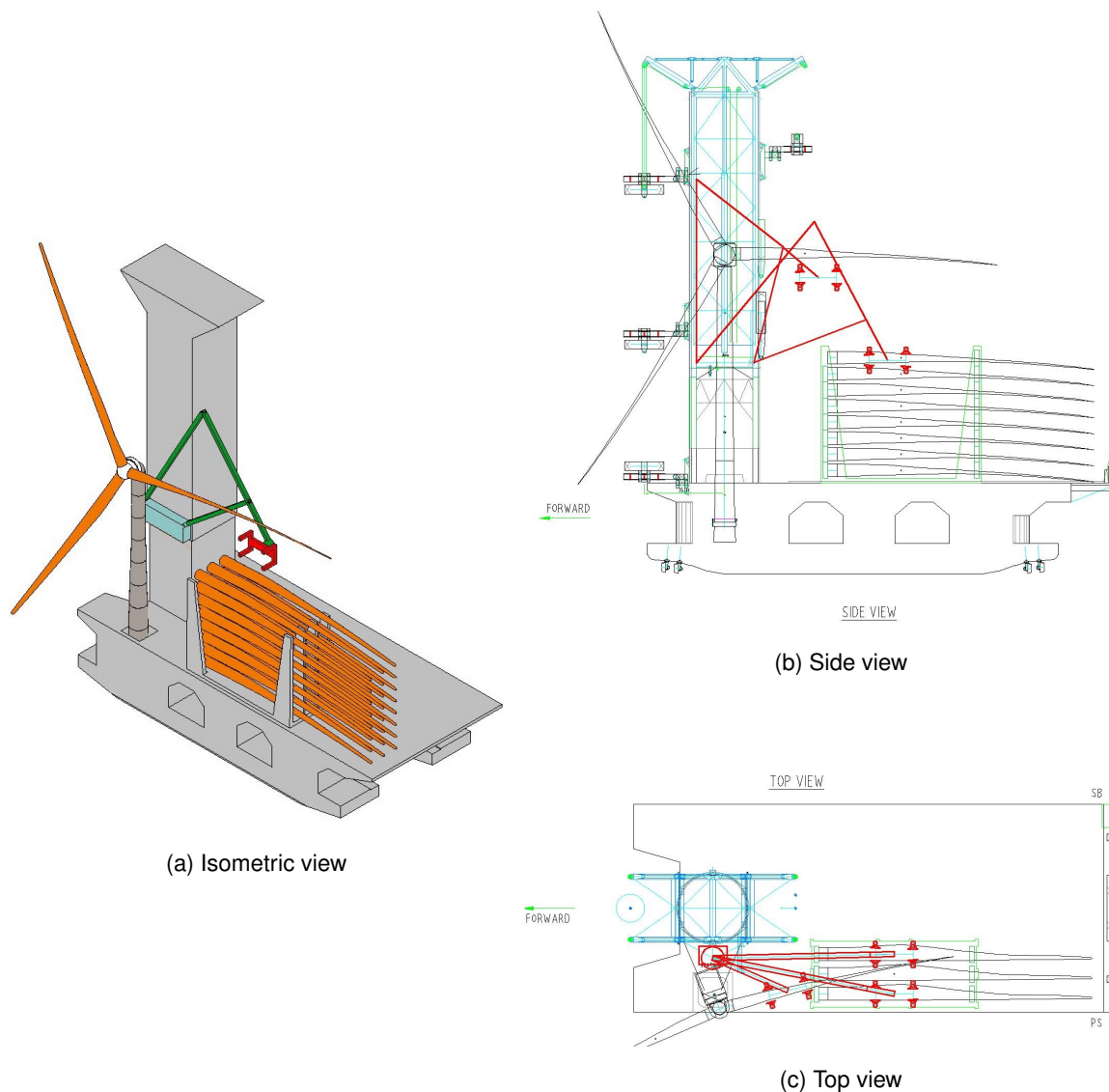


Figure 3.12: Concept 3 – Four-bar linkage

The third concept consists of a four-bar linkage, shown in Figure 3.12. The trajectory in the xz-direction is defined and optimised for this particular case. The movement in the y-direction is made possible by a slew bearing on the installation tower. The blades are picked up by the gripper from above and transported upwards along the predefined path.

The advantage of this design is that the arm always follows a predefined path. This mechanism can pick up all the blades from the rack.

The disadvantage is that the length of the arms is long, approximately 60 ± 20 m. The whole mechanism becomes heavy to create a stiff structure. Furthermore, this mechanism must be optimised before it can be used for another type of wind turbine.

3.2.7. Concept 4 – Conventional Crane

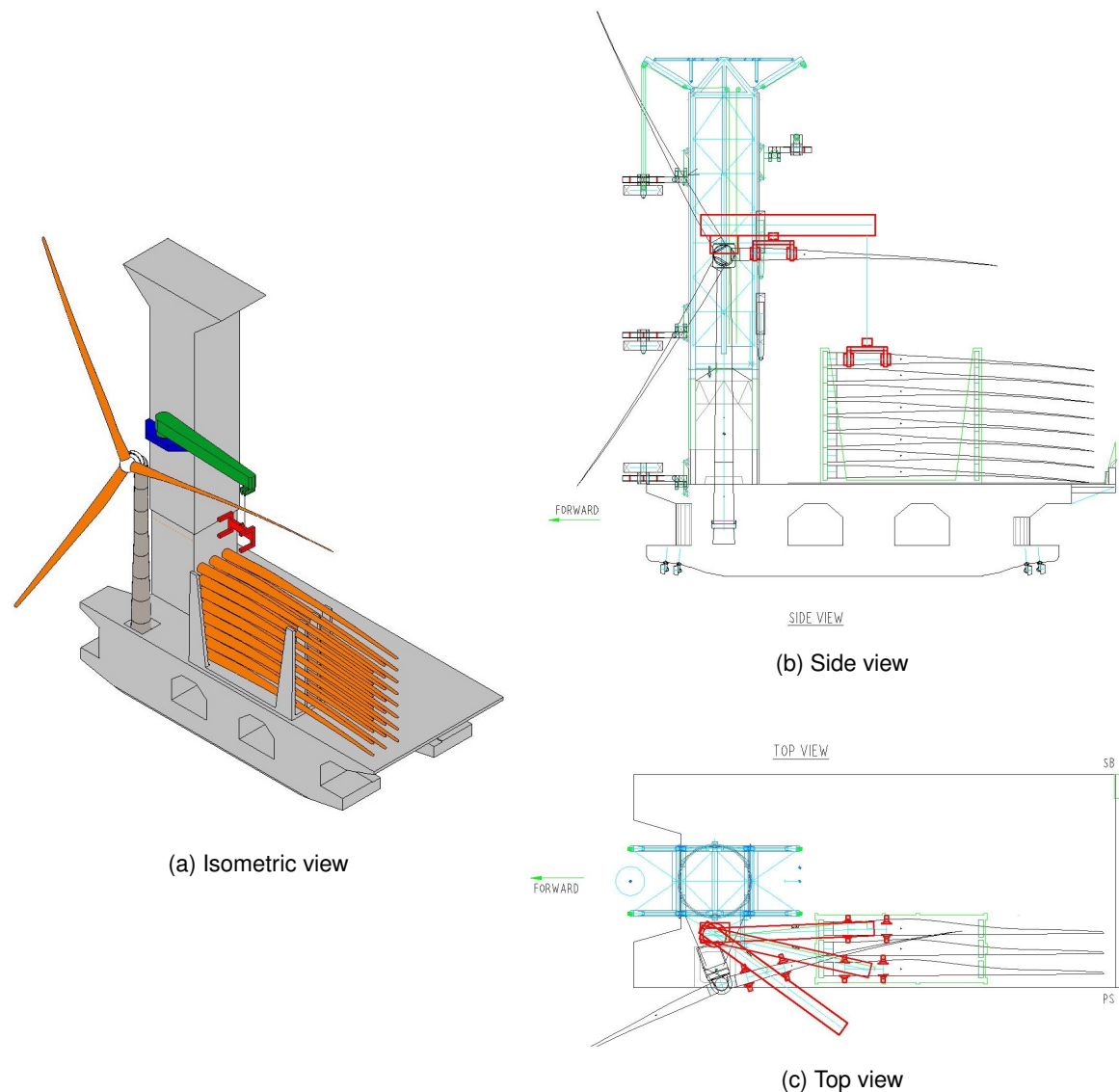


Figure 3.13: Concept 4 – Conventional crane

The fourth concept is a variation of the conventional method to install wind turbine blades. A visual representation of the concept can be seen in Figure 3.13. The crane slews to the right angle, so that the tip is exactly above the desired location. The gripper is lowered and picks up the blade. Consequently, the blade is lifted up and installed on the hub of the wind turbine.

The advantage of this concept is that an existing model can be used with minimal modifications. The gripper can reach all the blades in the blade rack.

The disadvantage of this concept is that it is sensitive to weather conditions because the gripper hangs from a wire rope. Therefore, it can only operate during ca. 2 months per year instead of the intended 85 % per year.

3.2.8. Concept 5 – Translational Arm

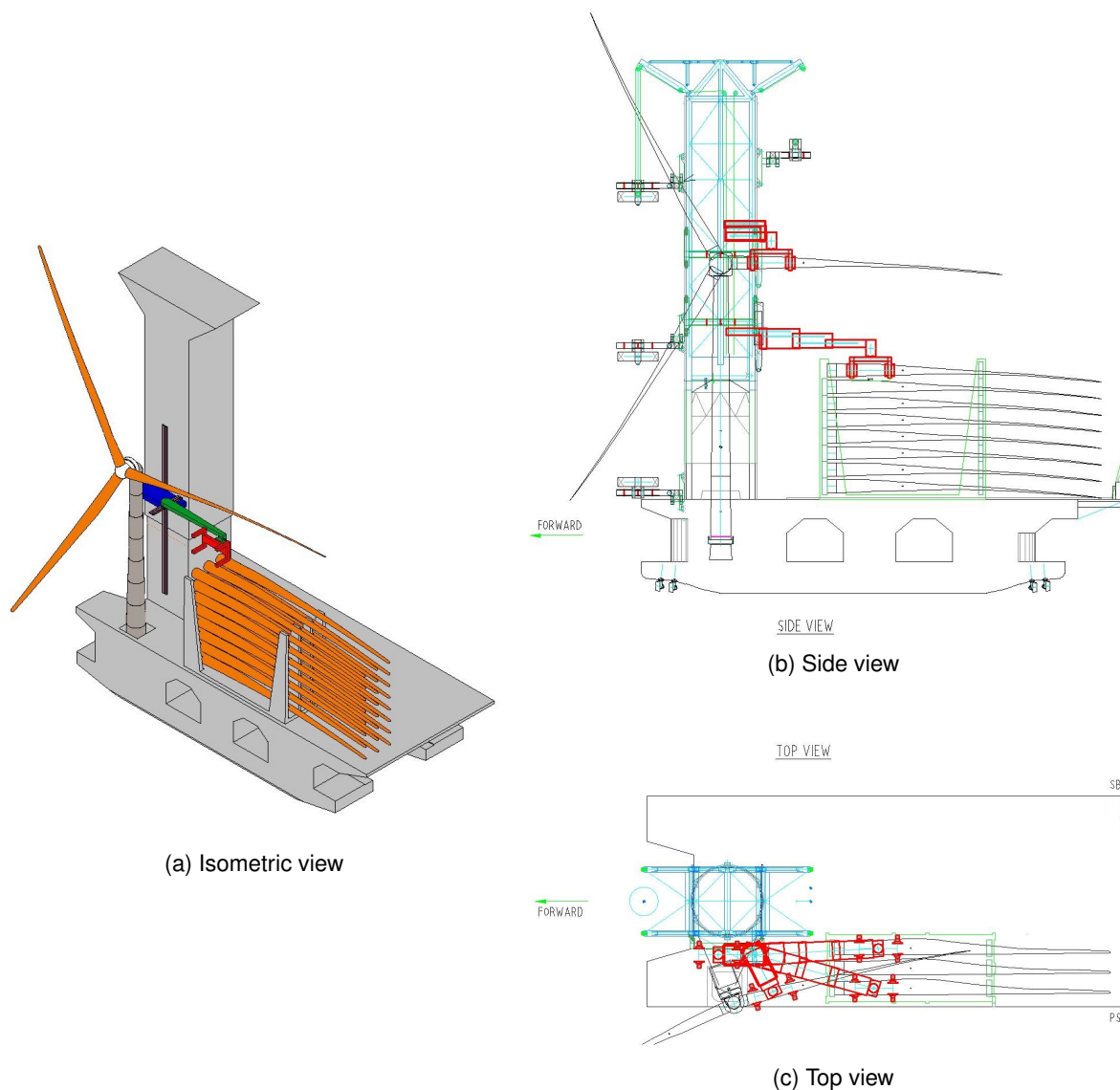


Figure 3.14: Concept 5 – Translational arm

Concept 5 is a telescopic arm, shown in Figure 3.14. To move the arm in the z-direction, a trolley with the whole arm attached to it moves over the installation tower. To ensure that the arm can reach everywhere in the xy-plane, a bearing is present in addition to the telescopic arm. At the head of the telescopic arm, there is a gripper. This gripper also has a slew bearing to ensure that the gripper is always parallel to the blade. To install a blade on the hub, the gripper picks up the blade and the trolley on the installation tower raises the manipulator. During this movement, the extending telescopic arm is retracted to bring the blade closer to the hub.

The advantage of this concept is that it is relatively easy to operate with only 4 Degree of Freedom (DoF) and that this concept is easily scalable for other sizes of wind turbines.

The disadvantages are that only the upper-level blades can be reached and that there are large forces on the linear bearings in the telescopic arm.

3.2.9. Concept 6 – Robotic Arm

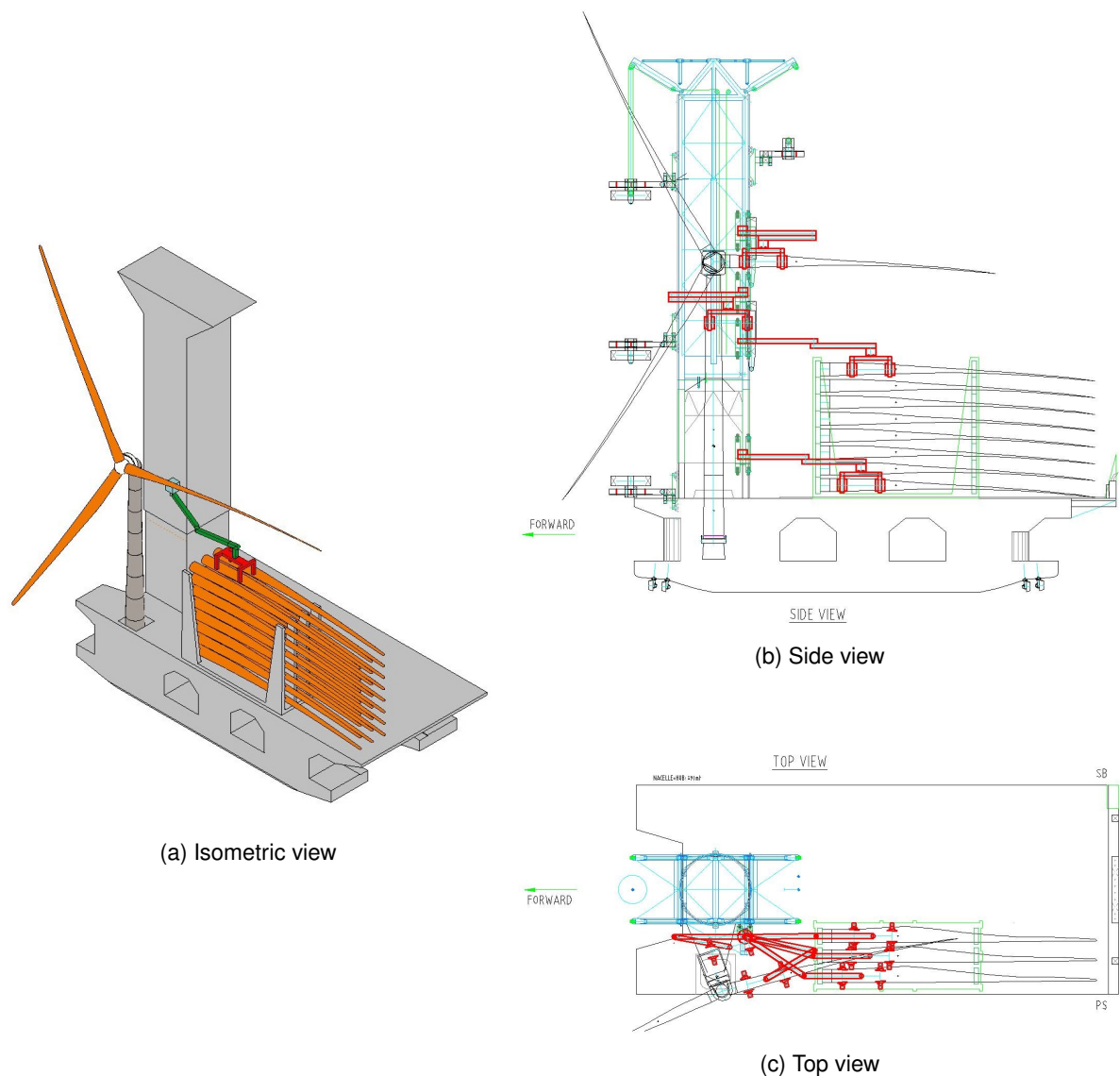


Figure 3.15: Concept 6 – Robotic arm

The sixth and final concept is a robotic arm, shown in Figure 3.15. The manipulator moves in the z-direction with a trolley. In the xy-plane, this concept moves with two arms and three pivot points, one at the installation tower, one between the two arms and one at the gripper. The latter is to assure that the gripper is always parallel to the blade. To pick up the blade, the manipulator moves to the correct z-coordinate and the second arm and the gripper are parallel to the blade. The second arm is also parallel to the blade, so that the arm can reach through the blade stretch and thus reach all the blades. After the blade is lifted out of the rack, it can be installed on the hub.

The advantages of this manipulator are that it can reach all the blades in the blade rack.

The disadvantages are that the manipulator must pass through the rack, making it less safe and less reliable.

3.3. Concept Selection

The concepts described in the previous section have not yet been realized. This makes it difficult to make a selection objectively based on criteria and their quantifications. Saaty [39] has developed a multi-criteria decision-making approach, the Analytic Hierarchy Process (AHP). With this method, difficult decisions can be made using a mathematical model where the different concepts are compared with each other using different criteria [40, 41].

To assess the previously presented concepts, eight criteria are used. These are presented in Table 3.6. First, these criteria are compared with each other to obtain the weighting factors. The scale of relative importance given to the comparison is shown in Table 3.7. This scale has a range of 1 to 9 where 1, 3, and 5 are assigned based on experience and judgement. 7 or 9 is given when one activity is significantly better than the other and has been proven in practice. 2, 4, 6, or 8 are intermediate values in case a compromise is needed.

Table 3.6: Criteria for concept selection with description

| Criterion | Description |
|-------------------------------------|--|
| 1. Ease of manufacturing | Purchase of raw materials and complexity of the manufacturing process |
| 2. Technology Readiness Level (TRL) | Type of measurement system used to assess the maturity level of a technology |
| 3. Economic feasibility | Manufacturing and operating costs of the parts needed for the mechanism |
| 4. Scalability | The capacity to use the concept for different wind turbine sizes |
| 5. Installation time | The time needed for the installation of the blade |
| 6. Reliability | Reliable performance under designated operating conditions |
| 7. Safety | The degree of human interaction and the number of moving parts |
| 8. Sustainability | The degree of sustainability of the kind and quality of materials and the drive system |

Table 3.7: Scale of relative importance [39]

| Intensity of importance | Definition | Description |
|-------------------------|---|--|
| 1 | Equal importance | Two activities contribute equally to the objective |
| 3 | Moderate importance of one over another | Experience and judgment moderately favour one activity over another |
| 5 | Essential or strong importance | Experience and judgment strongly favour one activity over another |
| 7 | Very strong importance | An activity is strongly favoured, and its dominance has been demonstrated in practice |
| 9 | Extreme importance | The evidence favouring one activity over another is of the highest possible order of affirmation |
| 2,4,6,8 | Intermediate values | When compromise is needed |

With the scale of relative importance, given in Table 3.7, a comparison between the different criteria can be made. This comparison is presented in Table 3.8. The ($n \times n$) judgement matrix shows that when, for example, technical feasibility is compared with economic feasibility, this scores a 5. This means that technical feasibility is more important than economic feasibility. Looking at the comparison between technical feasibility and safety, technical feasibility is less important than the safety and thus scores only 1/3. When technical feasibility is compared with itself, it scores a 1. If the first criterion is assigned one of the above numbers compared to another criterion, then the other criterion has the

reciprocal value compared to the first criterion.

With the complete judgement matrix, all criteria can be compared, and the eigenvector and eigenvalue can be calculated. By normalizing the eigenvector, the priority vector can be calculated, which is the last column in Table 3.8. The sum of the values in this column equals 1. In the case of the comparison between the different criteria in Table 3.8, the priority vector is equal to the weight factor that is used at the end of the selection process. When comparing the different concepts per single criterion this is not the case. It can be seen that the criterion *Safety* has the highest score and is, therefore, the most important criterion, followed by *Installation time* and *Economic feasibility*.

Table 3.8: Judgement matrix

| | Ease of manufacturing | TRL | Economic feasibility | Scalability | Installation time | Reliability | Safety | Sustainability | Priority Vector/ Weight factor |
|-----------------------|-----------------------|-----|----------------------|-------------|-------------------|-------------|--------|----------------|-----------------------------------|
| Ease of manufacturing | 1 | 3 | 1/3 | 3 | 1/5 | 1/3 | 1/5 | 3 | 0.072 |
| TRL | 1/3 | 1 | 1/3 | 3 | 1/5 | 1/3 | 1/5 | 3 | 0.054 |
| Economic feasibility | 3 | 3 | 1 | 3 | 1/3 | 3 | 1/3 | 5 | 0.147 |
| Scalability | 1/3 | 1/3 | 1/3 | 1 | 1/5 | 1/3 | 1/5 | 3 | 0.041 |
| Installation time | 5 | 5 | 3 | 5 | 1 | 3 | 1/3 | 5 | 0.236 |
| Reliability | 3 | 3 | 1/3 | 3 | 1/3 | 1 | 1/3 | 5 | 0.111 |
| Safety | 5 | 5 | 3 | 5 | 3 | 3 | 1 | 5 | 0.312 |
| Sustainability | 1/3 | 1/3 | 1/5 | 1/3 | 1/5 | 1/5 | 1/5 | 1 | 0.028 |

To check whether the judgement matrix is consistent, the Consistency Ratio (*CR*) is used. When the *CR* is less than 10 % the matrix is considered to be adequately consistent. To calculate the consistency ratio, the Consistency Index (*CI*) must first be calculated. This is done by taking the principal eigenvalue of the judgment matrix (λ_{max}), subtracting *n*, and dividing it by *n*-1; as shown in Equation 3.1. In the case of the judgement matrix of the different criteria shown in Table 3.8, $\lambda_{max} = 8.819$ and *n* = 8. This results in a *CI* of 0.117, as shown in Equations 3.1 and 3.2.

$$CI = \frac{\lambda_{max} - n}{n - 1} \quad (3.1)$$

$$CI = \frac{8.819 - 8}{8 - 1} = 0.117 \quad (3.2)$$

Next, the value obtained in Equation 3.1 is divided by the predefined Random Consistency Index (*RCI*), which can be found in Table 3.9, to obtain the *CR*. The value of *n* is 8 in the case of the judgement matrix presented in Table 3.8. This results in an *RCI* of 1.41. Filling in Equation 3.3 with these values results in a *CR* of 0.083, as shown in Equation 3.4. Thus, the judgement matrix is considered consistent.

Table 3.9: Random Consistency Index values for different values of *n* [41]

| n | 1 | 2 | 3 | 4 | 5 | 6 | 7 | 8 | 9 |
|------------|---|---|------|------|------|------|------|------|------|
| <i>RCI</i> | 0 | 0 | 0.58 | 0.90 | 1.12 | 1.24 | 1.32 | 1.41 | 1.45 |

$$CR = \frac{CI}{RCI(n)} \quad (3.3)$$

$$CR = \frac{0.117}{1.41} = 0.083 \quad (3.4)$$

In Tables 3.10 to 3.17 the judgement matrices are given per criterion for the 6 different concepts. For each of these matrices, the priority vector, eigenvalue, consistency index and consistency ratio are calculated. To calculate the consistency index and the consistency ratio, an n of 6 is used, because 6 concepts are compared with each other and therefore 6x6 matrices are created. Furthermore, since n is 6 an RCI of 1.24 is used, as in Table 3.9.

Criterion 1 – Ease of manufacturing

When looking at ease of manufacturing, we look at the material from which the final product is made and how easy the manufacturing process is. Concept 4, conventional crane, is the easiest to manufacture in this respect because it is a variation of a conventional concept and therefore many parts are already available. Concept 1, the rotational arm, is also relatively easy to construct because it is only one arm with actuators. Concept 2, knuckle boom crane, is a type of crane that is already on the market. However, it must be enlarged and adapted for this application, which makes it less easy to manufacture than concepts 1 and 4. Concept 3, four-bar linkage, is more difficult to build than the above concepts, because more parts have to be manufactured and fit together. Concepts 5 and 6 are relatively difficult to manufacture because there are many moving parts and they have to fit together.

Table 3.10: Criterion 1 – Ease of manufacturing

| | C1 | C2 | C3 | C4 | C5 | C6 | Priority Vector |
|-------------------------------|-----|-----|-----|-----|----|-----|-----------------|
| C1: Rotational arm | 1 | 3 | 5 | 1/3 | 5 | 3 | 0.258 |
| C2: Knuckle boom crane | 1/3 | 1 | 3 | 1/3 | 3 | 3 | 0.147 |
| C3: Four-bar linkage | 1/5 | 1/3 | 1 | 1/5 | 3 | 3 | 0.091 |
| C4: Conventional crane | 3 | 3 | 5 | 1 | 5 | 5 | 0.397 |
| C5: Translational arm | 1/5 | 1/3 | 1/3 | 1/5 | 1 | 1/3 | 0.042 |
| C6: Robotic arm | 1/3 | 1/3 | 1/3 | 1/5 | 3 | 1 | 0.066 |

Table 3.10 shows the scores linked to the concepts based on the criterion *Ease of manufacturing*. The eigenvalue λ_{max} is 6.56, which results in a CI of 0.112 and a CR of **0.09**, using Equations 3.1 and 3.3. CR is less than 10 % which means that this matrix is considered to be adequately consistent.

Criterion 2 – Technology Readiness Level

TRL rates technologies on their maturity. Conventional crane, concept 4, is already being used for this application. However, the aim is to handle larger wind turbine blades over a longer period of time per year, with more extreme weather conditions. This means that this method is not technically feasible. Concepts 2 and 5 are methods that are already used to handle objects. However, these methods are not applied at the desired scale. To make these methods possible, they have to be scaled up considerably, which involves scaling internal forces. The translational arm, concept 5, is a proven technique, which could be used for this system. It is important that the dimensions are optimised so that the path that the gripper travels is optimal.

In the case of concepts 1 and 5, an extra system is needed to lift the blades into the top position in the rack.

Table 3.11: Criterion 2 – Technology Readiness Level (TRL)

| | C1 | C2 | C3 | C4 | C5 | C6 | Priority Vector |
|-------------------------------|----|-----|-----|-----|-----|-----|-----------------|
| C1: Rotational arm | 1 | 1/7 | 1/7 | 1/5 | 1/7 | 1/5 | 0.030 |
| C2: Knuckle boom crane | 7 | 1 | 3 | 1/3 | 1 | 3 | 0.205 |
| C3: Four-bar linkage | 7 | 1/3 | 1 | 1/3 | 1/2 | 2 | 0.120 |
| C4: Conventional crane | 5 | 3 | 3 | 1 | 3 | 5 | 0.381 |
| C5: Translational arm | 7 | 1 | 2 | 1/3 | 1 | 3 | 0.187 |
| C6: Robotic arm | 5 | 1/3 | 1/2 | 1/5 | 1/3 | 1 | 0.077 |

The eigenvalue λ_{max} is 6.44, which results in a CI of 0.08 and a CR of **0.07**. CR is less than 10 % which means that this matrix is considered to be adequately consistent.

Criterion 3 – Economic feasibility

The cost of a product is primarily linked to its weight: the heavier a product the more material costs. These are the sunk costs that are spent once for the product. In addition to the material costs, the longer the installation time, the more expensive the process. These are the usage costs. To simplify the comparison of the concepts, estimated sunk costs are only considered in this analysis. This comparison matrix is simply a direct comparison of the weight of the concepts. The weight is estimated by the size and required stiffness of the components. Large constructions and long stiff arms are heavier to achieve a functional design. Installation time is separately considered as criterion 5.

Table 3.12: Criterion 3 – Economic feasibility

| | C1 | C2 | C3 | C4 | C5 | C6 | Priority Vector |
|-------------------------------|-----|-----|-----|-----|----|-----|-----------------|
| C1: Rotational arm | 1 | 5 | 5 | 3 | 5 | 3 | 0.413 |
| C2: Knuckle boom crane | 1/5 | 1 | 3 | 1/3 | 3 | 1 | 0.115 |
| C3: Four-bar linkage | 1/5 | 1/3 | 1 | 1/5 | 3 | 1 | 0.074 |
| C4: Conventional crane | 1/3 | 3 | 5 | 1 | 5 | 3 | 0.254 |
| C5: Translational arm | 1/5 | 1/3 | 1/3 | 1/5 | 1 | 1/3 | 0.043 |
| C6: Robotic arm | 1/3 | 1 | 1 | 1/3 | 3 | 1 | 0.100 |

The eigenvalue λ_{max} is 6.38, which results in a *CI* of 0.08 and a *CR* of **0.06**. *CR* is not higher than 10 % which means that this matrix is considered to be adequately consistent.

Criterion 4 – Scalability

The prospect is to install wind turbines with a power output of up to 20 MW. At present, wind turbines are mostly installed between 10 and 15 MW. This means that it is useful if the manipulator is easily scalable to handle other wind turbine blades than the IEA 15 MW blades. Concept 1, the rotational arm, can easily be used for larger and smaller wind turbines because of the slider present on the arm. Concept 5, the translational arm, can also be scaled for the same reason. Concept 2, knuckle boom crane, and concept 4, conventional crane, also do not require any modifications due to their design to accommodate other sizes of wind turbine blades. Concept 3, four-bar linkage, and concept 6, robotic arm, need to be adapted for other sizes. These, therefore, score lower than the rest.

Table 3.13: Criterion 4 – Scalability

| | C1 | C2 | C3 | C4 | C5 | C6 | Priority Vector |
|-------------------------------|-----|-----|----|-----|-----|-----|-----------------|
| C1: Rotational arm | 1 | 1/2 | 5 | 1/3 | 1/3 | 3 | 0.117 |
| C2: Knuckle boom crane | 2 | 1 | 5 | 1/3 | 3 | 3 | 0.228 |
| C3: Four-bar linkage | 1/5 | 1/5 | 1 | 1/7 | 1/5 | 1/2 | 0.034 |
| C4: Conventional crane | 3 | 3 | 7 | 1 | 3 | 5 | 0.384 |
| C5: Translational arm | 3 | 1/3 | 5 | 1/3 | 1 | 5 | 0.183 |
| C6: Robotic arm | 1/3 | 1/3 | 2 | 1/5 | 1/5 | 1 | 0.054 |

The eigenvalue λ_{max} is 6.46, which results in a *CI* of 0.09 and a *CR* of **0.07**. *CR* is less than 10 % which means that this matrix is considered to be adequately consistent.

Criterion 5 – Installation time

The installation time has already been mentioned in Criterion 3, economic feasibility. However, this is an important selection criterion and is therefore assessed independently. For the installation time, the time is taken into account from the moment the manipulator moves downwards to pick up the blade from the blade rack until the point that the blade has been installed on the hub and the gripper has released the blade. Parallel activities are quicker when looking at the installation time. This means that concept 1, rotational arm, and concept 5, translational arm, are quicker than the other concepts. This is because the process of moving the blade upwards in the rack is simultaneous with picking up the upper blade and installing it on the hub. If the manipulator itself has to pick up all the blades and also has to pick up the lower blades in the blade rack, this takes longer. In this case, the manipulator must move more carefully to prevent critical events, which means that this process takes longer. This

applies to concepts 2, 3, 4 and 6. Concept 6, the robotic arm, has the additional difficulty that the manipulator does not approach the blade rack from above but from the root side, which takes more time. Concept 4, a conventional crane, takes the longest time of all concepts, because this concept is most dependent on weather conditions due to the gripper hanging on a cable. Therefore, this concept cannot be used for a large part of the year.

Table 3.14: Criterion 5 – Installation time

| | C1 | C2 | C3 | C4 | C5 | C6 | Priority Vector |
|-------------------------------|-----------|-----------|-----------|-----------|-----------|-----------|------------------------|
| C1: Rotational arm | 1 | 3 | 5 | 7 | 2 | 5 | 0.375 |
| C2: Knuckle boom crane | 1/3 | 1 | 2 | 5 | 1/3 | 3 | 0.139 |
| C3: Four-bar linkage | 1/5 | 1/2 | 1 | 5 | 1/5 | 3 | 0.099 |
| C4: Conventional crane | 1/7 | 1/5 | 1/5 | 1 | 1/7 | 1/3 | 0.030 |
| C5: Translational arm | 1/2 | 3 | 5 | 7 | 1 | 5 | 0.299 |
| C6: Robotic arm | 1/5 | 1/3 | 1/3 | 3 | 1/5 | 1 | 0.057 |

The eigenvalue λ_{max} is 6.35, which results in a *CI* of 0.07 and a *CR* of **0.06**. *CR* is less than 10 % which means that this matrix is considered to be adequately consistent.

Criterion 6 – Reliability

Under stated operational conditions, no critical event is intended to occur. Concept 4, a conventional crane, is the most likely to fail. As described under criterion 5, installation time, in the literature [21], this concept is susceptible to weather influences. If the gripper is hanging on a cable the gripper moves when there is more wind than 10 m/s. This can cause the gripper and the blade to collide with other objects on the vessel, which can lead to a critical event. Therefore, concept 4 scores the lowest. Concept 6, the robotic arm, must be lowered through the rack with the long arm at the blade root. This manoeuvre must be done precisely to ensure that no critical events take place. Therefore this concept also scores low on reliability. Concept 2, knuckle boom crane and concept 3, four-bar linkage, must reach all the way to the bottom of the blade rack to pick up blades, this must be done with precision to prevent failure. Concept 1, the rotational arm and concept 5, the translational arm, are reliable systems. Both systems are the most reliable of all systems because they can fail the least.

Table 3.15: Criterion 6 – Reliability

| | C1 | C2 | C3 | C4 | C5 | C6 | Priority Vector |
|-------------------------------|-----------|-----------|-----------|-----------|-----------|-----------|------------------------|
| C1: Rotational arm | 1 | 3 | 3 | 5 | 1/3 | 3 | 0.244 |
| C2: Knuckle boom crane | 1/3 | 1 | 3 | 5 | 1/3 | 3 | 0.167 |
| C3: Four-bar linkage | 1/3 | 1/3 | 1 | 3 | 1/3 | 3 | 0.106 |
| C4: Conventional crane | 1/5 | 1/5 | 1/3 | 1 | 1/5 | 1/3 | 0.039 |
| C5: Translational arm | 3 | 3 | 3 | 5 | 1 | 5 | 0.378 |
| C6: Robotic arm | 1/3 | 1/3 | 1/3 | 3 | 1/5 | 1 | 0.066 |

The eigenvalue λ_{max} is 6.50 which results in a *CI* of 0.10 and a *CR* of **0.08**. *CR* is less than 10 % which means that this matrix is considered to be adequately consistent.

Criterion 7 – Safety

Safety looks at the amount of human interaction and the number of moving parts. In addition, the safety of the process on the entire vessel is evaluated. Concept 4, a conventional crane, and concept 6, robotic arm, are unsafe. Concept 4, conventional crane is subject to movement due to weather conditions. This is especially dangerous during the mating of the blade root with the hub. During this part of the process, people are present in the hub to guide the blade into the hub and then to mount the blade onto the hub. If a critical event occurs here, it can have far-reaching consequences. When the manipulator goes all the way down into the blade rack to pick up blades, this is dangerous because extreme failures can occur in the form of collisions. This is why concept 6, the robotic arm, is also dangerous; it moves down along the root side of the blade rack. Concept 2, knuckle boom crane and concept 3, four-bar linkage, equal each other in terms of safety. Concept 1, the rotational arm, and

concept 5, the translational arm are also safe. It is assumed that concepts 2 and 3 are safer than concept 1 because of the system which must be in place to bring the blades up in concept 1.

Table 3.16: Criterion 7 – Safety

| | C1 | C2 | C3 | C4 | C5 | C6 | Priority Vector |
|-------------------------------|-----------|-----------|-----------|-----------|-----------|-----------|------------------------|
| C1: Rotational arm | 1 | 3 | 3 | 5 | 3 | 3 | 0.369 |
| C2: Knuckle boom crane | 1/3 | 1 | 1 | 3 | 3 | 3 | 0.189 |
| C3: Four-bar linkage | 1/3 | 1 | 1 | 3 | 3 | 5 | 0.205 |
| C4: Conventional crane | 1/5 | 1/3 | 1/3 | 1 | 1/3 | 3 | 0.072 |
| C5: Translational arm | 1/3 | 1/3 | 1/3 | 3 | 1 | 3 | 0.114 |
| C6: Robotic arm | 1/3 | 1/3 | 1/5 | 1/3 | 1/3 | 1 | 0.052 |

The eigenvalue λ_{max} is 6.53 which results in a *CI* of 0.11 and a *CR* of **0.08**. *CR* is less than 10 % which means that this matrix is considered to be adequately consistent.

Criterion 8 – Sustainability

Sustainability is the last criterion on which the concepts are compared. Emissions, materials used and ways of recovering energy are considered. Electric is better than hydraulic or a diesel generator. The type of material is almost the same for each design: steel. However, it is more sustainable to use less material. So, the lighter the design, the better. Concepts 1, 2, and 3 mainly use hydraulic actuators. Concepts 4, 5, and 6 mainly use electrical components. In addition, concepts 1 and 4 perform better in terms of weight than concepts 2, 3, 5, and 6. When these considerations are taken together, the outcome is that concepts 1, 4, 5, and 6 are the best in terms of sustainability.

Table 3.17: Criterion 8 – Sustainability

| | C1 | C2 | C3 | C4 | C5 | C6 | Priority Vector |
|-------------------------------|-----------|-----------|-----------|-----------|-----------|-----------|------------------------|
| C1: Rotational arm | 1 | 3 | 5 | 1/3 | 1 | 1/2 | 0.148 |
| C2: Knuckle boom crane | 1/3 | 1 | 3 | 1/5 | 1/2 | 1/3 | 0.072 |
| C3: Four-bar linkage | 1/5 | 1/3 | 1 | 1/5 | 1/3 | 1/5 | 0.041 |
| C4: Conventional crane | 3 | 5 | 5 | 1 | 4 | 3 | 0.403 |
| C5: Translational arm | 1 | 2 | 3 | 1/4 | 1 | 1/3 | 0.112 |
| C6: Robotic arm | 2 | 3 | 5 | 1/3 | 3 | 1 | 0.224 |

The eigenvalue λ_{max} is 6.29 which results in a *CI* of 0.06 and a *CR* of **0.05**. *CR* is less than 10 % which means that this matrix is considered to be adequately consistent.

Concept selection Results

After all concepts have been weighed against all criteria, a result can be calculated. This is done by putting all priority vectors in a matrix as done in Table 3.18. Then all columns of this matrix are multiplied with the transposed of the weight factors. When all the values per concept are added up, the final score is obtained. Concept 1, the rotational arm is the most feasible option.

Table 3.18: Local and global priority vectors

| | Crit.1 | Crit.2 | Crit.3 | Crit.4 | Crit.5 | Crit.6 | Crit.7 | Crit.8 | Score |
|-------------------------------|---------------|---------------|---------------|---------------|---------------|---------------|---------------|---------------|--------------|
| <i>Weight factor</i> | 0.072 | 0.054 | 0.147 | 0.041 | 0.236 | 0.111 | 0.312 | 0.028 | |
| C1: Rotational arm | 0.258 | 0.030 | 0.413 | 0.117 | 0.375 | 0.244 | 0.369 | 0.148 | 0.320 |
| C2: Knuckle boom crane | 0.147 | 0.205 | 0.115 | 0.228 | 0.139 | 0.167 | 0.189 | 0.072 | 0.160 |
| C3: Four-bar linkage | 0.091 | 0.120 | 0.074 | 0.034 | 0.099 | 0.106 | 0.205 | 0.041 | 0.125 |
| C4: Conventional crane | 0.397 | 0.381 | 0.254 | 0.384 | 0.030 | 0.039 | 0.072 | 0.403 | 0.147 |
| C5: Translational arm | 0.042 | 0.187 | 0.043 | 0.183 | 0.299 | 0.378 | 0.114 | 0.112 | 0.178 |
| C6: Robotic arm | 0.066 | 0.077 | 0.100 | 0.054 | 0.057 | 0.066 | 0.052 | 0.224 | 0.069 |

3.4. Conclusion

The VDI 2221 guideline is used for the systematic development of concepts. There are a number of boundary conditions that each concept must meet.

The blade manipulator should be installed on top of the installation tower, above the swing bearing. The manipulator has a working area between the blade rack on the deck and station 3 of the WIV. The rotation of the installation tower on the WIV requires clearance to prevent the protruding material from colliding with the wind turbine. The blade must be installed horizontally on the hub of the wind turbine. The blades of the wind turbine are stored in a blade rack on the deck of the WIV. This rack is adapted so that the manipulator has access to the blades.

Using a morphological overview with several sub-functions, six different concepts were created. Using the analytic hierarchy process together with the weight factors, the results of the concept selection can be calculated. The results of the concept selection are shown in Table 3.19, together with the resulting ranking. Concept 1 is the most feasible option.

Table 3.19: Results

| Rank | Concept | Score |
|------|------------------------|-------|
| 1 | C1: Rotational arm | 0.320 |
| 2 | C5: Translational arm | 0.178 |
| 3 | C2: Knuckle boom crane | 0.160 |
| 4 | C4: Conventional crane | 0.147 |
| 5 | C3: Four-bar linkage | 0.125 |
| 6 | C6: Robotic arm | 0.069 |

4

Final Concept

This chapter presents the functional design of the final concept: the rotational arm and thus answers the third sub-question: *What is the best mechanical design for the selected method?* First, the final design is presented with the dimensions and the material used, and then the functioning of this concept is explained. The reasoning behind the drive systems is given subsequently, followed by the steel structure and the interfaces of all the sub-parts.

4.1. Functional Design

The purpose of the manipulator, see Figure 4.1b, is to transport a blade from the blade rack to the hub of the wind turbine.

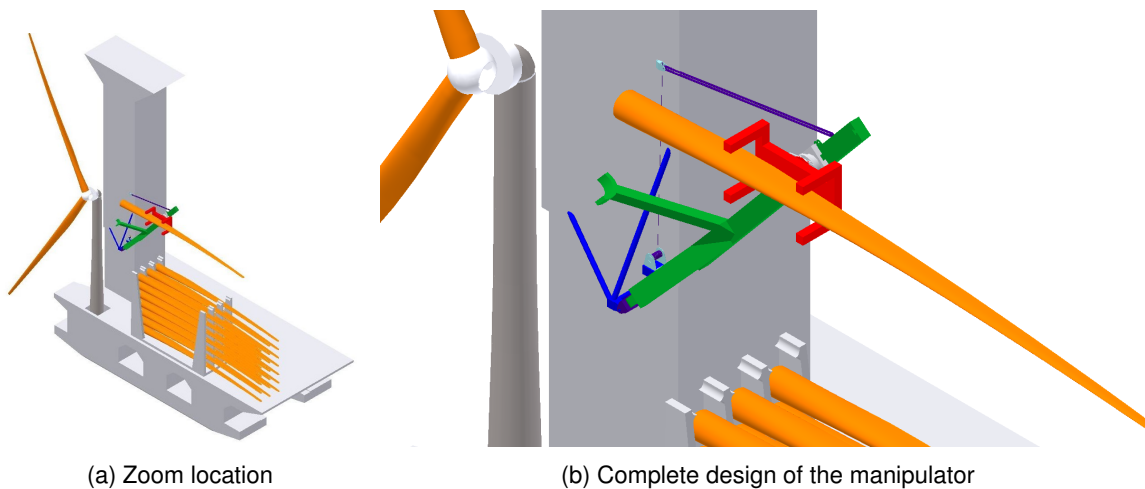


Figure 4.1: General layout

The blade rack has to be adapted to make this possible. The top part of the blade rack on the top level must be removed so that there is enough clearance for the manipulator, see Figure 4.2. Furthermore, a mechanism must be added to the blade rack to ensure that the blades are always at the top level for the manipulator to pick up. Examples for this mechanism are described in Subsection 3.1.3 and are not further elaborated on in this report, because it is beyond the scope of the project.

The blades are stacked in the blade rack horizontal and parallel. The blades lie with the chord horizontally so that the blade rack with the blades is subjected to as little wind load as possible. Therefore, the blades are picked up from the side instead of from the top.

The gripper lifts the blade from the blade rack around the CoG of the blade. Consequently, the gripper slides over a distance towards the pivot point to obtain the correct radius for installation. After this, the manipulator moves upwards by means of a rotating movement, after which the blade can be installed on the hub of the wind turbine, see Figure 4.3.

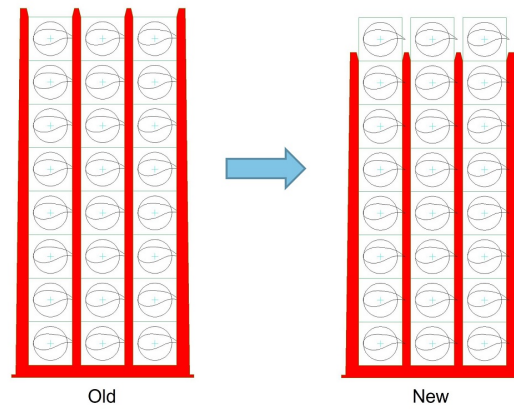


Figure 4.2: New blade rack size, the blade supports at the top level have been removed

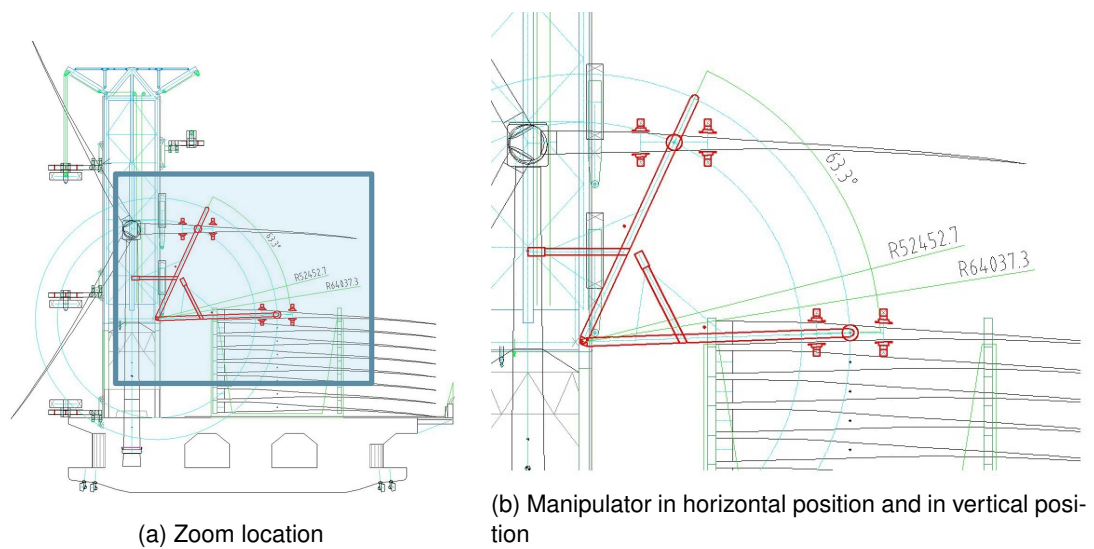


Figure 4.3: Overview of manipulator movement

When the arm of the manipulator is in a horizontal position to grab a blade from the blade rack, there are three positions the gripper should be able to reach, see Figure 4.4. Further, the gripper comes from the side to pick up the blade. A hydraulic cylinder and a hinge point provide a rotational movement to reach these locations.

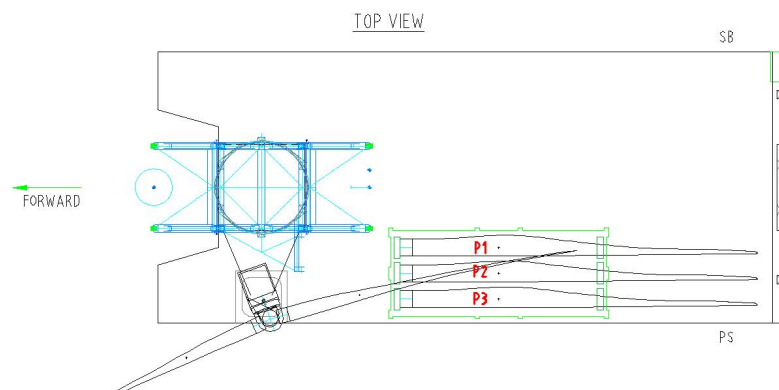


Figure 4.4: Locations (P1, P2, and P3) shown in red of the blade the gripper must be able to reach

To keep the gripper horizontal in any circumstance, a slew bearing is used. To ensure that the gripper can tilt, cylinders are used. For the sliding movement along the arm of the manipulator, a slider with a hydraulic cylinder is used. A winch with a wire rope is used to lift the manipulator. The winch is fixed approx. 60 m above the rotation point of the manipulator and the wire rope is connected to the arm of the manipulator around the location of the gripper. An overview of the manipulator can be seen in Figure 4.5. The actuators are indicated in the figure, as well as the horizontal and vertical position.

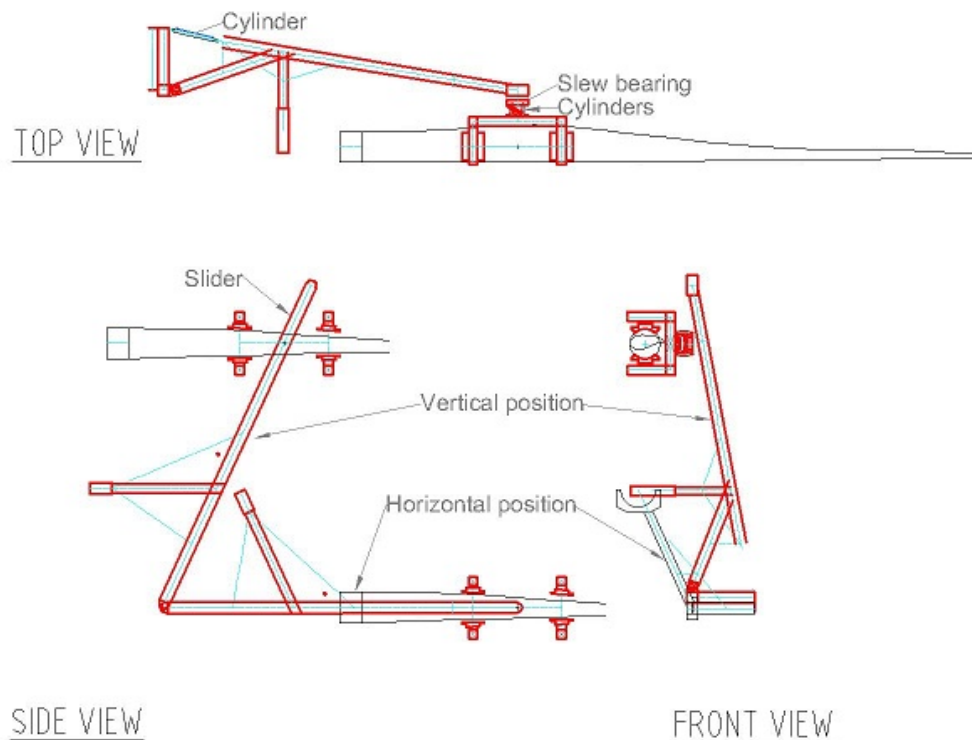


Figure 4.5: Drawing manipulator

4.2. Material

The material used for the manipulator is ST52-3N-Plate. Table 4.1 shows the properties of ST52-3N-Plate. It is a strong type of steel that is suitable for this construction. This type of steel requires a thicker structure than other types of steel with higher yield strength, such as S690. However, a thicker and heavier structure is stiffer and has less deflection.

Table 4.1: Material properties ST52-3N-Plate

| Description | Value |
|---------------------------------|-------------------------|
| Tensile strength (UTS) | 510 N/mm^2 |
| Yield strength (σ_y) | 355 N/mm^2 |
| Poisson ratio (ν) | 0.29 |
| Mass density (ρ_{steel}) | 7.85 g/cm^3 |
| Young's modulus (E) | 210000 N/mm^2 |
| Shear modulus (G) | 82 GPa |

4.3. Load Factor

The load factor (LF) must be determined before the loads on the manipulator can be calculated. The forces are multiplied by this load factor. The offshore standard DNVGL-OS-C101 for the design of offshore steel structures is used for this purpose and states a load factor of **1.2** may be used since the permanent loads and the variable functional loads are well defined [42].

4.4. Load Cases

To determine the structure of the blade manipulator, several load cases must be evaluated. The load cases are listed below:

LC1 – Manipulator Horizontal Picking up blades is the first event to take place. The manipulator picks up the blade from the blade rack. The manipulator boom is in horizontal orientation.

LC2 – Slided Blade The blade is moved slightly inwards over the boom of the manipulator. This case looks at the state after this translation. There are reaction forces in the support and in the winch.

LC3 – Lifting Blade Full/ Blade Installation at the Hub In this load case, the manipulator is vertical and the blade is at hub height.

LC4 – Empty Lifting This is the case when the manipulator is lowered after the blade has been installed, or when the manipulator is lifted without a load.

LC5 – Storage When the installation tower rotates, the manipulator must provide enough clearance for this to work. This is done by putting the manipulator vertically against the installation tower.

LC 6 – Survival During survival mode, there is no blade in the gripper. What is meant by survival mode is storm, test conditions, emergency stop and load release system.

4.5. Load Calculation

The load on the system is calculated here. The load is divided into different parts: the gravitational load, the wind load on the manipulator, the wind load on the gripper and the wind load on the blade.

4.5.1. Gravitational Load

Initially, only the gravitational loads acting on the system are considered. The accelerations due to the movement of the vessel are neglected because it is considered statical. This results in a gravitational acceleration (g) of 9.81 m/s^2 . The masses used for the calculations are:

- $m_{blade} = 65.25 \text{ mt}$
- $m_{gripper} = 80 \text{ mt}$
- $m_{boom} = 1.6 \text{ mt/m}$

The different nodes are shown in Figure 4.6. Two forces are also drawn in this figure. These are the gravitational forces caused by the blade end the gripper. The force drawn at node A is when the gripper is at that location. The force drawn with a dashed line and in italics is when the gripper is at location B. The exact locations of the different nodes when the manipulator is in horizontal position are given in Table 4.2.

Table 4.2: Location nodes as shown in Figure 4.6

| Node | x [m] | y [m] | z [m] |
|------|-------|-------|-------|
| A | 63.6 | -10.5 | 0 |
| B | 31.8 | -5.25 | 0 |
| C | 21.2 | -3.50 | 0 |
| D | 0 | 0 | 0 |
| E | 0 | -11.0 | 0 |
| F | -11.0 | 0 | 0 |
| G | 0 | 0 | 11.0 |
| H | 0 | 0 | 50.5 |

The manipulator is represented as a simple beam problem. A force acts downwards at node A or B. This is the gravitational force of the gripper together with the blade ($F_{g,blade+gripper}$). This gravitational force of the blade ($F_{g,blade}$) and the gripper ($F_{g,gripper}$) are shown in Equations 4.1, 4.2 and 4.3. The gripper weighs 80 mt as mentioned in Subsection 3.1.4, the blade weighs 65 mt as mentioned in Section 2.3. The gravitational acceleration (g) for this first approximation is set at 9.81 m/s^2 . The

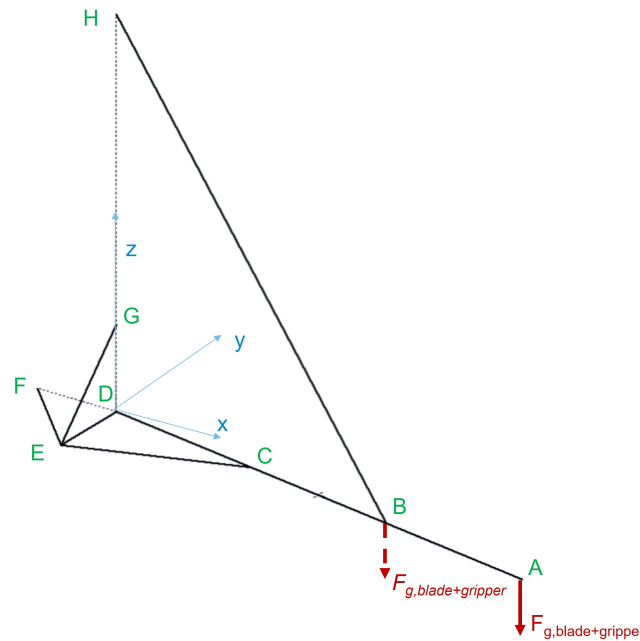


Figure 4.6: Schematic 3D representation of the manipulator

moment induced by the blade and the gripper ($M_{blade+gripper}$) due to the distance between their CoG and the tip of the boom ($r_{CoG,blade}$ and $r_{CoG,gripper}$) is stated in Equation 4.4. The mass of the boom itself is modelled as a distributed load over the whole length of the arm. The length of the beam (L) is initially 65.5 m. For now, it is assumed that this distributed load of the boom ($F_{g,boom/m}$) equals 19 kN/m. The gravitational force of the boom of the manipulator ($F_{g,boom}$) is shown in Equation 4.5.

$$F_{g,blade} = m_{blade} \times g \times LF = 65.25 \times 9.81 \times 1.2 = 768 \text{ kN} \quad (4.1)$$

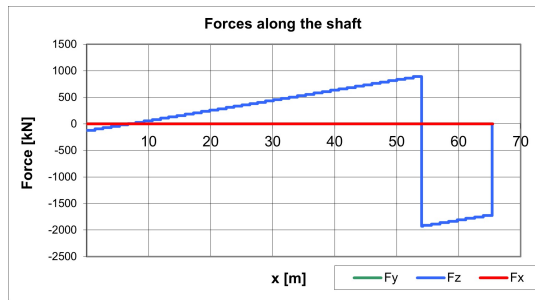
$$F_{g,gripper} = m_{gripper} \times g \times LF = 80 \times 9.81 \times 1.2 = 941 \text{ kN} \quad (4.2)$$

$$F_{g,blade+grripper} = F_{g,blade} + F_{g,grripper} = 768 + 941 = 1.71 \times 10^3 \text{ kN} \quad (4.3)$$

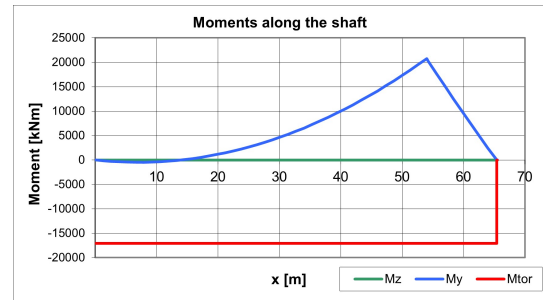
$$\begin{aligned} \oplus \sum M_{blade+gripper} &= r_{CoG,blade} \times F_{g,blade} + r_{CoG,gripper} \times F_{g,gripper} \\ &= \begin{bmatrix} 0 \\ 10 \\ 0 \end{bmatrix} \times \begin{bmatrix} 0 \\ 0 \\ -768 \end{bmatrix} + \begin{bmatrix} 0 \\ 10 \\ 0 \end{bmatrix} \times \begin{bmatrix} 0 \\ 0 \\ 941 \end{bmatrix} = \begin{bmatrix} -1.71 \times 10^4 \\ 0 \\ 0 \end{bmatrix} \text{ kNm} \end{aligned} \quad (4.4)$$

$$F_{g,boom} = F_{g,boom/m} \times L = 19 \times 65.5 = 1.24 \times 10^3 \text{ kN} \quad (4.5)$$

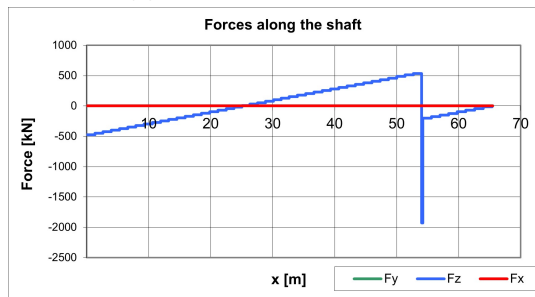
A reaction force acts on node E, which acts as a pin support. A wire rope with a winch on the installation tower is connected to the boom, creating a second reaction force. The mounting location of the winch to the boom is node B. This point provides, on average, a lower maximum shear force and bending moment than in the case of a mounting location at node A or C. The estimation of the shear force and the bending moment of the boom are shown in Figure 4.7 for the different load cases. The coordinate system used here is always in the same orientation with respect to the boom, a transformation matrix is used to achieve this.



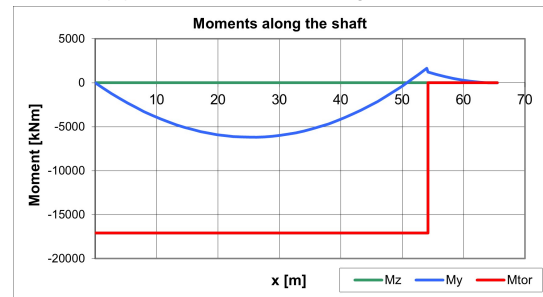
(a) Load case 1, shear force



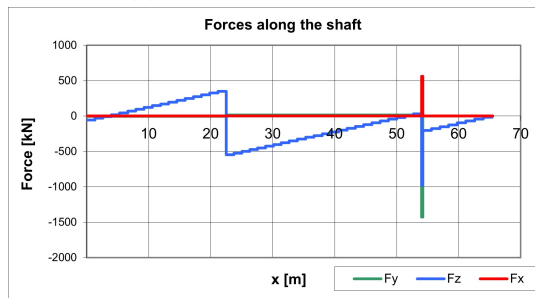
(b) Load case 1, bending moment



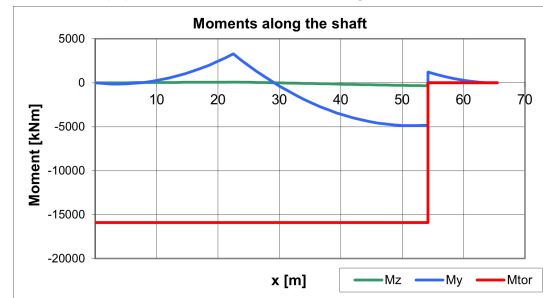
(c) Load case 2, shear force



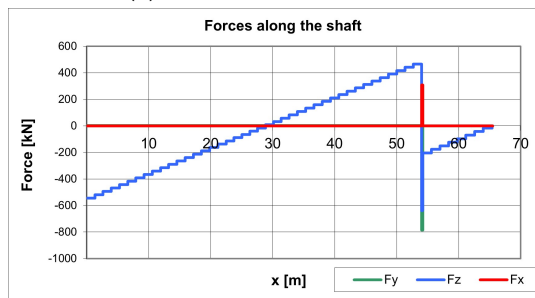
(d) Load case 2, bending moment



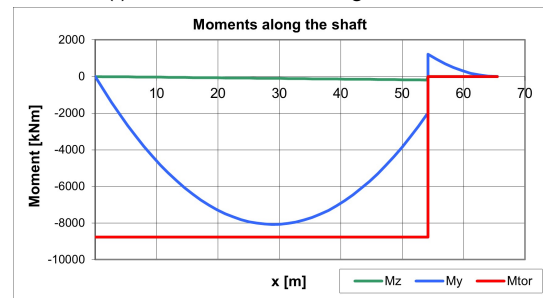
(e) Load case 3, shear force



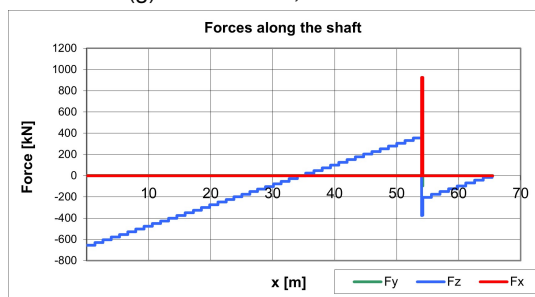
(f) Load case 3, bending moment



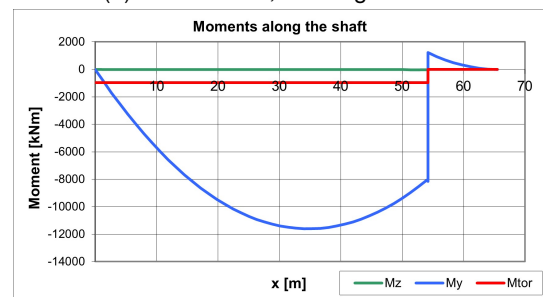
(g) Load case 4, shear force



(h) Load case 4, bending moment



(i) Load case 5, shear force



(j) Load case 5, bending moment

Figure 4.7: Shear force and bending moment diagrams for different load cases

4.5.2. Wind Load Manipulator

The wind force on the boom of the manipulator is calculated using Equation 4.6. Here, F_W is the wind force, the air density (ρ_{air}) is 1.225 kg/m^3 , the wind speed (U_W) is 12 m/s , the surface area (A) depends on the surface on which the wind is blowing, and the drag coefficient (C_D) can be derived from White [43]. The wind load in this calculation is applied in the surface centroid.

$$F_W = \frac{1}{2} \rho v^2 A C_d \quad (4.6)$$

Wind loads are minimal in the operational state, due to wind limitations on the operation. This means the wind load is not the leading force to determine the size of the manipulator. Wind loads for the structural design are checked after the primary concept design.

4.5.3. Wind Load Gripper

Similar to the wind load of the manipulator, the wind load on the gripper is also not considered in the concept design. Additionally, the wind load is not checked after the concept design due to the limited surface area. The wind load is linearly dependent on the surface area, where the gripper surface area is negligible compared to the manipulator and blade. Therefore, for a concept design, this load is not considered.

4.5.4. Wind Load Blade

The wind force acting on the wind turbine blade can be approximated in two ways. The first method is the same as the one mentioned above. For a wind turbine blade, this is a very rough approximation. Assuming the blade has 6 sides and thus 6 different surfaces, as shown in Figure 4.8, the wind force is calculated for those six different surfaces. The second approximation is more precise. Here, the blade is divided into different segments and the load is calculated for those different segments. Equation 4.6 is used to calculate the wind force roughly for the different surfaces. The drag coefficient for the root can be approximated as a cylinder and thus gets a C_D of 1.2, the tip of the blade can be approximated as a cone with a small angle and then gets a C_D of 0.5. The leading edge and the trailing edge can both be approximated by an airfoil and get a C_D of 0.3, the upwind and downwind wind surface can both be approximated by a rectangle and get a C_D of 1.6. The resulting wind force per surface is shown in the last column of Table 4.3.

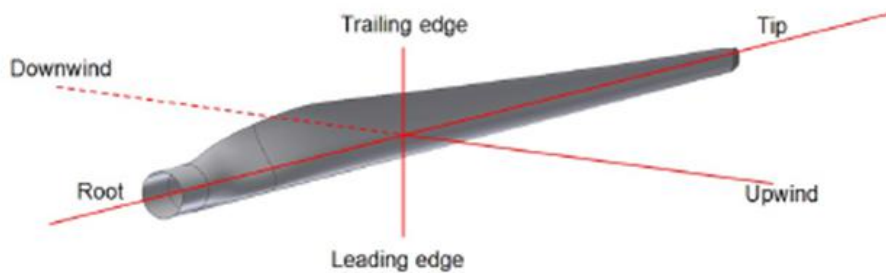


Figure 4.8: Different surfaces of a wind turbine blade [44]

Table 4.3: Wind force on wind turbine blade

| Surface | $A \text{ [m}^2\text{]}$ | C_D | $A \times C_D \text{ [m}^2\text{]}$ | $F_W \text{ [kN]}$ |
|--------------|--------------------------|-------|-------------------------------------|--------------------|
| Root | 21.2 | 1.2 | 25.4 | 2.244 |
| Tip | 21.2 | 0.5 | 10.6 | 0.935 |
| Leading edge | 270 | 0.3 | 81.0 | 7.144 |
| Tailing edge | 270 | 0.3 | 81.0 | 7.144 |
| Upwind | 470 | 1.6 | 752.0 | 66.326 |
| Downwind | 470 | 1.6 | 752.0 | 66.326 |

However, the wind loads can also be calculated in a more comprehensive way. A wind turbine blade can be divided into i segments. For each segment, the force and moment caused by the wind can be calculated. Figure 4.9 shows the wind turbine blade with the various segments and the location of the origin of the coordinate system used.

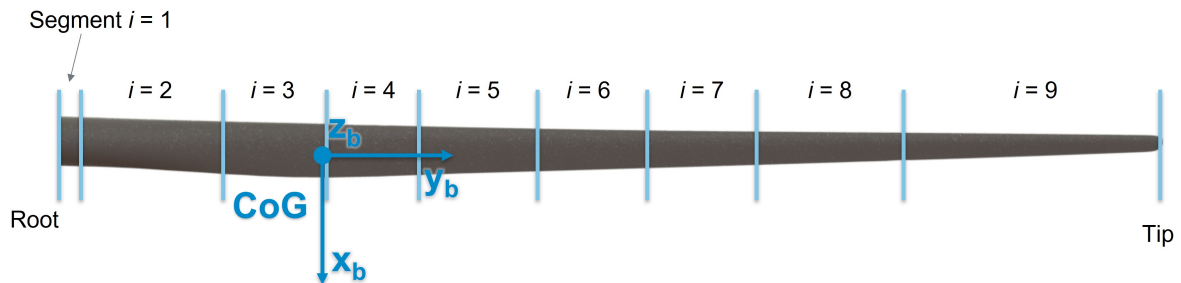


Figure 4.9: Blade segments and coordinate system top view

Figure 4.10 shows the cross-section of a wind turbine blade with the relevant angles and forces. Here U_W is the average wind speed, and the relevant wind speed is indicated by V_{rel} . The angle of the blade with the x-axis is the inclination angle for section i (θ) added by the AoA . AoA is the angle between V_{rel} and the chord line of the blade. The lift force (F_L) is perpendicular to V_{rel} and the drag force (F_D) is an extension of V_{rel} .

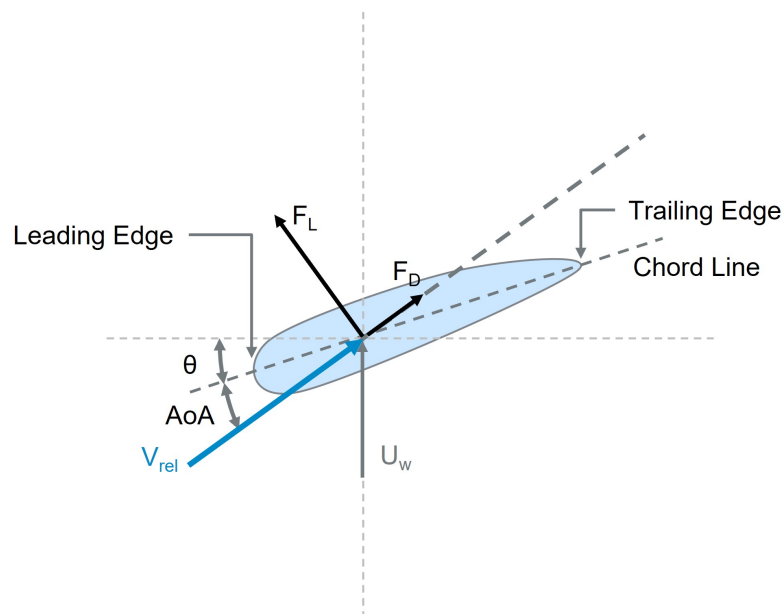


Figure 4.10: Intersection wind turbine blade and coordinate system

The data per section of the IEA 15 MW wind turbine are shown in Table 4.4. The wind turbine blade is divided into sections with a relatively uniform cross-section, which means that the length is not evenly distributed. The approximation of the spanwise position is shown in italics. These values with corresponding parameters are used in further calculations.

Table 4.4: Parameters per section

| i | Spanwise position [r/R] | Airfoil name | Relative thickness | Spanwise position [r/R] | Chord [m] | Twist [rad] | Pitch axis [x/c] | Span [m] | Prebend [m] | Spancenter [m] |
|----|-------------------------|-----------------|--------------------|-------------------------|-----------|-------------|------------------|----------|-------------|----------------|
| 1 | 0.00 | circular | 1.00 | 0.00 | 5.20 | 0.27 | 0.50 | 0.00 | 0.00 | 0.00 |
| 2 | 0.02 | circular | 1.00 | 0.02 | 5.21 | 0.27 | 0.49 | 2.39 | -0.02 | 1.19 |
| 3 | 0.15 | SNL-FFA-W3-500 | 0.50 | 0.14 | 5.62 | 0.20 | 0.38 | 16.7 | -0.20 | 9.55 |
| 4 | 0.25 | FFA-W3-360 | 0.36 | 0.24 | 5.70 | 0.13 | 0.32 | 28.7 | -0.25 | 22.7 |
| 5 | 0.33 | FFA-W3-330blend | 0.33 | 0.33 | 5.17 | 0.08 | 0.31 | 38.2 | -0.24 | 33.4 |
| 6 | 0.44 | FFA-W3-301 | 0.30 | 0.45 | 4.43 | 0.04 | 0.29 | 52.5 | -0.10 | 45.4 |
| 7 | 0.54 | FFA-W3-270blend | 0.27 | 0.53 | 4.00 | 0.02 | 0.29 | 62.1 | 0.16 | 57.3 |
| 8 | 0.64 | FFA-W3-241 | 0.24 | 0.63 | 3.53 | 0.00 | 0.29 | 74.0 | 0.70 | 68.1 |
| 9 | 0.77 | FFA-W3-211 | 0.21 | 0.78 | 2.88 | -0.03 | 0.31 | 90.7 | 1.74 | 82.4 |
| 10 | 1.00 | FFA-W3-211 | 0.21 | 1.00 | 0.50 | -0.02 | 0.37 | 117 | 4.00 | 103.9 |

The blade nodes are positioned at the beginning of each segment as seen from the root. The y-value is zero at the CoG. d_{CoG} represents the distance between the node and the CoG. θ is the section twist angle in degrees. Chord represents the length of the chord and t_{rel} is the relative thickness. The AoA is calculated as in Equation 4.7, with β as the rotation angle around the yb axis, θ as the twist angle per node, and α as the angle of the incoming wind. For now, β and α are kept zero. The resulting AoA per node is shown in bold in Table 4.5.

$$AoA_i = \beta + \theta_{twist,i} + \alpha \quad (4.7)$$

For the IEA 15 MW wind turbine the lift, drag and moment coefficients are given per AoA per airfoil. To be able to use these values, the nearest value for the AoA per airfoil is used in Table 4.5, indicated in italics. The corresponding lift, drag and moment coefficients (C_L , C_D , and C_M) are shown in the last three columns of Table 4.5.

Table 4.5: Blade nodes

| Node | xb [m] | yb [m] | zb [m] | d_{CoG} [m] | θ [°] | Chord [m] | t_{rel} [-] | AoA [°] | AoA approx. [°] | C_L [-] | C_D [-] | C_M [-] |
|------|--------|--------|--------|---------------|--------------|-----------|---------------|--------------|-------------------|-----------|-----------|-----------|
| 1 | 0 | -26.8 | 0 | 26.8 | 15.6 | 5.20 | 1.00 | 0.27 | 3.140 | 0.000 | 0.350 | 0.000 |
| 2 | 0 | -24.4 | 0 | 24.4 | 15.6 | 5.21 | 1.00 | 0.27 | 3.140 | 0.000 | 0.350 | 0.000 |
| 3 | 0 | -10.1 | 0 | 10.1 | 11.4 | 5.62 | 0.50 | 0.20 | 0.199 | 1.615 | 0.090 | -0.121 |
| 4 | 0 | 1.85 | 0 | 1.85 | 7.19 | 5.70 | 0.36 | 0.13 | 0.122 | 1.413 | 0.017 | -0.149 |
| 5 | 0 | 11.4 | 0 | 11.4 | 4.80 | 5.17 | 0.33 | 0.08 | 0.087 | 1.107 | 0.014 | -0.134 |
| 6 | 0 | 25.7 | 0 | 25.7 | 2.41 | 4.43 | 0.30 | 0.04 | 0.035 | 0.650 | 0.012 | -0.113 |
| 7 | 0 | 35.3 | 0 | 35.3 | 1.30 | 4.00 | 0.27 | 0.02 | 0.017 | 0.502 | 0.010 | -0.104 |
| 8 | 0 | 47.2 | 0 | 47.2 | 0.24 | 3.53 | 0.24 | 0.00 | 0.017 | 0.498 | 0.008 | -0.099 |
| 9 | 0 | 63.9 | 0 | 63.9 | -1.62 | 2.88 | 0.21 | -0.03 | -0.035 | 0.128 | 0.007 | -0.083 |
| 10 | 0 | 90.2 | 0 | 90.2 | -1.24 | 0.50 | 0.21 | -0.02 | -0.017 | 0.252 | 0.007 | -0.085 |

The segments are defined in Table 4.6. This defines the starting, ending, and centre points of each segment. Subtracting y_{begin} from y_{end} gives the span length of each segment ($l_{segment}$). The area of each segment ($A_{segment}$) is calculated, using Equation 4.8.

$$A_{segment,i} = l_{chord,i} \times t_{rel,i} \times l_{segment,i} \quad (4.8)$$

Table 4.6: Blade segments

| Segment | y_{begin} [m] | y_{end} [m] | x_{center} [m] | y_{center} [m] | z_{center} [m] | $l_{segment}$ [m] | $A_{segment}$ [m ²] |
|---------|-----------------|---------------|------------------|------------------|------------------|-------------------|---------------------------------|
| 1 | -26.8 | -24.4 | 0 | -25.6 | 0 | 2.39 | 12.4 |
| 2 | -24.4 | -10.1 | 0 | -17.2 | 0 | 14.3 | 74.6 |
| 3 | -10.1 | 1.85 | 0 | -4.11 | 0 | 11.9 | 33.6 |
| 4 | 1.85 | 11.4 | 0 | 6.62 | 0 | 9.55 | 19.6 |
| 5 | 11.4 | 25.7 | 0 | 18.6 | 0 | 14.3 | 24.4 |
| 6 | 25.7 | 35.3 | 0 | 30.5 | 0 | 9.55 | 12.7 |
| 7 | 35.3 | 47.2 | 0 | 41.3 | 0 | 11.9 | 12.9 |
| 8 | 47.2 | 63.9 | 0 | 55.6 | 0 | 16.7 | 14.2 |
| 9 | 63.9 | 90.2 | 0 | 77.1 | 0 | 26.3 | 16.0 |

The lift force, drag force and pitching moment can then be calculated per segment as in Equations 4.9 till 4.11. These loads can be combined according to Equations 4.12 and 4.13.

$$F_{L,i} = \frac{1}{2} \rho_{air} v^2 A_{segment,i} C_{L,i} (AoA_i) \quad (4.9)$$

$$F_{D,i} = \frac{1}{2} \rho_{air} v^2 A_{segment,i} C_{D,i} (AoA_i) \quad (4.10)$$

$$M_i = \frac{1}{2} \rho_{air} v^2 A_{segment,i} C_{M,i} (AoA_i) \quad (4.11)$$

$$F_W = \begin{bmatrix} F_{xb} \\ F_{yb} \\ F_{zb} \end{bmatrix} = \sum_{i=1}^n \begin{bmatrix} F_{L,i,x} - F_{D,i,x} \\ 0 \\ F_{L,i,z} + F_{D,i,z} \end{bmatrix} = \begin{bmatrix} -5.14 \\ 0.00 \\ 19.6 \end{bmatrix} \text{ kN} \quad (4.12)$$

$$M_W = \begin{bmatrix} M_{xb} \\ M_{yb} \\ M_{zb} \end{bmatrix} = \sum_{i=1}^n \begin{bmatrix} 0 \\ M_i \\ 0 \end{bmatrix} \sum_{i=1}^n \begin{bmatrix} F_{zb,i} \times y_{center,i} \\ 0 \\ F_{xb,i} \times y_{center,i} \end{bmatrix} = \begin{bmatrix} -83.6 \\ -2.17 \\ 65.3 \end{bmatrix} \text{ kNm} \quad (4.13)$$

The lift and drag forces can also be combined into an x and y component per segment, shown in Figure 4.11. The strongest force on the blade is at segment 2.

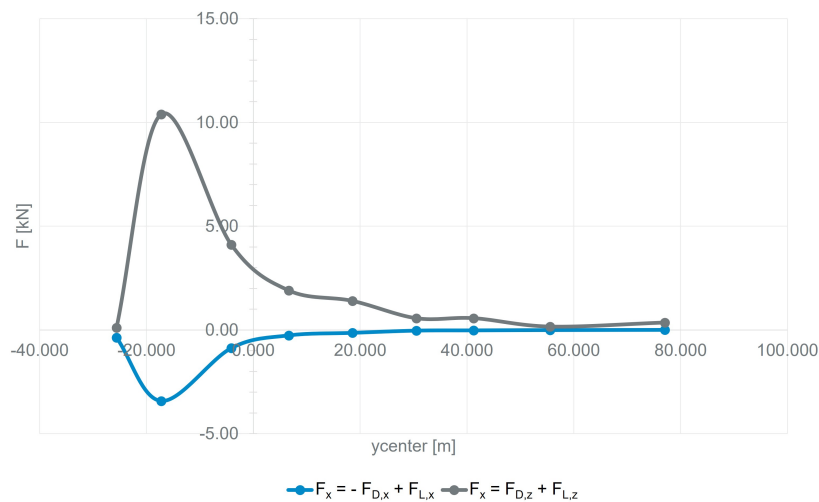


Figure 4.11: Distribution of wind forces on the blade. The nodes represent the different segments of the blade.

4.6. Structural Design

Designing the structure of the manipulator can now be done with the previously determined loads. The cross-section of the manipulator needs to stay within the desired deflections and stresses. The load case considered for this concept design is when the manipulator is in the horizontal position loaded with a blade. This is when moments are highest around the points of interest.

When considering the wind forces on the blade, two factors are relevant when considering the load on the manipulator. Namely the weight of the blade and the lift of the blade. Figure 4.11 shows the distribution of wind forces on the blade. When adding these wind loads up at the highest limit winds, the blade creates more lift than the weight of the blade, which negates these forces. Therefore, the load case of the structural design considered no wind, to maximize the bending moment experienced by the manipulator, which is a critical force to design for.

With the loads defined, the segment size can now be determined. With the aid of a box segment calculation tool by Huisman, the segment dimensions are determined for the windless horizontal load case. The dimensions are shown in Table 4.7 and the cross-section is shown in Figure 4.12. These dimensions result in a mass moment of inertia (I) of $3.57 \times 10^{11} \text{ mm}^4$, a polar moment of inertia (J) of $2.26 \times 10^{11} \text{ mm}^4$ and weight of $1.64 \times 10^3 \text{ kg/m}$. With these segments, the displacement and stresses in the beam can be checked to see if they are within the design requirements.

Table 4.7: Dimensions segment

| Description | Value |
|-----------------------------|---------|
| Height | 3500 mm |
| Width | 2000 mm |
| Thickness left | 12 mm |
| Thickness right | 12 mm |
| Thickness top | 15 mm |
| Thickness bottom | 15 mm |
| Amount of stiffeners left | 3 |
| Amount of stiffeners right | 3 |
| Amount of stiffeners top | 2 |
| Amount of stiffeners bottom | 2 |

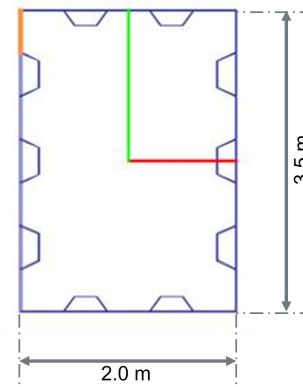


Figure 4.12: cross-section boom

4.6.1. Allowable Deflection

Deflection is the degree to which a part of a structural element is deformed under load. This can be deformation or torsion. The displacement (δ) of the manipulator can be calculated using Equation 4.14. Using the data from Tables 4.1 and 4.7 the displacement of the beam is determined for the boom in horizontal position. From this, it is found that the displacement is 50 mm, within the design limits when fully loaded.

$$\begin{aligned} \delta &= \delta_{distributed\ load} + \delta_{point\ load} \\ &= \frac{1}{8} \times \frac{F_{g,boom/m} \times L^4}{E \times I} + \frac{1}{3} \times \frac{F_{g,blade+gripper} \times L^3}{E \times I} \end{aligned} \quad (4.14)$$

Additionally, the torsion (ϕ) of the non-centre loads on the manipulator can also be calculated. Using Equations 4.15 and 4.16 it is found that the manipulator beam rotates 1.1° , resulting in an additional 190 mm of blade drop. This is a minimal torsion which should be considered in the installation phase for alignment purposes, but this does not influence the operational phase of the WIV.

$$G = \frac{E}{2(1 + \nu)} \quad (4.15)$$

$$\phi = \frac{M_{blade+gripper} \times L}{G \times J} \quad (4.16)$$

Relative to the size of the system, the deflection and rotation of the manipulator beam are minimal. Using large lifting equipment in operations already considered these deflections. When a load is being lifted, it gradually shifts its weight onto the equipment, meaning that the deflection occurs slowly. When completely loading the equipment, the deflection stays consistent and can be accounted for as the load consistently maintains the deflection.

4.6.2. Allowable Stress

Acceptable stress ($\sigma_{occurring}$) in a system is determined by a safety factor and the yield strength (σ_y) of the materials used. The stresses in the system should be chosen to ensure no plastic deformation or permanent damage occurs. The safety factor (SF_{actual}) is calculated using Equation 4.17. If the resulting value is above the chosen safety factor ($SF_{required}$) for this component, the stresses in the system are allowed. In the case of the manipulator, the chosen safety factor is 1.5, which is conform to the industry standard.

$$SF_{actual} = \frac{\sigma_y}{\sigma_{occurring}} \quad (4.17)$$

$$SF_{actual} > SF_{required} \rightarrow ok. \quad (4.18)$$

The cross-section as described in Figure 4.12 is present along the entire length of the boom. For various locations across the boom, the actual safety factor is calculated for the section using the load cases. With the current cross-section, this safety factor is always higher than the required safety factor. These estimates lead to the conclusion that no plastic deformation or permanent damage will occur in the boom.

4.7. Drive Systems

With a basic structure of the manipulator defined, the actuation of the system is another essential aspect. The manipulator has multiple degrees of freedom which need to be controlled. This is done by drive systems on the manipulator. The drive systems are dealt with per DoF, as each actuation requires its own specifications to be acceptable within the design.

4.7.1. Winch

To raise the arm of the manipulator, a winch is needed. The winch is calculated according to DNV standards.

A wire rope with a diameter of 50 mm is chosen, as this is the most commonly used. The 8xK36WS+EPIWRC cable is chosen for this purpose [45]. Figure 4.13 shows the cross-section of this cable and Table 4.8 shows the main specifications.

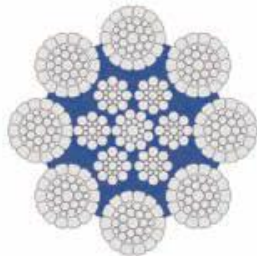


Figure 4.13: Crosssection wire rope 8xK36WS+EPIWRC [45]

Table 4.8: Characteristics 8xK36WS+EPIWRC [45]

| Description | Value |
|-----------------------------|----------------------|
| Nominal diameter | 50 mm |
| Cross-section | 1333 mm ² |
| Weight | 11.4 kg/m |
| Minimum Breaking Load (MBL) | 2365 kN |
| Tolerance on diameter | ± 5 % |
| Filling factor | 0.678 |
| Spinning factor | 0.820 |
| Modulus of elasticity | 105 GPa |

The load on this subsystem is 500 mt. The cable has a Minimum Breaking Load (MBL) of 2365 kN. Usually, a safety factor of 3.35 is used for lifting loads above 122 mt. However, this manipulator lifts almost all the time at maximum load. Therefore, a safety factor of 4 is used. This results in an allowable load of approximately 600 kN per cable. Dividing the total load by the allowable load per cable shows that 8 cables must be used. The maximum distance between the deflection sheave and the lower block is 67 m and the minimum distance is 16 m. Using the maximum distance and the number of falls results in a required wire storage of 405 m.

The minimum ratio of drum diameter per rope diameter (D/d) that may be applied is 21. This results in a minimum drum diameter of 1.05 m.

The fleet angle is the angle between the drum and the wire. It should not exceed 1.5°. This is to ensure that the first winding of the new layer is spooled properly. The deflection sheave is at a height of 40 m above the winch. This results in a maximum width of the drum of 2.09 m, which allows 40 windings side by side on the drum. The number of layers equals 3. Therefore, the total storage capacity on the drum is 438 m. This is sufficient for the required capacity of 405 m.

The outer radius of the flange is diameter of the maximum amount of layers plus one extra layer, which results in an outer flange diameter of 1.45 m.

The parameters of the drum described above are summarised in Figure 4.14.

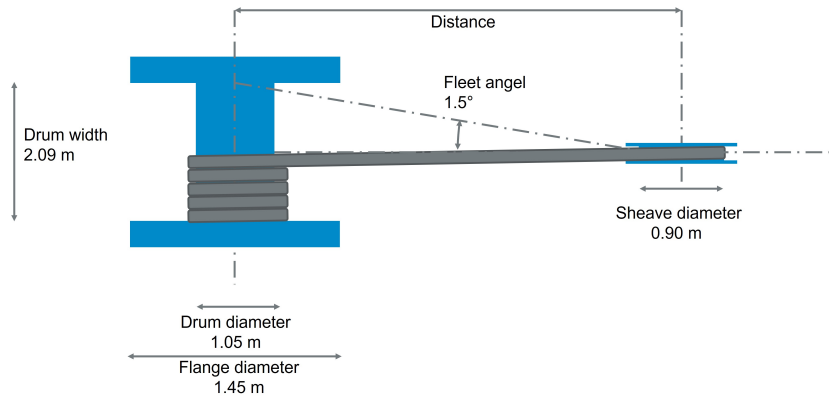


Figure 4.14: Dimensions winch

4.7.2. Hydraulic Cylinder

To move the arm of the manipulator in the xy-plane, a hydraulic cylinder is used, shown in Figure 4.15. The maximum force applied to the cylinder is 913 kN. This is when the manipulator is in the storage position. The retracted length of the cylinder has to be 4.3 m and the extended length has to be 8.45 m. This results in a stroke of 4.15 m.

A cylinder of IHC Vremac is used. It must be ensured that the cylinder does not buckle at the mentioned forces. From the Piston rod buckling load diagrams of Vremac [46], it appears that a rod diameter of 220 mm must be used to prevent buckling. This rod diameter results in a cylinder with the characteristics shown in Table 4.9.

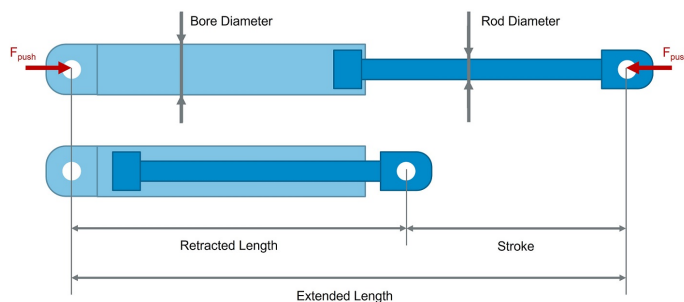


Figure 4.15: Layout cylinder

Table 4.9: Characteristics hydraulic cylinder [46]

| Description | Value |
|-------------------------|---------------------|
| Bore | 320 mm |
| Piston Rod | 220 mm |
| Piston area | 804 mm ² |
| Rod area | 380 mm ² |
| Piston area / Ring area | 1.90 |
| Pushing force 210 bar | 1689 kN |
| Pushing force 320 bar | 2574 kN |
| Pulling force 210 bar | 891 kN |
| Pulling force 320 bar | 1357 kN |

4.7.3. Slew Drive

To tilt the gripper, a slew drive is added between the arm of the manipulator and the gripper. This bearing has a diameter of 4 m and a ball diameter of 70 mm.

The load on this bearing is a shear force (V) and a moment (M), as shown in Figure 4.16, caused by the mass of the gripper and the blade. The shear force is equal to the mass of the gripper and the blade times the gravitational acceleration and the load factor. This results in a shear force of 1.71×10^3 kN (radial load). The bending moment is equal to this force times the arm. The CoG of the gripper and blade has a distance of 8.45 m to the slew drive. This results in a bending moment of 1.44×10^4 kNm.

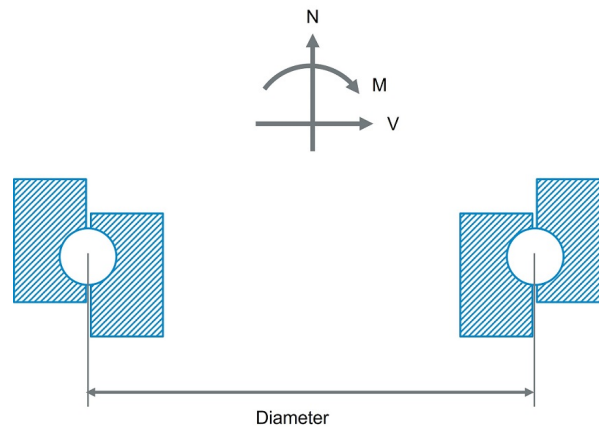


Figure 4.16: Cross-section bearing

4.7.4. Slider

The gripper with the blade is slid in over a length of 11.5 m to ensure that the arm of the manipulator has the correct length to install the blade properly on the hub of the wind turbine. The load on the slider is the mass of the gripper together with the blade.

The trolley is driven by a rack and pinion. Equations 4.19 and 4.20 show the tangential force (F_r) on the rack for horizontal and vertical application. Both applications are needed because the manipulator operates in both horizontal and vertical positions. The coefficient of friction (μ) is 0.003. This results in a force of 8.1 kN on the rack in horizontal position and 1713 kN in vertical position.

$$F_{r,horizontal} = (m_{blade} + m_{gripper}) \times g \times \mu + (m_{blade} + m_{gripper}) \times a \quad (4.19)$$

$$F_{r,vertical} = (m_{blade} + m_{gripper}) \times g + (m_{blade} + m_{gripper}) \times a \quad (4.20)$$

4.8. Safety

Safe use and operation of the manipulator are essential for this system. Safety comes in many forms, considering short and long-term influences on the operators. As actuators directly drive the different movements of the manipulator, this can be done autonomously or remotely. Remote and autonomous work reduces the exposure time of people to dangers and accidents.

In addition, long-term effects could also pose a threat. In the case of the manipulator, accelerations experienced by operators to join the blade to the hub could pose health risks. It was found that extended exposure to high acceleration, around 20 m/s² could have fatal consequences if experienced longer than 2 days [47]. Considering the worst case, accelerations barely exceed 1G in the worst circumstances. In the X, Y, and Z directions, the accelerations are 0.5, 0.75, and 10.41 m/s² respectively.

4.9. Conclusion and Storyboard

This manipulator can cope with normal operational conditions throughout most of the year. This means that this manipulator is operational with a mean wind speed of 12 m/s and a significant wave height of 3.5 m. When looking at the load case with the boom of the manipulator horizontal, just after picking up the blade, the deflection of the boom is 50 mm and the torsion is 1.1°, which results in the blade dropping an extra 190 mm. The deflection is less than 1 % of the total length of the boom which is considered acceptable. As larger wind turbines will make their appearance in the future, a WIV applied to these wind turbines will be needed. This manipulator can be scaled for this purpose. The slider makes it already possible to handle smaller blades.

Figure 4.17 shows the storyboard of different movements of the manipulator.

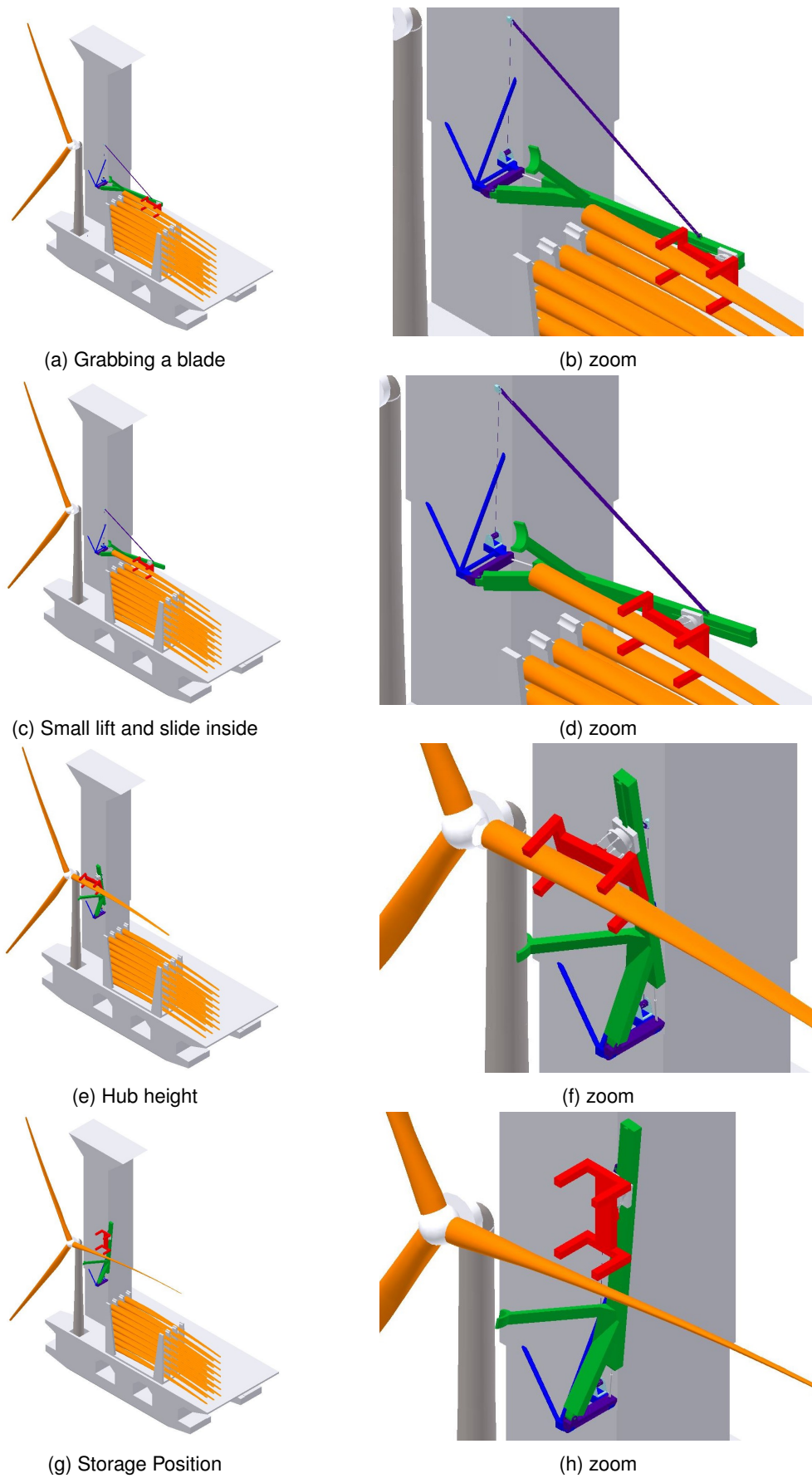


Figure 4.17: Storyboard

Conclusion and Recommendations

Demand for offshore wind farms is growing rapidly, as is the size of the wind turbines themselves. Currently, Huisman is working on the design of a Windfarm Installation Vessel (WIV), which approaches the installation of offshore wind turbines as an industrial robotised process. The objective of this thesis is to develop a blade manipulator that is able to install wind turbine blades on a customised floating vessel, the WIV, in severe weather conditions. The following research question is formulated:

How can a blade manipulator be used to quickly and accurately install blades on a 15 MW wind turbine on a floating vessel?

Currently, the installation method for offshore wind turbine blades is usually executed by using a jack-up vessel. The blade installation only takes place for a few months per year to avoid extreme weather conditions, which can cause a critical event. The WIV is developed for more severe environmental conditions. The WIV should be operational at 85 % per year with a mean wind speed of 12 m/s and a significant wave height of 3.5 m. The offshore wind turbine selected for the design of the blade manipulator is the IEA 15-MW wind turbine. This is the largest reference wind turbine with all the blade properties and specifications available.

Based on the VDI 2221 guidelines, a systematic approach, six concepts are developed. Using the analytic hierarchy process, the rotational arm was selected to be the most feasible one. This manipulator grabs the blade around the centre of gravity and picks it up. The gripper with the blade is moved over the arm towards the hinge point. After this, the blade is lifted using a rotational movement to hub height. Here, the blade is installed and the manipulator can move back to the blade rack to pick up the next blade.

The manipulator is designed to be operational with an average wind speed of 12 m/s and a significant wave height of 3.5 m. This enables the WIV to operate through most of the year. When looking at the load case with the boom of the manipulator horizontal, just after picking up the blade, the deflection of the boom is 50 mm and the torsion is 1.1° , which results in the blade dropping an extra 190 mm. The deflection is less than 1 % of the total length of the boom which is considered acceptable. As larger wind turbines will make their appearance in the future, a WIV applied to these wind turbines will be needed. Due to the slider mechanism, the manipulator is able to handle increasing blade sizes.

5.1. Recommendations

The subject of this thesis is to design a blade manipulator to install blades on a 15 MW wind turbine on a floating vessel. This goal has been achieved, however, follow-up research is required before realisation:

- During the development of the manipulator, several assumptions were made for the load cases. The load cases need to be more accurate. The motion of the ship should be added and wind loads should be included in the calculations of the main boom. With these calculations, the structure of the main boom can then be optimised in terms of shape to save weight.

- The actuators in the current design are worked out fundamentally. When the calculations with the different load cases are done more accurately, the loads on the actuators and the loads the actuators have to deliver can also be optimised more accurately. This optimisation should consider the design of the actuator and the interface of the actuator and manipulator.
- In the current design, there is no control system in place to control all actuators. The aim is to operate the manipulator autonomously to increase safety and workability. A control system must be added to realise this. The actuators need to work together and sensors need to be added to control the movement of the manipulator during operation.
- Once the above components are further developed, the accuracy of the manipulator can be considered. This can be done with calculations and later with model tests.
- The largest wind turbine currently available is 15 MW. There is already a plan for 20 MW wind turbines. The results from this thesis can be used for these larger wind turbines by applying the argumentation analysis and calculations to a larger wind turbine than 15 MW. However, it is advisable to use the 20 MW reference wind turbine when doing so, assuming it is published in the near future.

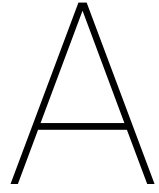
Bibliography

- [1] United Nations Climate Change, “The Paris Agreement,” <https://unfccc.int/process-and-meetings/the-paris-agreement/the-paris-agreement>, (accessed April 6, 2022).
- [2] European Commission, “2050 long-term strategy,” https://ec.europa.eu/clima/eu-action/climate-strategies-targets/2050-long-term-strategy_en, n.d., (accessed April 6, 2022).
- [3] —, “A European Green Deal,” https://ec.europa.eu/info/strategy/priorities-2019-2024/european-green-deal_en, 2019, (accessed April 6, 2022).
- [4] L. Ramirez, “Offshore wind energy 2022 mid-year statistics,” *Wind Europe*, 2022, (accessed August 30, 2022).
- [5] C. Bak, F. Zahle, R. Bitsche, T. Kim, A. Yde, L. C. Henriksen, M. H. Hansen, J. P. A. A. Blasques, M. Gaunaa, and A. Natarajan, “The dtu 10-mw reference wind turbine,” https://backend.orbit.dtu.dk/ws/portalfiles/portal/55645274/The_DTU_10MW_Reference_Turbine_Christian_Bak.pdf, Technical Univeristy of Denmark, Tech. Rep., 2013, (accessed April 6, 2022).
- [6] Vestas Wind Systems A/S, “V80-2.0 mw unsurpassed reliability and performance at high-wind sites,” <https://www.yumpu.com/en/document/read/9023342/v80-20-mw-vestas>, 2009, (accessed April 6, 2022).
- [7] Siemens AG, “New dimensions siemens wind turbine swt-3.6-107,” <https://pdf.archiexpo.com/pdf/siemens-gamesa/swt-36-107/88089-134485.html>, 2011, (accessed April 6, 2022).
- [8] J. Jonkman, S. Butterfield, W. Musial, , and G. Scott, “Definition of a 5-mw reference wind turbine for offshore system development,” <https://www.nrel.gov/docs/fy09osti/38060.pdf>, National Renewable Energy Laberatory, Golden, CO, Technical Report NREL/TP-500-38060, 2009, (accessed April 6, 2022).
- [9] Vestas, “V164-10.0 mw,” <https://www.vestas.com/en/products/offshore/V164-10-0-MW>, n.d., (accessed February 25, 2022).
- [10] Siemens Gamesa, “Sg 11.0-200 dd offshore wind turbine,” <https://www.siemensgamesa.com/en-int/products-and-services/offshore/wind-turbine-sg-11-0-200-dd>, n.d., (accessed April 6, 2022).
- [11] GE Renewable Energy, “Haliade-x offshore wind turbine,” <https://www.ge.com/renewableenergy/wind-energy/offshore-wind/haliade-x-offshore-turbine>, n.d., (accessed February 25, 2022).
- [12] E. Gaertner, J. Rinker, L. Sethuraman, F. Zahle, B. Anderson, G. Barter, N. Abbas, F. Meng, P. Bortolotti, W. Skrzypinski, G. Scott, R. Feil, H. Bredmose, K. Dykes, M. Shields, C. Allen, and A. Viselli, “Definition of the iea 15-megawatt offshore reference wind,” <https://www.nrel.gov/docs/fy20osti/75698.pdf>, National Renewable Energy Laboratory, Golden, CO, Technical Report NREL/TP-5000-75698, 2020, (accessed April 6, 2022).
- [13] Siemens Gamesa, “Sg 14-222 dd offshore wind turbine,” <https://www.siemensgamesa.com/products-and-services/offshore/wind-turbine-sg-14-222-dd>, n.d., (accessed February 25, 2022).
- [14] Project Cargo Journal, “Video: Siemens gamesa installs 14 mw wind turbine prototype,” <https://www.projectcargojournal.com/construction/2021/11/16/video-siemens-gamesa-installs-14-mw-wind-turbine-prototype/?gdp=accept>, 2021, (accessed April 13, 2022).
- [15] Vestas, “V236-15.0 mw,” <https://www.vestas.com/en/products/offshore/V236-15MW>, n.d., (accessed February 25, 2022).

- [16] P. H. Jensen, T. Chaviaropoulos, and A. Natarajan, "Lcoe reduction for the next generation off-shore wind turbines," *innwind.eu*, 2017, (accessed June 20, 2022).
- [17] M. Gaunaa, L. Bergami, S. Guntur, and F. Zahle, "First-order aerodynamic and aeroelastic behavior of a single-blade installation setup," *Journal of Physics: Conference Series*, vol. 524, p. 012073, 2014.
- [18] L. Kuijken, "Single blade installation for large wind turbines in extreme wind conditions: A quasi-steady aeroelastic study in high wind speeds under different inflow angles," Master of Science Thesis, Technical University of Denmark and Delft University of Technology, 2015.
- [19] Wind Monitor, "Wave heights and accessibility," http://windmonitor.iee.fraunhofer.de/windmonitor_en/4_Offshore/3_externe_Bedingungen/3_Wellen/, n.d., (accessed February 25, 2022).
- [20] Wind Energy The Facts, "Wind turbine technology for offshore locations: Availability, reliability and access," <https://www.wind-energy-the-facts.org/availability-reliability-and-access-7.html>, n.d., (accessed February 25, 2022).
- [21] K. J. van Dinther, "Blade installation for offshore wind turbines," Literature Survey, Delft University of Technology, 2022.
- [22] Huisman, "Windfarm Installation Vessel," https://www.huismanequipment.com/nl/products/renewables/offshore_wind/windfarm-installation-vessel, n.d., (accessed February 28, 2022).
- [23] Orsted, "Our experience with suction bucket jackets," <https://orsted.com/en/our-business/offshore-wind/wind-technology/suction-bucket-jacket-foundations>, n.d., (accessed August 30, 2022).
- [24] R. Chitteth Ramachandran, C. Desmond, F. Judge, J.-J. Serraris, and J. Murphy, "Floating offshore wind turbines: Installation, operation, maintenance and decommissioning challenges and opportunities," *Wind Energy Science Discussions*, pp. 1–32, 2021.
- [25] Seajacks, "Seajacks international awarded foundation installation contract for the akita port and noshiro port offshore wind farms," <https://www.seajacks.com/press-releases/seajacks-international-awarded-foundation-installation-contract-for-the-akita-port-and-noshiro-port-offshore-wind-farms/>, 2020, (accessed March 21, 2022).
- [26] D. Weston, "Offshore wind companies to test vibratory monopile driving," <https://www.windpowermonthly.com/article/1289182/offshore-wind-companies-test-vibratory-monopile-driving>, 2014, (accessed March 21, 2022).
- [27] N. Augusteijn and M. Buitendijk, "Boskalis: Kincardine is a prelude to more floating wind projects," <https://www.projectcargojournal.com/offshore/2021/02/18/boskalis-kincardine-is-a-prelude-to-more-floating-wind-projects/?gdpr=accept>, 2021, (accessed March 21, 2022).
- [28] Z. Ren, Z. Jiang, R. Skjetne, and Z. Gao, "Development and application of a simulator for offshore wind turbine blades installation," *Ocean Engineering*, vol. 166, pp. 380–395, 2018.
- [29] Z. Jiang, "Installation of offshore wind turbines: A technical review," *Renewable and Sustainable Energy Reviews*, vol. 139, p. 110576, 2021.
- [30] Gemini, "The building and installation of: The turbines and the nacelles," <https://www.geminiwindpark.nl/turbines--nacelles--rotorblades.html>, n.d., (accessed April 9, 2022).
- [31] J. Moeller, "Wind turbine lifting arrangement," U.S. Patent US2 021 284 506A1, 2021, (accessed April 5, 2022).
- [32] D. N. V. AS, "DNV-RP-C205: Environmental conditions and environmental loads," 2014.
- [33] J. Jänsch and H. Birkhofer, "The development of the guideline VDI 2221-the change of direction," in *DS 36: Proceedings DESIGN 2006, the 9th International Design Conference, Dubrovnik, Croatia*, 2006.

- [34] Dutch Water Sector, "Purpose built vessel to install 20 mw offshore wind turbines," <https://www.dutchwatersector.com/news/purpose-built-vessel-to-install-20-mw-offshore-wind-turbines>, n.d., (accessed August 1, 2022).
- [35] DEME, "Deme offshore awarded major hornsea two contract for foundation and turbine installation," <https://www.deme-group.com/news/deme-offshore-awarded-major-hornsea-two-contract-foundation-and-turbine-installation>, n.d., (accessed August 1, 2022).
- [36] Riviera, "Updated: Load-orienting technology will make offshore installation safer," <https://www.rivieramm.com/news-content-hub/news-content-hub/load-orienting-technology-could-make-offshore-wind-installation-safer-61316>, n.d., (accessed August 1, 2022).
- [37] ENABL, "Onshore blade lifting yokes: Onshore installation equipment," <https://enabl-wind.com/products/all-equipment/blade-lifting-yokes-onshore/>, 2022, (accessed March 4, 2022).
- [38] —, "Offshore blade-lifting yoke for b75 blades," <https://enabl-wind.com/cases/offshore-blade-lifting-yoke-for-b75-blades/>, 2021, (accessed March 4, 2022).
- [39] T. L. Saaty, "How to make a decision: The analytic hierarchy process," *European Journal of Operational Research*, vol. 48, no. 1, pp. 9–26, 1990, decision making by the analytic hierarchy process: Theory and applications.
- [40] O. S. Vaidya and S. Kumar, "Analytic hierarchy process: An overview of applications," *European Journal of operational research*, vol. 169, no. 1, pp. 1–29, 2006.
- [41] E. Triantaphyllou, S. H. Mann *et al.*, "Using the analytic hierarchy process for decision making in engineering applications: some challenges," *International journal of industrial engineering: applications and practice*, vol. 2, no. 1, pp. 35–44, 1995.
- [42] Det Norske Veritas AS, "DNV-OS-C101: Design of offshore steel structures, general - lrfd method," 2016.
- [43] F. White, *Fluid Mechanics*, 8th ed., ser. McGraw-Hill series in mechanical engineering. McGraw Hill Education, 2016.
- [44] M. Rodenburg, "Additional lifting days for single blade installation," master thesis, Delft University of Technology, 2015.
- [45] Eurocable, "Cable constructions," <https://www.eurocable.be/nl/producten/staalkabels/kabelconstructies>, 2022, (accessed September 11, 2022).
- [46] Vremac, "Cylinder Catalogue 210 bar / 320 bar," https://vremac.com/wp-content/uploads/sites/4/2020/11/Cylinder-Catalogue-V21-V32_zonder-logo.pdf, 2020, (accessed September 11, 2022).
- [47] M. McCORMACK, "Space handbook: Astronautics and its Applications," <https://history.nasa.gov/conghand/mannedev.htm>, 1959, (accessed September 14, 2022).
- [48] Office of Energy Efficiency & Renewable Energy, "Advanced wind turbine drivetrain trends and opportunities," <https://www.energy.gov/eere/articles/advanced-wind-turbine-drivetrain-trends-and-opportunities#:~:text=Direct%20drive%20systems%20do%20not,for%20a%20given%20turbine%20capacity.>, 2019, (accessed February 25, 2022).
- [49] C. Lavanya and N. D. Kumar, "Foundation types for land and offshore sustainable wind energy turbine towers," *E3S Web of Conferences*, vol. 184, no. 01094, 2020, (accessed February 18, 2022).
- [50] D. Mulazzani, "Avi iroll extreme control system: Setting new standards in off-shore foundations manufacturing," <https://www.offshorewind.biz/2021/10/06/davi-iroll-extreme-control-system-setting-new-standards-in-off-shore-foundations-manufacturing/>, 2021, (accessed February 25, 2022).
- [51] H. Díaz and C. Guedes Soares, "Review of the current status, technology and future trends of offshore wind farms," *Ocean Engineering*, vol. 209, p. 107381, 2020.

- [52] A. T. Rognstad and I. S. Nakstad, "Numerical study for single blade installation of an offshore wind turbine," Master of Science Thesis, Norwegian University of Science and Technology, 2020.
- [53] E. Konstantinidis and P. Botsaris, "Wind turbines: current status, obstacles, trends and technologies," *IOP Conference Series: Materials Science and Engineering*, vol. 161, p. 012079, 11 2016.
- [54] S. Tewolde, R. Höffer, h. haard, and J. Krieger, "Lessons learned from practical structural health monitoring of offshore wind turbine support structures in the north sea," in *The International conference on wind energy harvesting 2018*, Catanzaro Lido, Italy, 2018.
- [55] H. Bailey, K. Brookes, and P. Thompson, "Assessing environmental impacts of offshore wind farms: Lessons learned and recommendations for the future," *Aquatic biosystems*, vol. 10, p. 8, 2014.
- [56] D. Ahn, S. chul Shin, S. young Kim, H. Kharoufi, and H. cheol Kim, "Comparative evaluation of different offshore wind turbine installation vessels for korean west-south wind farm," *International Journal of Naval Architecture and Ocean Engineering*, vol. 9, no. 1, pp. 45–54, 2017.
- [57] N. Blenkey, "Turkish tugboats deliver big bollard pull on trials," <https://www.marinelog.com/news/turkish-tugboats-deliver-big-bollard-pull-on-trials/>, 2019, (accessed February 28, 2022).
- [58] Huisman, "Sheerleg kranen," https://www.huismanequipment.com/nl/products/cranes/floating_cranes, n.d., (accessed February 28, 2022).
- [59] Huisman, "Heavy lift mast cranes," https://www.huismanequipment.com/en/products/cranes/heavy_lift_mast_cranes, n.d., (accessed February 28, 2022).
- [60] Heavy Lift News, "Jack-up barge fitting dp2 system on jb117 – video," <https://www.heavyliftnews.com/jack-up-barge-fitting-dp2-system-on-jb117-video/>, 2019, (accessed February 28, 2022).
- [61] Huisman, "300mt pedestal mounted crane," https://www.huismanequipment.com/en/products/references/674-289_300mt-Pedestal-Mounted-Crane, 2012, (accessed February 28, 2022).
- [62] DC Velocity, "Pintsch bubenzer brakes for giant semi-submersible crane vessel," <https://www.dcvelocity.com/articles/44953-pintsch-bubenzer-brakes-for-giant-semi-submersible-crane-vessel>, 2019, (accessed February 25, 2022).



Scientific Research Paper

Offshore Blade Manipulator: Increased safety and workability for future wind turbine blade installation.

K.J. van Dinther, Dr.ir.H. Polinder, ir.W. van der Bos
Department of Maritime and Transport Technology
Delft University of Technology
 Delft, the Netherlands

D. Wijning
Product Manager Drilling
Huisman Equipment
 Schiedam, The Netherlands

Abstract—Demand for offshore wind farms is growing rapidly, as is the size of the wind turbines themselves. Currently, Huisman is working on the design of a Windfarm Installation Vessel (WIV), which approaches the installation of offshore wind turbines as an industrial robotised process. The objective of this paper is to describe a blade manipulator to install wind turbine blades on a customised floating vessel, the WIV, in severe weather conditions. The current methods for wind turbine blade installation are analysed, resulting in operational conditions for the blade manipulator. Several concepts are drawn up. Selection is made and the rotating arm proves to be the most feasible concept. The arm is hinged at the WIV installation tower. With a rotational movement is the blade installed at the hub. This manipulator can handle offshore operating conditions for most of the year and is equipped for wind turbines of different sizes.

Index Terms—Offshore wind turbine, Blade installation, Blade manipulator, Floating installation vessel

I. INTRODUCTION

RECENTLY, the drawing up of climate goals has been prioritized worldwide, notably in the 2015 Paris Agreement. 196 countries signed this agreement stipulating that global warming must be limited to a maximum of 2°C compared to the pre-industrial level [1]. The European Union has drawn up the European Green Deal targeting to become climate neutral with zero net greenhouse gas emissions by 2050 [2], [3]. To meet these goals, the way energy is generated needs to change drastically. Currently, most wind turbines placed at sea have a capacity of about 10 MW with a rotor diameter of approximately 160 m. In the future, wind turbines will inevitably become larger to account for the growing demand for renewable energy. Wind turbines of about 20 MW with a rotor diameter of approximately 260 m are considered [4]. Additionally, the challenge to install wind turbines in a larger weather window arises. Wind turbines are usually installed in the summer months when the weather window is favourable. This is because the maximum wind speed for the installation of blades is only about 10 m/s, to avoid critical events [5], [6]. Due to the use of jack-up vessels, is the allowable significant wave height (H_s) currently limited to 1.5 - 2.0 m [7], [8]. However, increasing the weather window means that wind turbine installations should also be feasible with wind speeds

up to 12 m/s and more extreme sea conditions with H_s of up to 3.5 m.

Currently, Huisman is working on the design of a Windfarm Installation Vessel (WIV), shown in Fig. 1, which approaches the installation of offshore wind turbines as an industrial robotised process. The WIV has four workstations, where different stages of the wind turbine assembly and installation take place simultaneously. The fast installation and high workability of this vessel lead to a higher installation capacity of wind turbines. In theory, the WIV is up to three times faster than conventional jack-up vessels. As wind turbines are getting larger, the installation of the larger wind turbine blades will be more challenging. This is compounded by more severe weather conditions during the installation process.



Fig. 1: Windfarm Installation Vessel

The objective of this paper is to develop a blade manipulator for wind turbine blade installation in severe weather conditions on a customized floating vessel, the WIV. The offshore wind turbine selected for this thesis is the IEA 15 MW wind turbine. This is the largest reference wind turbine with all the blade properties and specifications available [9]. This 15 MW wind turbine is used as a reference part for the capacity of the WIV. The following research question is formulated: **How can a blade manipulator be used to quickly and accurately install blades on a 15 MW wind turbine on a floating vessel?**

This paper first presents the problem analysis. It explains how offshore wind turbines are currently installed. Next, Huisman's WIV is presented. Then, different blade installation concepts are listed based on the concept requirements. The most feasible concept is selected by using an analytical hierarchical process. This concept is further developed with a functional design and a structural design. This paper ends with a conclusion.

II. PROBLEM ANALYSIS

This section presents the case for the design of the blade manipulator. First, the current method of wind turbine installation is explained, focusing on the installation of a single blade [10]. Subsequently, the current design of the WIV is explained, focusing on the process of simultaneous installation of the wind turbine on the vessel.

A. Current Wind Turbine Blade Installation

Currently, standard wind turbine installation takes place with a jack-up vessel during favourable weather conditions. The process starts with the transportation of the components to the offshore installation site. The foundation is already installed. The tower is upended and placed on the transition piece on the foundation. Subsequently, the nacelle, hub, and blades can be installed. This is done using the single blade installation method [10]. The flowchart of this method is shown in Fig. 2.

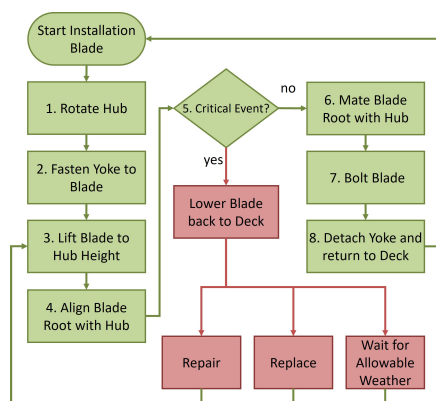


Fig. 2: Single Blade Installation

With single blade installation, the hub is first rotated to the right angle to insert the blade properly, this is block 1 in Fig. 2. In blocks 2 and 3 of the flowchart, a yoke lifts a blade out of the rack. The yoke is a specially designed lifting tool suspended at the crane hook, which is used to pick up the blade around its Center of Gravity (CoG). Sometimes, the tasks of the yoke are not limited to only gripping, in which case it is generally called a "blade manipulator". When there is no critical event, as indicated in block 5, such as a collision, the blade root is mated and mounted to the hub, as indicated

in blocks 6 and 7 respectively. Tag lines, also called tugger lines or tack lines, can be attached to the yoke and the crane boom to ensure that the blade does not move too much in the wind and to be able to manipulate the load horizontally. After successful installation, the yoke is detached and returned to deck, as indicated in block 8. Then the process is repeated until all three blades are installed.

B. Windfarm Installation Vessel

The WIV is a semi-submersible vessel that robotises the installation of both wind turbine foundations, as monopiles, and wind turbines. The wind turbine components are placed on deck at port or offshore supplied by a vessel. The WIV navigates to the appropriate location at sea, where a wind turbine foundation is located. The wind turbine is assembled on deck and installed on the foundation afterwards.

Fig. 3 shows a top view of the WIV with the different workstations to enable simultaneous assembly and installation. Station 1 is located on the starboard side of the vessel. Station 2 is located on the stern side of the vessel, station 3 on the port side and station 4 at the bow of the vessel. The tower of the wind turbine is upended at station 2 after which the electrical cabling is made ready for the nacelle. The nacelle is skid to the right place on deck to make it possible for it to be picked up at station 1. The installation tower rotates and picks up the nacelle at station 3. The installation tower rotates back and installs the nacelle on top of the tower in station 2. The electrical cabling is connected between the tower and the nacelle. Processes at all stations run simultaneously, increasing workability.

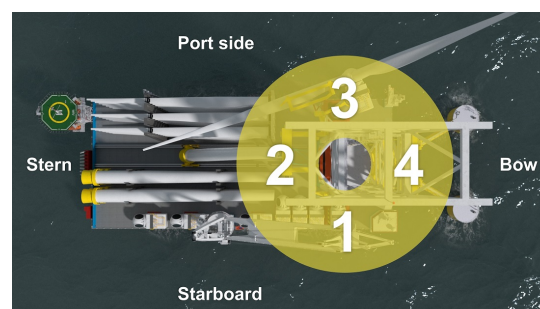


Fig. 3: Top view Windfarm Installation Vessel with the four different stations

During these first steps of the assembly process, the grippers at station 2 are tucked away, to create enough clearance to allow the installation tower to rotate. The grippers pick up the tower-nacelle assembly at station 2, after which the installation tower rotates and the tower-nacelle assembly is placed in the hole at station 3. Here, the blades are installed by the blade manipulator. After installing the blades, the wind turbine is picked up, the installation tower rotates and then the wind turbine is installed on the foundation.

III. CONCEPTS

With a clear overview of the problem analysis, concepts for the design goal can be created. Several concepts have been developed based on the VDI 2221 guideline. First, the problem is clarified and a list of concept requirements is drawn up, this is Phase I. Next, the different functions and a morphological overview are drawn up to systematically develop concepts. This is Phase II. Next, the concept selection takes place. This results in a single concept, which is elaborated in Phase III. Phase IV provides an overview of the complete concept with the final design of the manipulators.

A. Concept Requirements

1) *Clearance on Deck*: The blade manipulator has to be installed on top of the installation tower, above the slew bearing. The manipulator has a working area between the blade rack on the deck and station 3 of the WIV. Due to the rotation of the installation tower on the WIV, clearance is needed to prevent the protruding equipment from colliding with the wind turbine.

2) *Wind Turbine Installation Angle*: The blade has to be installed horizontally on the hub of the wind turbine. The maximum allowable angle is limited by the water level and equipment on deck. Blades are not allowed to contact water or other equipment, because this can cause damage.

3) *Blade Rack Layout*: The blades of the wind turbine are stored in a blade rack on deck of the WIV. This blade rack is modified to make it possible for the manipulator to access the blades. The top part of the blade rack must be removed to create enough clearance for the manipulator. Furthermore, a mechanism is added to ensure that the blades are always on the top level.

B. Conceptual Design

Using a morphological overview with several sub-functions, six different concepts were created. The concepts are shown in Fig. 4 and explained below.

Concept 1 – Rotational Arm: The blade is installed in one movement by a rotating arm with the hinge point at the installation tower.

Concept 2 – Knuckle Boom Crane: A knuckle boom crane picks up and installs the blade using a gripper directly connected to the boom. This manipulator can reach all the blades in the blade rack.

Concept 3 – Four-bar Linkage: The blade is picked up and installed by the four-bar linkage with an optimised predefined trajectory. The manipulator can reach all the blades in the blade rack.

Concept 4 – Conventional Crane: The blade is installed using a conventional crane using hoisting cables. This crane is extremely sensitive to weather conditions due to the gripper hanging from the crane.

Concept 5 – Translational Arm: Using a telescopic arm the blade is picked up. A trolley lifts the arm with the blade to hub height, where the blade is installed.

Concept 6 – Robotic Arm: The robotic arm moves between the blade rack at the root side of the blade to pick up the blade. A trolley moves the manipulator in the z-direction.

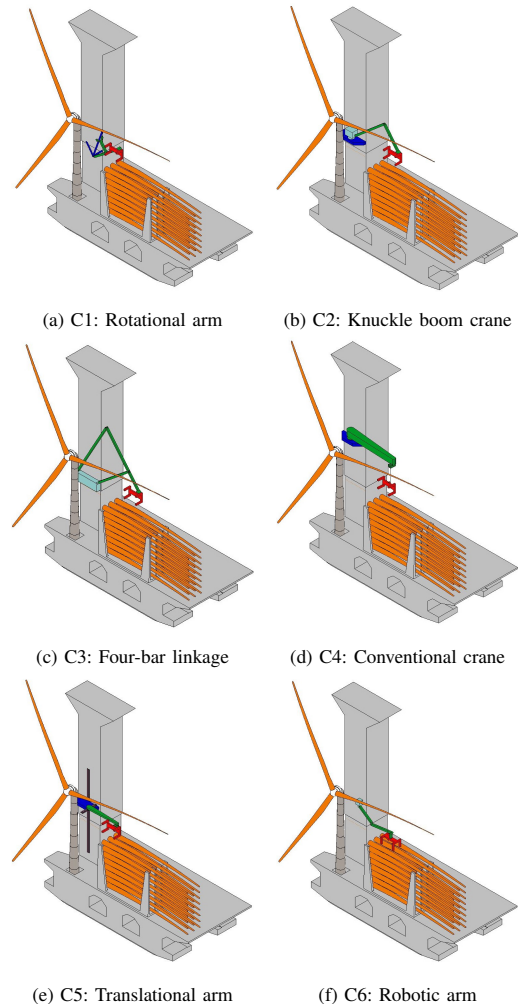


Fig. 4: Different concepts

C. Concept Selection

The concepts described in the previous section have not yet been realized. This makes it difficult to make a selection objectively based on criteria and their quantification. Saaty [11] has developed a multi-criteria decision-making approach, the analytic hierarchy process. With this method, difficult decisions can be made using a mathematical model where the different concepts are compared with each other using different criteria [12], [13]. To assess the previously presented concepts,

eight criteria are used. These are presented in Table I together with their weight factor. The weight factor is determined by the analytic hierarchy process.

TABLE I: Criteria for concept selection with description

| Criterion | Weight factor |
|----------------------------------|---------------|
| 1. Ease of manufacturing | 0.072 |
| 2. Technological Readiness Level | 0.054 |
| 3. Economic feasibility | 0.147 |
| 4. Scalability | 0.041 |
| 5. Installation time | 0.235 |
| 6. Reliability | 0.111 |
| 7. Safety | 0.312 |
| 8. Sustainability | 0.028 |

Using the analytic hierarchy process together with the weight factors, the results of the concept selection can be calculated. The results are presented in Table II. The rotational arm, concept 1, is the most feasible concept.

TABLE II: Results

| Rank | Concept | Score |
|------|------------------------|-------|
| 1 | C1: Rotational arm | 0.320 |
| 2 | C5: Translational arm | 0.178 |
| 3 | C2: Knuckle boom crane | 0.160 |
| 4 | C4: Conventional Crane | 0.147 |
| 5 | C3: Four-bar linkage | 0.125 |
| 6 | C6: Robotic arm | 0.069 |

IV. FUNCTIONAL DESIGN

This section presents the functional design of the blade manipulator. The manipulator is shown in Fig. 5. The manipulator is fixed to the top part of the installation tower of the WIV. This allows the manipulator to move with the installation tower as it rotates. The purpose of the manipulator is to transport a blade from the blade rack to the hub of the wind turbine.

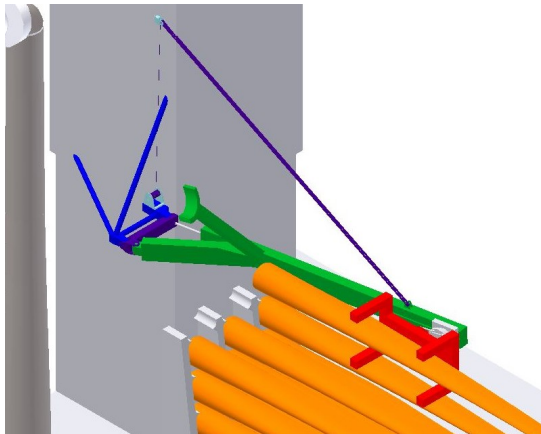


Fig. 5: Design of the manipulator

The rack stores the blades in a horizontal position parallel to each other, to minimize the wind load on the blades. Therefore, the blades are picked up from the side instead of from the top.

The gripper lifts the blade from the blade rack around the CoG of the blade. Consequently, the gripper translates towards the pivot point to obtain the correct radius for installation. Then, the manipulator moves upwards through a rotating movement, after which the blade can be installed on the hub of the wind turbine, see Fig. 6.

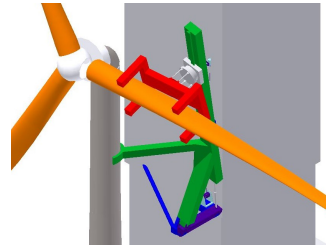


Fig. 6: Manipulator in vertical position

When the arm of the manipulator is in a horizontal position to grab a blade from the blade rack, there are three positions the gripper should be able to reach, see Fig. 7. The gripper comes from the side to pick up the blade. A hydraulic cylinder and a hinge point provide a rotational movement to reach these locations.

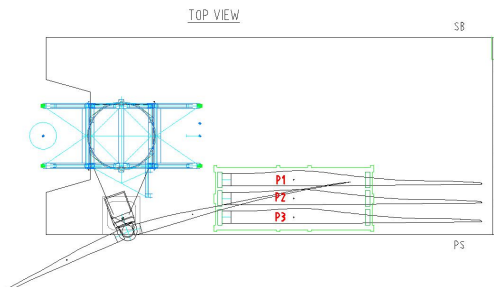


Fig. 7: Locations (P1, P2, and P3) shown in red of the blade the gripper must be able to reach

To keep the gripper horizontal in any circumstance, a slew bearing is used. To ensure that the gripper can tilt, cylinders are used. For the linear movement along the arm of the manipulator, a slider with a rack and pinion is used. A winch with a wire rope is used to lift the manipulator. The upper block is fixed approx. 40 m above the rotation point of the manipulator and the wire rope is connected to the arm of the manipulator around the location of the gripper. An overview of the manipulator can be seen in Fig. 8. The actuators are indicated in the figure, as well as the horizontal and vertical position.

V. STRUCTURAL DESIGN

The material used for the manipulator is ST52-3N-Plate. This is a strong type of steel that is suitable for this construction. This type of steel requires a thicker structure than

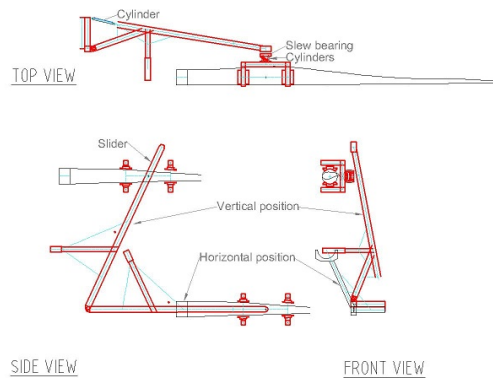


Fig. 8: Drawing manipulator

other types of steel with higher yield strength, such as S690. However, a thicker structure is stiffer and has less deflection.

The load factor must be determined before the loads on the manipulator can be calculated. The forces are multiplied by this load factor. The offshore standard DNVGL-OS-C101 for the design of offshore steel structures is used for this purpose and states a load factor of 1.2 may be used since the permanent loads and the variable functional loads are well defined [14].

To determine the structure of the blade manipulator, several load cases are evaluated with the manipulator in various positions and survival state. Only in the survival state the movement of the vessel and the wind loads are included. This is because during normal environmental conditions both of these loads are negligible. The wind load on the blade is calculated for a wind speed of 12 m/s when the chord of the blade is horizontal. The blade is divided into several segments with their own lift, drag, and moment coefficients. This results in the wind loads as stated in Equations 1 and 2. These are significantly smaller than the loads created by the mass of the blade, which is 65.25 mt. The operational accelerations of the vessel are as stated in Equation 3. This is without a gravitational acceleration of $g = 9.81 \text{ m/s}^2$. Since the gravitational acceleration is significantly higher than the accelerations due to the movement of the vessel, these operational accelerations are neglected in all load cases except in the survival case.

$$F_{W,blade} = \begin{bmatrix} F_{xb} \\ F_{yb} \\ F_{zb} \end{bmatrix} = \begin{bmatrix} 0.00 \\ -5.14 \\ 19.56 \end{bmatrix} \text{ kN} \quad (1)$$

$$M_{W,blade} = \begin{bmatrix} M_{xb} \\ M_{yb} \\ M_{zb} \end{bmatrix} = \begin{bmatrix} 2.17 \\ -83.6 \\ 65.3 \end{bmatrix} \text{ kNm} \quad (2)$$

$$a_{operational} = \begin{bmatrix} a_x \\ a_y \\ a_z \end{bmatrix} = \begin{bmatrix} 0.50 \\ 0.75 \\ 0.60 \end{bmatrix} \text{ m/s}^2 \quad (3)$$

The masses of the blade gripper and boom are as follows:

- $m_{blade} = 65.25 \text{ mt}$
- $m_{grripper} = 80 \text{ mt}$
- $m_{boom} = 1.6 \text{ mt/m}$

The blade and the gripper cause a force downward of $1.71 \times 10^3 \text{ kN}$ and a moment of $-1.71 \times 10^4 \text{ kNm}$ around the x-axis at the tip of the boom. Using these values, the loads can be calculated for all the load cases. These estimations of shear forces and bending moments are used to determine the steel structure of the boom. The cross-section of the boom together with the dimensions can be seen in Fig. 9. The cross-section is uniform along the entire length of the boom.

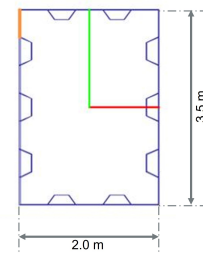


Fig. 9: Cross-section boom manipulator

The cross-section can be used to determine the deflection and rotation of the boom during different load cases. Calculations show that the largest deflection and torsion take place when the boom of the manipulator is horizontal, just after picking up the blade. In this case, the deflection of the boom is 50 mm and the torsion 1.1° , resulting in an additional 190 mm of blade drop. The deflection is less than 1 % of the total length of the boom, which is considered acceptable. Using large lifting equipment in operations considered these deflections already. When a load is being lifted, it gradually shifts its weight onto the equipment meaning that the deflection occurs slowly. Once completely loading the equipment, the deflection stays consistent and can be accounted for as the load consistently maintains the deflection.

VI. CONCLUSION

The objective of this paper is to design a blade manipulator to install wind turbine blades on a customised floating vessel, the WIV, in severe weather conditions. Based on a systematic approach, six concepts are developed. The rotational arm is selected to be most feasible. This is the rotational arm. This manipulator grabs the blade around the centre of gravity and picks it up. The gripper with the blade is moved over the arm towards the hinge point. Subsequently, the blade is lifted using a rotational movement to hub height. Here the blade is installed and the manipulator moves back to the blade rack to pick up the next blade.

The manipulator is designed to be operational with an average wind speed of 12 m/s and a significant wave height of 3.5 m. This enables the WIV to operate through most of

the year. As larger wind turbines will make their appearance in the future, a WIV equipped to install these wind turbines is needed. Due to the slider mechanism, the manipulator is able to handle increasing blade sizes.

Follow-up research is required before realisation of the blade manipulator. The steel structure of the boom should be optimised. The wind loads and ship movements should be added to the load cases. This can then be used to consider the optimal cross section for each section. Additionally, the actuators in the current design are determined fundamentally. They should be more extensively designed and optimised. Finally, a control system needs to be added and the accuracy calculated and determined with model tests.

The largest wind turbine currently available is 15 MW. There is already a plan for 20 MW wind turbines. The results from this thesis can be used for these kinds of larger wind turbines by applying the argumentation analysis and calculations to a larger wind turbine than 15 MW. However, it is advisable to use the 20 MW reference wind turbine when doing so, assuming it will be published in the near future.

REFERENCES

- [1] United Nations Climate Change, "The Paris Agreement." <https://unfccc.int/process-and-meetings/the-paris-agreement/the-paris-agreement>. (accessed April 6, 2022).
- [2] European Commission, "2050 long-term strategy." https://ec.europa.eu/clima/eu-action/climate-strategies-targets/2050-long-term-strategy_en, n.d. (accessed April 6, 2022).
- [3] European Commission, "A European Green Deal." https://ec.europa.eu/info/strategy/priorities-2019-2024/european-green-deal_en, 2019. (accessed April 6, 2022).
- [4] P. H. Jensen, T. Chavariopoulos, and A. Natarajan, "Lcoe reduction for the next generation offshore wind turbines," *innwind.eu*, 2017. (accessed June 20, 2022).
- [5] M. Gaunaa, L. Bergami, S. Guntur, and F. Zahle, "First-order aerodynamic and aeroelastic behavior of a single-blade installation setup," *Journal of Physics: Conference Series*, vol. 524, p. 012073, 2014.
- [6] L. Kuijken, "Single blade installation for large wind turbines in extreme wind conditions: A quasi-steady aeroelastic study in high wind speeds under different inflow angles," master of science thesis, Technical University of Denmark and Delft University of Technology, 2015.
- [7] Wind Monitor, "Wave heights and accessibility." http://windmonitor.iec.fraunhofer.de/windmonitor_en/4_Offshore/3_externe_Bedingungen/3_Wellen/, n.d. (accessed February 25, 2022).
- [8] Wind Energy The Facts, "Wind turbine technology for offshore locations: Availability, reliability and access." <https://www.wind-energy-the-facts.org/availability-reliability-and-access-7.html>, n.d. (accessed February 25, 2022).
- [9] E. Gaertner, J. Rinker, L. Sethuraman, F. Zahle, B. Anderson, G. Barter, N. Abbas, F. Meng, P. Bortolotti, W. Skrzypinski, G. Scott, R. Feil, H. Bredmose, K. Dykes, M. Shields, C. Allen, and A. Viselli, "Definition of the IEA 15-megawatt offshore reference wind," Technical Report NREL/TP-5000-75698, National Renewable Energy Laboratory, Golden, CO, 2020. (accessed April 6, 2022).
- [10] K. J. van Dinther, "Blade installation for offshore wind turbines," literature survey, Delft University of Technology, 2022.
- [11] T. L. Saaty, "How to make a decision: The analytic hierarchy process," *European Journal of Operational Research*, vol. 48, no. 1, pp. 9–26, 1990. Decision making by the analytic hierarchy process: Theory and applications.
- [12] O. S. Vaidya and S. Kumar, "Analytic hierarchy process: An overview of applications," *European Journal of operational research*, vol. 169, no. 1, pp. 1–29, 2006.
- [13] E. Triantaphyllou, S. H. Mann, *et al.*, "Using the analytic hierarchy process for decision making in engineering applications: some challenges," *International journal of industrial engineering: applications and practice*, vol. 2, no. 1, pp. 35–44, 1995.
- [14] Det Norske Veritas AS, "DNV-OS-C101: Design of offshore steel structures, general - Lrfd method," 2016.

B

Nomenclature

This appendix presents a nomenclature of definitions that are assumed to be general knowledge in this thesis. The information here is copied from literature study by van Dinther [21].

B.1. Wind Turbine

A wind turbine is a turbine that converts the energy of the wind into electricity by means of a generator. Figure B.1 shows a schematic overview of a wind turbine. When the wind arrives on the left side of this figure, the blades will catch the wind. This will cause the rotor, consisting of the blades in the hub, to rotate. The speed of the rotor is increased in the gearbox. The generator converts the kinetic energy from the gearbox into electricity. Another option is a Direct Drive (DD) generator. With this method, electricity is generated at a lower speed. The advantage of Direct Drive (DD) is that there are fewer moving parts and therefore less maintenance is required. The disadvantage, however, is that it requires permanent magnets made of rare-earth materials. Moreover, the hub cannot be rotated during installation because there is no gearbox to deliver a large moment [18, 48]. The generator (and gearbox) are located in the nacelle, which is on top of the tower. The generated electricity is then transported via power lines to an offshore and onshore substation after which it is connected to the electrical grid.

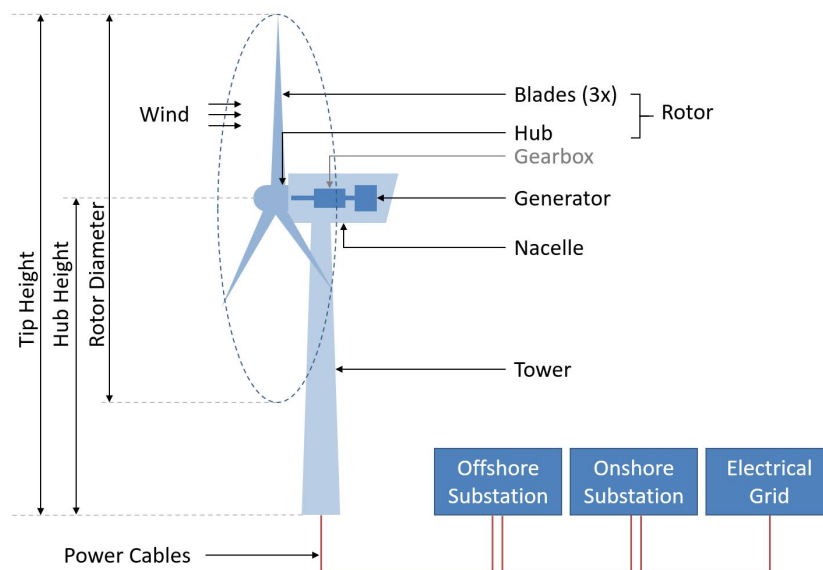


Figure B.1: Schematic overview of a wind turbine [21]

B.2. Foundation

A wind turbine is relatively easy to install onshore with a foundation of concrete [49]. However, this is more difficult to carry out offshore. The foundation type depends on the depth of the water. In shallow water (0-45 m) a monopile can be used. A monopile currently has a diameter of up to up to 15 m [50]. For a water depth of 50-70 m a Tripod or Jacket is used. Off the coast of the Netherlands these solutions are usually adequate, as shown in Figure B.2a. However, when looking at deeper locations a different foundation is needed for the wind turbine. Figure B.2b shows the average distance to shore of an installed offshore wind farm against the water depth. What can be noted is that most wind farms have been installed close to shore, within a distance of 120 km [51]. This is what has been installed until 2020. However, the goal is to build more wind farms; there are already permits to build wind farms further from the coast in deeper waters [52]. Different floating structures can be used for this purpose: a Tension Leg Platform is an example of a mooring line stabilised tension leg platform with suction pile anchors; a semi-submersible is an example of a buoyancy stabilised platform with catenary mooring lines; and a Spar Buoy is a ballast stabilised platform with catenary mooring drag embedded anchors [29, 53]. The different types of foundations for wind turbines at sea are shown in Figure B.3.

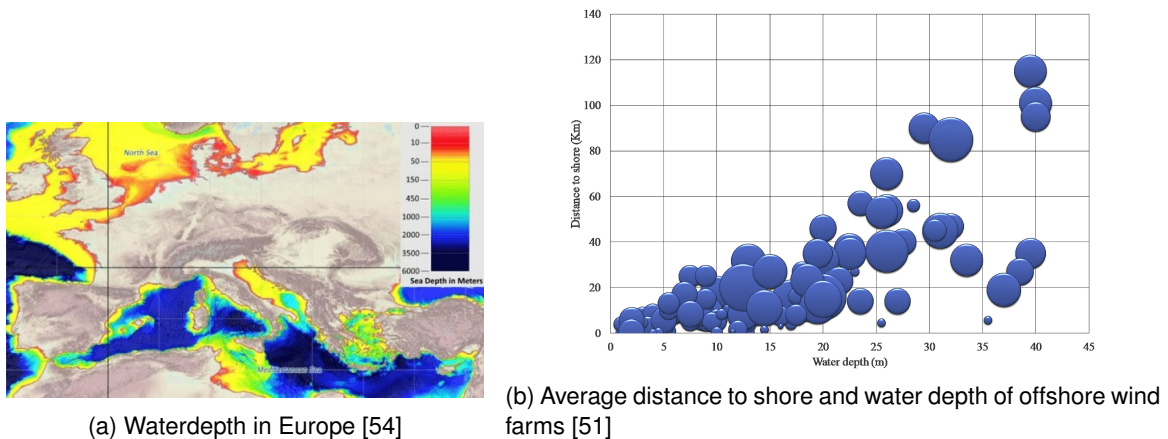


Figure B.2: Water depth

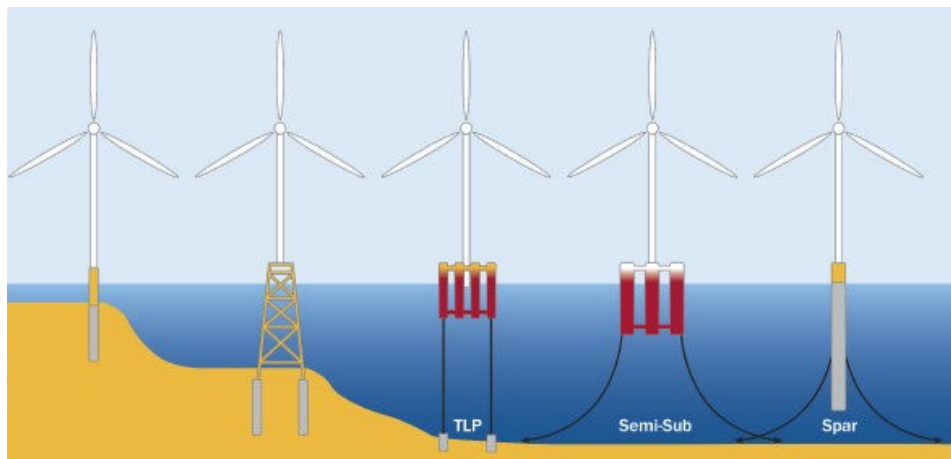


Figure B.3: Types of offshore wind turbine foundation. From left to right: Monopile, Tripod or Jacket, Tension Leg Platform (TLP), Semi-submersible, and Spar Buoy [55]

B.3. Installation Vessels

A vessel is required to install a wind turbine offshore. Figure B.4 shows the most common vessels which are currently in use. Tugboats, shown in Figure B.4a are used to guide non-self-propelled barges to its destination by pushing or pulling. An example of a barge is a crane barge, visible in Figure B.4b. A heavy lift vessel, as shown in Figure B.4c, has large cargo holds. Such vessels usually employ one or more cranes with a large SWL. This allows the vessel to transport and handle heavy components. A jack-up barge or jack-up vessel, see Figure B.4d and Figure B.4e, is a floating platform that can lift the platform, also known as hull, out of the sea. This makes the unit more or less independent of the sea swell and waves. However, a jack-up vessel is not suitable for floating offshore wind turbines because the legs of the jack-up vessel are not long enough for the greater water depth. A semi-submersible vessel is the solution to this. A semi-submersible vessel, shown in Figure B.4f, has the largest capacity of all the vessels mentioned here. The vessel is de-ballasted during transport to a draught at which the pontoons are partially above water. During lifting operations, ballasting is carried out in such a way that the pontoons are well under water. The required stability is obtained by placing the columns far apart, which makes it possible to hoist the enormous weights [29, 56].



(a) Tugboat [57]



(b) Crane Barge [58]



(c) Heavy Lift Vessel [59]



(d) Jack-up Barge [60]



(e) Jack-up Vessel [61]



(f) Semi-submersible Heavy Lift Vessel [62]

Figure B.4: Offshore Wind Turbine Installation Vessels

C

Additional Information Windfarm Installation Vessel

Figure C.1 shows the flowchart for installing a monopile using the WIV. The upending of a monopile takes place at station 2; a visual representation of this is shown in Figure C.2a. After this, the monopile is picked up and the installation tower rotates to part of the monopile at station 1 or 2, as can be seen in Figure C.2b. Here, the monopile is parked until the monopile is ready to be installed. To install the monopile, the installation tower picks up the monopile again and rotates so the monopile ends up at station 4. The monopile is lowered to the seabed, see Figure C.2c, and hammered into the seabed.

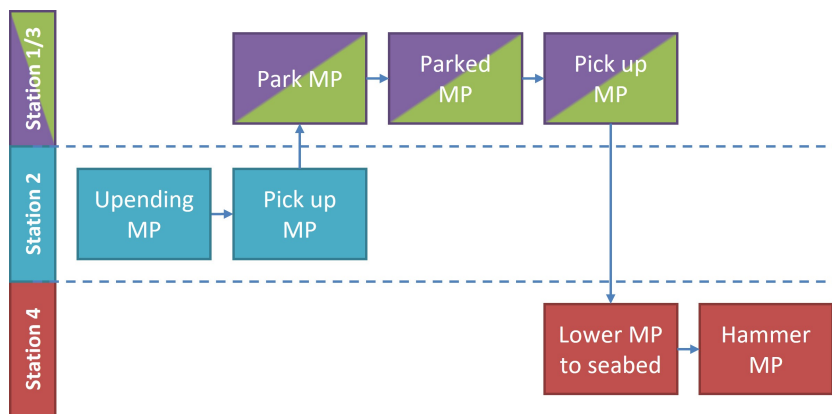


Figure C.1: Flowchart for installing a Monopile (MP)



(a) Upending of the Monopile

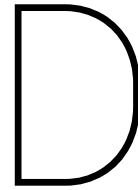


(b) Pick up and Rotate Monopile



(c) Lower Monopile to Seabed

Figure C.2: Monopile installation by WIV



Concept Selection

```
1 clear;clc;
2
3 %% parameters
4 [status,sheets] = xlsfinfo('AHP.xlsx'); % Upload file info
5 comparison=xlsread('AHPweegfactoren.xlsx'); % Upload content from Excel
6 comparison(:,1)=[]; % Remove header column
7 comparison(1,:)=[]; % Remove header row
8
9 for k = 1:length(sheets)
10 criterion(:,k)=xlsread('AHP.xlsx',k); % Fill 3d-matrix with all the criteria and their score
11 end
12 n = size(criterion,1); % Count amount of concepts
13 m = size(comparison,1); % Count amount of criteria
14 RCI = [1 2 3 4 5 6 7 8 9 10; 0 0 0.58 0.9 1.12 1.24 1.32 1.41 1.45 1.49]; % Random Consistency index
15
16 %% calculate eigenvector and eigenvalue
17 for k = 1:length(sheets)
18 [W(:,k),l(:,k)] = eig(criterion(:,k)); % Calculate eigenvector(W) and eigenvalue(l) of the comparison matrices
19 end
20 lambda = max(l,[],1 2); % Calculate the maximum eigenvalue per comparison matrix
21
22 [V,D] = eig(comparison); % Calculate the eigenvector (V) and eigenvalue (D) of pairwise comparison matrix
23 lambdac = max(D,[],'all'); % Calculate the maximum eigenvalue per comparison
24
25 %% calculate priority vector and indices
26 PV = W(:,1,:)./sum(W(:,1,:)); % Calculate the priority vector (PV) per comparison matrix
27 CI = (lambdac-n)/(n-1); % Calculate the consistency index (CI) per comparison matrix
28 [row,col] = find(RCI==n); % Find the row and column of the RCI value for the amount of different concepts n
29 CR = CI/RCI(2,col); % Calculate the consistency ration (CR)
30 PV(isinf(PV)) = 1/n;
31
32 Pvc= V(:,1)/sum(V(:,1)); % Calculate the priority vector/ weighing factor (PV) per pairwise comparison matrix
33 C Ic = (lambdac-m)/(m-1); % Calculate the consistency index (CI) per pairwise comparison matrix
34 [rowc,colc] = find(RCI==m); % Find the row and column of the RCI value for the amount of different concepts m
35 CRc = C Ic/RCI(2,colc); % Calculate the consistency ration (CR)
36
37 %% print results
38 % print the pairwise comparison matrix with the priority vector and its eigenvalue, CI and CR
39 fprintf('Comparison criteria:\n')
40 fprintf('\t%.2f %.2f %.2f %.2f %.2f %.2f | %.4f\n', [comparison,Pvc].')
41 fprintf('\tlambda_{max} = %.3f\n\tConsistency index (CI) = %.3f\n\tConsistency ratio (CR) = %.3f\n', lambdac, C Ic, CRc)
42 if CRc > 0.1
43 fprintf(2,'<strong>Look at the rating of the criteria, the consistency ratio is larger than 10%%</strong>\n');
44 % Check the consistency ration weather this comparison can be accepted
45 end
46
47 % Print the comparison matrices with the priority vector and their eigenvalue, CI and CR
48 for j=1:length(sheets)
49 fprintf('Criterion %d:\n', j)
50 fprintf('\t C1 C2 C3 C4 C5 C6 | PV\n')
51 fprintf('\t%.2f %.2f %.2f %.2f %.2f %.2f | %.3f\n', [criterion(:,j),PV(:,j)].')
52 fprintf('\t$lambda_{max}$ = %.3f\n\tConsistency index (CI) = %.3f\n\tConsistency ratio (CR) = %.3f\n', lambda(:,j), CI(:,j), CR(:,j))
53 if (CR(:,j) > 0.1)
54 fprintf(2,'<strong>Look at the rating of this criterion (criterion %d), the consistency ratio is larger than 10%%</strong>\n', CR(:,j))
55 % Check the consistency ration weather this comparison can be accepted
56 end
57 end
```

```
58
59 for j=1:length(sheets)
60     priorities(:,j) = PV(:,j)*PVC(j);    % Combine all the priority vectors in one matrix and multiply them with their
        corresponding weighing factor
61 end
62 result = sum(priorities,2);                % Calculate the normalized results per concept.
63 fprintf('Results:\n')
64 for j=1:n
65     fprintf('Concept %d: %.3f\n', j, result(j))
66 end
```